ON THE GLOBAL ATTRACTOR OF 2D INCOMPRESSIBLE TURBULENCE WITH RANDOM FORCING

by

Pedram Emami

A thesis submitted in partial fulfillment of the requirements for the degree of

Master of Science

in

Applied Mathematics

Department of Mathematical and Statistical Sciences
University of Alberta

Abstract

The importance of simulating fluid flow is indisputable. From weather forecasting to aviation to the blood flow inside our arteries, fluid flow significantly influences our everyday life. Among all possible fluid regimes, one is dominant in many physical applications. Turbulence, sometimes characterized as the "last great unsolved problem of classical mechanics," is complicated enough that it still does not have a unified and thoroughly validated theory. Understanding the nature of turbulence even in the simplest and most ideal homogeneous isotropic incompressible case has been underway since the beginning of the twentieth century. Although there have been brilliant breakthroughs, we are far from a complete understanding of this important physical phenomenon. Among many approaches available for studying turbulence, a recent method exploits modern mathematical tools to analyze turbulence on a solid foundation. This functional analysis approach is based on the Navier–Stokes equation, the most widely adopted deterministic governing equation for Newtonian fluid flow. This study revisits bounds on the projection of the global attractor in the energy–enstrophy plane obtained by Dascaliuc, Foias, and Jolly [2005, 2010]. In addition to providing more elegant proofs of some of the required nonlinear identities, the treatment is extended from the case of constant forcing to the more realistic case of white-noise forcing typically used in numerical simulations of turbulence. Finally, these analytical bounds, which have not previously been demonstrated numerically in the literature, even for the case of constant forcing, are illustrated numerically in this work for the case of white-noise forcing.

Dedicated with love to my parents

Acknowledgements

I would like to thank profoundly Professor John C. Bowman for all he has done for me in my master of science program. Undoubtedly, without his kindness and also his extremely useful support and guidance, this work could not have been achieved. His friendly behaviour and patience, along with his great level of knowledge in the field, were the driving force of this work and the main source of my motivation and enthusiasm. I would also like to thank Dr. Clement W. Bowman for the generous financial support provided by the Clement W. Bowman Mathematical Turbulence Scholarship.

Table of Contents

List of Figures

Chapter 1

Introduction

Turbulence is sometimes characterized as the "last great unsolved problem of classical mechanics." Attempts to understand and predict turbulent flow have been undertaken since the very beginning of the emergence of classical mechanics. While there have been some influential breakthroughs in the last century by great researchers like Kolmogorov, Kraichnan, Batchelor, Leith, Ruelle, Takens, Orszag, Frisch and others, the problem of turbulence is complicated enough that there is not even a unified model adopted by all researchers in the field. The nature of turbulence is still controversial. Is it a deterministic or stochastic phenomenon? While the majority of researchers in the field might agree that this phenomenon is governed by a deterministic system of partial differential equations, the Navier–Stokes equation, and so it is usually categorized as a fully deterministic problem, there are some core assumptions for the validity of this perspective. Even with the emergence of chaos theory in the 1980s and the understanding of nonlinear dynamical systems using the concepts of attractors, basins, intermittency, and coherent structures, the problem of turbulence cannot be completely described. The complex nature

and essence of turbulence deserves much further study. The paucity of our knowledge about turbulence is such that we are in danger of being on the wrong track even after all of our attempts to understand it. In this chapter we are going to discuss what is known about turbulence and what progress has been made in the field, taking the deterministic approach adopted by the majority of researchers.

1.A What is turbulence?

> Turbulence is that state of fluid motion which is characterized by apparently random and chaotic flow. When turbulence is present, it usually dominates all other flow phenomena and results in increased energy dissipation, mixing, heat transfer, and drag. George [2013]

There is no universally accepted definition for turbulence. It is such a multifaceted phenomenon that the word *turbulence* is viewed from different perspectives by different researchers. From the mathematician's viewpoint, the *turbulence problem* is mostly about the well-posedness, regularity, ergodicity, and uniqueness of solutions of a partial differential equation. On the other hand, physicists typically focus on universality and statistical descriptions, while engineers tend to be more interested in the enhanced mixing and drag attributed to turbulent interactions. So the reader must pay attention to the word *apparently random* in the above general definition, as we now explain.
For a long time researchers were in doubt about the origin of randomness in turbulence. Is there is a hidden randomness in the nature of turbulence, with some specific stochastic quantity playing a major role? Or does the randomness arise only from the uncertainty in initial conditions and physical

measurements, in view of the chaotic nature of the underlying deterministic governing equations? These questions remain relevant even today, as there is no universal consensus among researchers on how precisely to view turbulence.

The emergence of dynamical system theory and the way it changed our view of the physical world has persuaded many researchers, especially the most influential ones, that turbulence is a deterministic phenomenon and is a problem of dynamical systems. This viewpoint leads to the description of turbulence as an apparently, but not really, random physical phenomenon. It is also believed that the apparently random behaviour of turbulence is caused by nonlinear terms in the governing equations, which make the results extremely sensitive to the initial conditions. Although the dynamical systems viewpoint might seem more justifiable, especially in view of supporting experimental evidence, turbulence is in fact not just a time-dependent initial value problem, but also involves spacial propagation, exhibiting both temporal and spatial intermittency. Spatial intermittency is typically not addressed by dynamical systems theory.

Up to this point we have presented the uncertainty we are dealing with in the field of turbulence. The historical efforts in this field reflect the depth of the difficulties that researchers have confronted, and so the reader should expect to face many simplifying assumptions that have been taken into consideration by many influential researchers. Later on in this chapter we will turn our focus to the simplest idealistic case of turbulence. The reader who is not profoundly familiar with the notion of turbulence will observe the difficulties buried in the nature of turbulence, which make even the simplest case resistant to both theoretical and numerical analysis, even under a deterministic governing partial differential equation, derived under many simplifying but tenable assumptions.

1.B Why study turbulence?

From weather forecasting to aviation to the blood flow inside our arteries, fluid flow significantly influences our everyday life. Among all possible fluid regimes, there is one that is dominant in many physical applications. Turbulent flows surround us so much in our everyday life that we can easily lose awareness of their ubiquity. The above question can be answered with at least two fairly independent reasons:

- Turbulence, the pure scientific study of chaotic fluid flow, affects almost every underlying part of our life, from health and biology to advanced technologies.
- The conveniences of our modern life style, which depends on efficient transportation, reliable weather forecasting, and advanced instrumentation, are intricately connected to turbulent phenomenon.

On one hand, our curiosity for understanding this fascinating phenomenon motivates mathematicians and physicists to put a certain amount of energy and attention into this challenge. On the other hand, the promise of a better life encourages engineers to come up with a solution for obstacles to progress in advanced technologies, many of which deal with different facets of turbulence. So even if we can suppress our curiosity for studying such a complicated phenomenon, our motivation for studying turbulence is empowered by our enthusiasm for a better life and more advanced technologies. So in fact the second reason can itself be divided into two aspects:

- Turbulence is predominant in fluid flows.
- The cost of our ignorance is unbelievably high.

In order to elucidate these reasons to the reader, it is enough to recall the billions of dollars that almost all countries have to spend renovating damages caused by floods, tornadoes, hurricanes, and typhoons, because of poor weather forecasting, not to mention the sorrow of lost life.

Our modern life is intricately connected with technological innovation. Having safer, more efficient and comfortable transportation technologies is just one among many examples where we have to deal with the presence of turbulence as an indispensable effect of fluid flow. Besides these simple examples, the reader can readily appreciate the vital effects of turbulence in our arteries, contributing at the same time to both our survival and death.

What we have mentioned above is just a short note to emphasize the importance of studying turbulence; we believe that it is informative enough to motivate the interested reader to follow up on their interests in this field.

1.C The way we look at turbulence

1.C.1 Deterministic governing equations; no stochastic parameters

Just as classical mechanics has been greatly successful in predicting the future state of time-dependent mechanical systems composed of particles, there is a parallel view of fluid flows in the form of continuum mechanics. Although we strongly believe that fluids are made up of molecules whose dynamical behaviours are governed by Newtonian mechanics, dealing with a countless number of molecules in a fluid is another difficulty that makes it almost impossible to solve the resulting system. Here is the main place where statistical mechan-

ics comes in, an approach that applies Newtonian mechanics to a system of many particles, based on a molecular collision model. The fluid flow at the macroscopic level is thus governed by the laws of statistical mechanics. The statistical representation can be obtained by solving the Boltzmann equation for the governing distribution function of particle positions and velocities. There is an integral collision operator that describes the collisions between particles, using a many-particle distribution. This results in an extremely complicated system that is essentially impossible to analyze precisely. This approach can be applied to a dilute gas, considering the evolution of a single particle distribution, subjected only to binary collisions. For this simplified approximation the collision operator can be represented based on its first- and second-order spatial derivatives, where the former becomes the familiar pressure gradient and the latter becomes the Laplacian of the velocity, multiplied by a constant known as the viscosity. This simplified approximation makes it possible to obtain conservation equations for mass and momentum, respectively.

Although this kind of approximation can be taken as a successful model for a suitable range of pressure and densities of dilute gases, deriving the corresponding model for fluids remains an open problem. The difficulty is that in the case of fluid flows, ternary and higher-order collisions become important. Consequently, because of the lack of a better option, the only accessible approaches, given limited theoretical and computational resources, are based on continuum mechanics models like the Navier–Stokes equation. This equation can be derived using a few simplifying assumptions (which define a Newtonian fluid): the relation between the stress and strain tensors is considered to be linear, with a proportionality constant called the fluid viscosity. The viscosity encapsulates all those extremely complicated microscopic

interactions between fluid molecules into a simple constant. The viscosity assumption imposes a limit on the domain of validity of the resulting Navier–Stokes equation, so that fluid phenomena having length scales comparable to the mean free path cannot be described using a continuum model like the Navier–Stokes equation. As this approach has been very successful in describing the evolution of *laminar* fluid flows, it is tempting to adopt this model also for turbulent flows. Again, the paucity of our knowledge and the lack of better alternatives persuade us to take the Navier–Stokes equation as the main governing equation underlying turbulent flow, with the precaution that this model would be inappropriate for flows in which turbulent fluctuations are comparable to thermal fluctuations at the microscopic level.

1.C.2 Predictable vs. unpredictable phenomena

It may seem strange that a fully deterministic phenomenon is truly unpredictable. Here we address the meaning of predictability and show that there is nothing in conflict with having a deterministic but unpredictable phenomenon. To resolve this apparently paradoxical behaviour, we must return to the exact meaning of predictability.

We call the dynamical behaviour of a system *predictable* if there exists a mapping from the current state of the system to future states. If the system is deterministic, that mapping must be the explicit solution of the governing equations for each possible initial and boundary condition. Examining this notion carefully, it can be easily observed that there could be many complicated systems of governing equations, whose explicit solutions are not obtainable, even though their existence might be proven using advanced mathematical

tools. Now if we turn back to the turbulence problem, we have to consider some extra difficulties. Adopting the deterministic point of view and applying dynamical system theory, turbulence can be considered as fully chaotic state of fluid flow, and it has been well understood that in the case of chaos, every numerical simulation of the governing equations is quite sensitive to the initial conditions. Numericists have long observed that even if an explicit solution of the Navier–Stokes equation exists, it is so sensitive to the initial conditions that restarting a numerical simulation from a specific state (with a slight perturbation arising from precision loss during the restart process) toward a future state can yield results dramatically different from those obtained by evolving directly from the initial condition to the final state [Lorenz 1963].

The above discussion should be helpful enough to understand the subtle difference between predictability and determinacy.

1.C.3 Stochastic models for turbulence

Alternatively, turbulence can be regarded as an intrinsically random and stochastic phenomenon. Although for natural fluids that we work with in everyday life, the majority of researchers believe that turbulence is a deterministic phenomenon, there is some justification for the alternative viewpoint. The main empirical justification is the observation of turbulent phenomena in superfluids like helium at $T \approx 4K$, even though these surprising fluids have zero viscosity. Although we are not dealing with superfluidity in our everyday life, it is possible to investigate such fluids in laboratories. Classical turbulence is thought to be the result of viscous dissipation acting on vortices that interact via a nonlinearity to produce new vortices. However, in the case of

superfluids there must be another underlying phenomenon since no viscous forces are present. These observations can be used to justify the existence of an intrinsic randomness property for turbulence other than the nonlinearity of the governing equations.

1.D Different approaches toward studying turbulence

According to the surviving art work of Leonardo da Vinci, it is clear that our first recognition of turbulence goes back at least 500 years. However, it seems that there was little methodological understanding of turbulence until the late 19th century and the beginning of the twentieth century, when the study of turbulence was revolutionized by important breakthroughs made by mathematicians and engineers in both theoretical and experimental fields. If we look at the twentieth century as the modern era of studying turbulence, we can categorize the approaches taken by different researchers as follows:

- Statistical approach
- Phenomenological approach
- Structural method
- Deterministic approach
  - Subgrid scale models (SGS)
  - Functional analysis approach

In the rest of this chapter we will mostly focus on the overview of the history of turbulence, focusing on the most influential and remarkable discoveries pertaining to each of the above outlooks.

1.E An overview of turbulence history [1]

In the late 19th century, Boussinesq [1877] made the pioneering assumption that turbulence stresses are linearly dependent on strain rates (equivalently, there is a linear operator that maps the strain rate tensor to the stress tensor), an assumption on which many later models of turbulence have been built.

The famous tube experiment by Osborne Reynolds [Reynolds 1894] are among the most influential results ever produced on the subject of incompressible homogeneous turbulence. His experimental results were the main motivation for defining the Reynolds number as the only dimensional number involved in a sequence of flow transitions leading from laminar to fully turbulent flow over a smooth surface. Besides introducing the dimensionless Reynolds number, which we denote here by R_e, he also noticed that only a few transitions are required to reach a turbulent state, a fact that was not fully understood until late in the 20th century. As the main impact of his experiment, he stated that turbulence is too complicated to be studied in detail, an understanding that led him to separate the velocity field into two separate fields: the mean flow and fluctuations. This result for a long time led to a specific belief by many researchers, especially engineers, that turbulence is a random phenomenon and consequently studying its details would be pointless. It is really interesting to know that at about the same time, Poincaré & Magini [1899] were establishing

[1] [McDonough 2007]

the theory of chaos, which demonstrates that even a relatively simple deterministic nonlinear dynamical system can exhibit apparently random behaviour. Although many researches began working on nonlinear dynamical systems, it was about 70 years later that the American meteorologist Lorenz [1963] first proposed possible links between *deterministic chaos* and turbulence. Until this time, almost all attempts in the field of turbulence applied statistical methods to describe turbulence, pursuing the idea of random phenomenon proposed by Reynolds. The first important result of the statistical approach that added significant credibility to this discipline was obtained by Prandtl [1925]. His *mixing-length theory* was established by drawing an analogy between turbulent eddies (swirls) and the molecules of a gas in order to make use of *kinetic theory*.

In the 1930s, another breakthrough was made by G.I. Taylor, the first researcher who utilized a more advanced level of mathematical rigour, introducing formal statistical methods involving correlations, Fourier transforms, and power spectra for studying turbulence [Taylor 1935]. He explicitly assumed that turbulence is a random phenomenon and explained his experimental data generated by wind tunnel flow using a mesh to show that the flow could be viewed as homogeneous isotropic turbulence. The success of his approach was so influential that the effects of his viewpoint continue to the present. Taylor also made a great contribution to experimental research by introducing the *Taylor hypothesis*, which provides a means of converting temporally distributed data to spatially distributed data.

The first truly mathematically rigorous analysis of the Navier–Stokes equations was done by Leray exactly during the period of the most celebrated work of Taylor [Leray 1933], [Leray 1934]. In fact Leray's work can be thought of as a cornerstone for developing and utilizing the analytical tools required for

studying the Navier–Stokes equation in the context of deterministic dynamical systems.

In 1941, the historically most important and oft-quoted turbulence theory was proposed by the Russian mathematician A.N. Kolmogorov through three seminal papers. The first and third of these papers, often referred to as the *K41 theory* [Kolmogorov 1941a], [Kolmogorov 1941b] introduced a statistical method distinct from Reynolds' approach. Although before the late 20th century, insufficient computational power was available to test these theories numerically, the phenomenological K41 result was highly influential in furthering turbulence theory. Except for the work of Kolmogorov, most other research in the 1940s can be viewed as a consolidation of Reynolds' method. Among many of such works we can refer to the most often cited: Batchelor [1948], Burgers [1948], Corrsin [1949], Heisenberg [1948], von Karman [1948], Obukhov [1949], Townsend [1947] and Yaglom [1948], among which the works of Corrsin, Obukhov and Townsend were experimental. Although the 1940s can be viewed as a decade of consolidating and codifying the statistical approach proposed by Reynolds and later on by Prandtl, Taylor, von Karaman, and others, the results of the experimental work during this period were beginning to cast doubt on the validity and consistency of the random approach for describing turbulence. Particularly, according to the early work of Emmons [1951], it was not rational to accept the random nature of turbulence. Later on, the application of sophisticated measurement methods in the late 1950s characterized the existence of long-lived vortices known as *coherent structures* in turbulent flow, which was seen to contradict the random and unpredictable nature of turbulence.

Although experimental instruments had been improved considerably by

the beginning of 1960s, the measurements were still not advanced enough to yield significant progress in developing a comprehensive theory of turbulence. Nevertheless, researchers in computer science were laying the groundwork for a sweeping change in the treatment of turbulence based on the advent of the digital computer. In 1963 the MIT meteorologist E. Lorenz investigated the deterministic solution of a highly truncated Fourier model of the Navier–Stokes equation [Lorenz 1963]. He showed that the numerical results are so erratic that is it is difficult to distinguish them from a fully random process. In addition, he demonstrated the extreme sensitivity of the solution to small changes in the initial conditions, with implications for weather forecasting. The other extremely interesting result (not truly understood at that time) hidden in his numerical simulation was the existence of structures that were later appreciated by McWilliams [1984], McDonough *et al.* [1998], Mukerji *et al.* [1998] and Yang *et al.* [2003] as potentially being associated to the experimentally observed coherent structures. The most important point of Lorenz's work was the existence of a solution to a highly simplified form of the Navier–Stokes equation that exhibited an apparently random behaviour quite similar to turbulence. This led to further mathematical studies of the Navier–Stokes equation undertaken both in pure mathematical contexts (focusing on existence, uniqueness and regularity of the solutions) [Ladyzhenskaya 1963] and in the context of dynamical systems [Smale 1965], [Arnold 1964].

In the 1960s there was another movement by researchers toward tackling turbulence, based on solving the so-called *closure problem*. The goal was to devise a reasonable model for the higher-order moments that arise in the equations of lower-order moments in the statistical formulation of turbulence. For tackling this problem many new mathematical and statistical tools were

introduced by researchers, especially through the work of Kraichnan, who applied mathematical perturbation methods from quantum field theory to turbulence [Kraichnan 1958], [Kraichnan 1959], [Kraichnan 1961]. He used Fourier representations (both series and transforms) and Feynman diagrams, building on connections to the Liouville and Fokker–Planck equations to approximate the higher-order moments appearing in the moment equations. While these new tools and equations were of educational value in learning about different kinds of turbulent interactions, in the end, they unfortunately did not solve the problem of turbulence.

More relevant to this work is the generalization of Kolmogorov's ideas to two-dimensional incompressible homogeneous isotropic turbulence by Kraichnan [1967], Kraichnan [1971], Leith [1968], and Batchelor [1969]. Although the mere existence and formation of 2D turbulence is somewhat controversial, due to the absence of a vortex-stretching mechanism in two dimensions, it was immediately understood that 2D turbulence is complicated by the presence of an additional quantity called the *enstrophy*, which cascades towards the smaller scales (the *direct cascade*), while energy cascades to the large scales (the *inverse cascade*).

The 1960s was also the decade of underlying advancements in experimental studies of turbulence: major improvements in experimental measurements of decay rates in isotropic turbulence, the return to isotropy in homogeneous anisotropic turbulence [Comte-Bellot & Corrsin 1966], [Lumley & Newman 1977], details of boundary layer transitions [Wygnanski & Fiedler 1970], the transition to turbulence in pipes and ducts [Tucker & Reynolds 1968], and the effects of turbulence on scalar transport [Gibson 1968].

The seminal paper by Ruelle & Takens [1971] marks a turning point in the history of turbulence, initiating what we call the modern view of turbulence. They showed that the full Navier–Stokes equation as a dynamical system can produce chaotic solutions that are very sensitive to small changes in the initial conditions. In that work it is shown that this dynamical system exhibits apparently random behaviour associated with an abstract mathematical notion called the *global attractor*. As the Reynolds number increases, the system undergoes a sequence of bifurcations that finally arrives at a chaotic state that manifests itself as fully developed turbulence. Typically, the sequence of states that the flow undergoes can be expressed as

$$\text{steady} \rightarrow \text{periodic} \rightarrow \text{quasi-periodic} \rightarrow \text{turbulent}.$$

The main motivation of many experiments in the 1970s and 1980s was the investigation of the explicit predictable sequence of states proposed by Ruelle. These investigations confirmed the existence of such a sequence of states. During these experiments, other short sequences of turbulent transitions were repeatedly confirmed, particularly the period-doubling subharmonic sequence observed by Feigenbaum [1978], the sequences involving intermittency demonstrated in the work of Pomeau & Manneville [1980], and some specific sequences of transitions recognized in flows associated with natural convection by Gollub & Benson [1980].

Although the experiments done in the 1970s and 1980s primarily revolved around the work of Ruelle, there were two other important aspects of these experiments. The first aspect was an attempt to perform a detailed test of the Kolmogorov theory of turbulence, the outcome of which was approximate overall agreement with the theory, despite some anomalies in the precise scaling

exponents. Further investigation of this *anomalous scaling* ensued. The second aspect of these experiments was an emphasis on inhomogenous and anisotropic turbulence beyond the realm of the K41 theory.

Since the beginning of the modern view of turbulence in the 1970s, with the seminal work of Ruelle, the most important progress made in the field was in the advancement of techniques for *direct numerical simulation* (DNS) of turbulence. The first and one of the most successful of these methods was the Large Eddy Simulation (LES) method proposed by Smagorinsky [1963] and Deardorff [1970]. Shortly thereafter, the highly accurate but expensive pseudospectral method was proposed by Patterson Jr. & Orszag [1971]. The lack of sufficient computational resources in the 1970s, which in turn made the DNS and even LES impractical, led to the introduction of, and subsequent preoccupation with, a wide range of Reynolds-averaged Navier–Stokes (RANS) methods, in spite of their obvious shortcomings and pitfalls (see e.g., Launder & Spalding [1974] and Launder *et al.* [1975]). This trend was partially reversed by the beginning of the 1990s with the rapid increase in computational resources and power that made using LES in simple practical problems finally possible. Even today, about 25 years after the introduction of the LES method, it is still the most feasible simulation technique that can be used for real practical problems, while the pseudospectral method is primarily used for theoretical and fundamental investigations in very simple domains. This difficulty in implementing the most accurate and advanced numerical simulation method is still the main motivation behind research in advanced subgrid scale models than are more accurate than traditionally LES methods and still more feasible than pseudospectral collocation. These include the dynamic models of Germano *et al.* [1991] and

Piomelli [1993] and various forms of *synthetic-velocity* models, such as those of Domaradzki and coworkers (e.g., Domaradzki & Saiki [1997]), Kerstein and coworkers (e.g., Echekki *et al.* [2001]) and McDonough and coworkers (e.g., McDonough & Yang [2003]).

1.F Eras of turbulence studies

In the spirit of Chapman & Tobak [1985], the brief history of turbulence described in the previous section, from the famous Reynolds experiments in 1883 to the present can be divided into fairly separate eras of noticeable "movements", as illustrated in Figure 1.1.

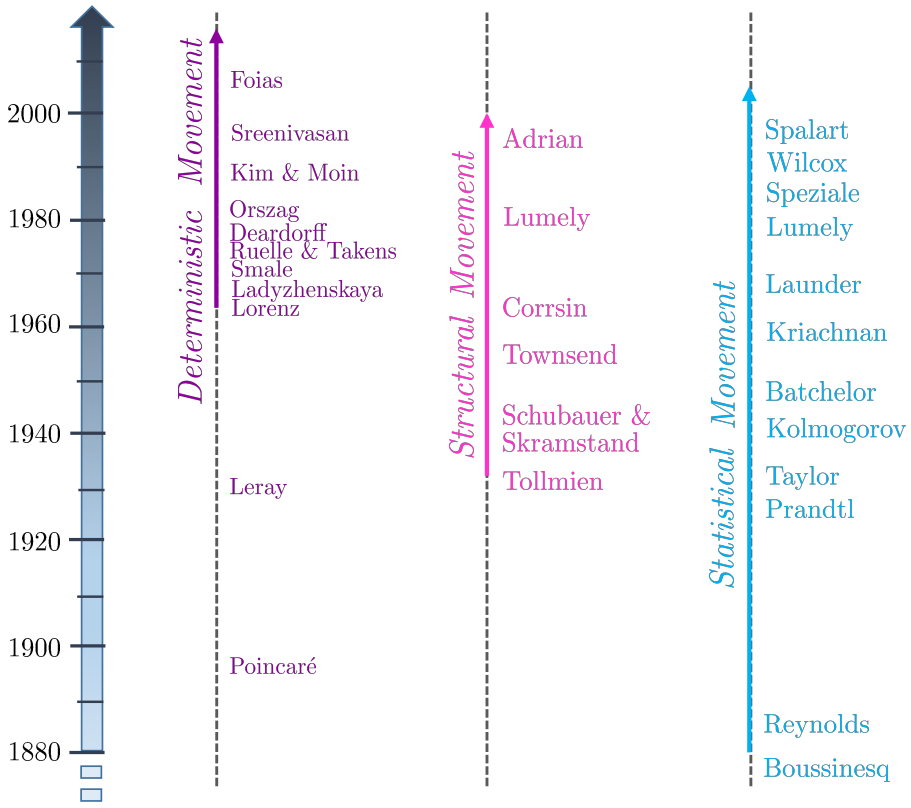

Figure 1.1: Movements in the study of turbulence

In the rest of this section we will talk about each era briefly, based on the above discussion.

1.F.1 Statistical approach

As we discussed earlier, the genesis of this influential approach is the seminal work of Reynolds 1883, which motivated many researchers to consider turbulence as a thoroughly random phenomenon. In spite of latter experiments showing the existence of *coherent structures*, which in turn contradicts the assumption of looking at turbulence as a fully random phenomenon, this approach has continued even up to the present time. Besides, many mathematical and statistical advances brought into the field have not been successful in reliably predicting the behaviour of turbulence. It is also somewhat paradoxical that researchers in this era expected to obtain a completely random solution from the deterministic Navier–Stokes equation. Taking the average of that equation to develop RANS models seems even worse: if turbulence is really a random phenomenon, perhaps one should look instead for a set of stochastic governing equations.

1.F.2 Structural movement

Chapman and Tobak considered the structural movement as beginning with the work of Schubauer & Skramstad [1947] and the observations of Tollmien–Schlicting waves in 1948. However, even the early experiment done by Reynolds indicated the existence of coherent structures and short bifurcation sequences. This structural movement led to a better understanding of the intrinsic structure of turbulence and cast severe doubt on the statistical approach that envisions

turbulence as a completely structureless phenomenon. While it is capable of describing the structures of turbulence, this movement suffered from the lack of a comprehensive theory.

1.F.3 Phenomenological approach

This era began with the breakthroughs of Kolmogorov in his famous K41 paper. Although this approach is still dependent on the statistical method, it is viewed as the first major departure from the completely random view of turbulence developed since the experiment of Reynolds. The work of Kraichnan, Leith, and Batchelor in 1967–1969 generalized Kolmogorov's ideas to the case of two-dimensional turbulence. Although this approach could not describe turbulence in detail, it was so successful and influential that it is still the main inspiration for much research in the field.

1.F.4 Modern deterministic approach

As Chapman and Tobak stated in their paper, the actual deterministic movement began with the work of Lorenz [1963] and, a bit later, Ruelle & Takens [1971]. However, as we mentioned above, even about 70 years before Lorenz's work, Poincaré & Magini [1899] initiated a new deterministic approach to study dynamical systems. The success of this approach led to a considerable amount of research up to the late 1980s, exactly when the community came to a conclusion about this new approach. They concluded that although the modern deterministic approach so far provides the best description of turbulence, it suffers from a lack of applicability due to limited computational resources. Consequently, none of the methods proposed in this area provides a successful

means for simulating turbulent flows, particularly the pseudospectral method, which unlikely will continue to be impractical for simulating high Reynolds number turbulence well into the mid-21st century.

A successful theory of turbulence will likely incorporate both the statistical and deterministic approaches. Even at the current time, LES can be viewed as a model that has arisen out of both deterministic and statistical approaches. In fact, while it is based on the deterministic governing equations, the subgrid modelling included in LES relies on statistical approaches. The combination of deterministic and statistical approaches is not the only ongoing activity, as there are recent attempts in proposing new subgrid models influenced by both the deterministic and structural perspectives. Figure 1.2 lists the most important subgrid scale models.

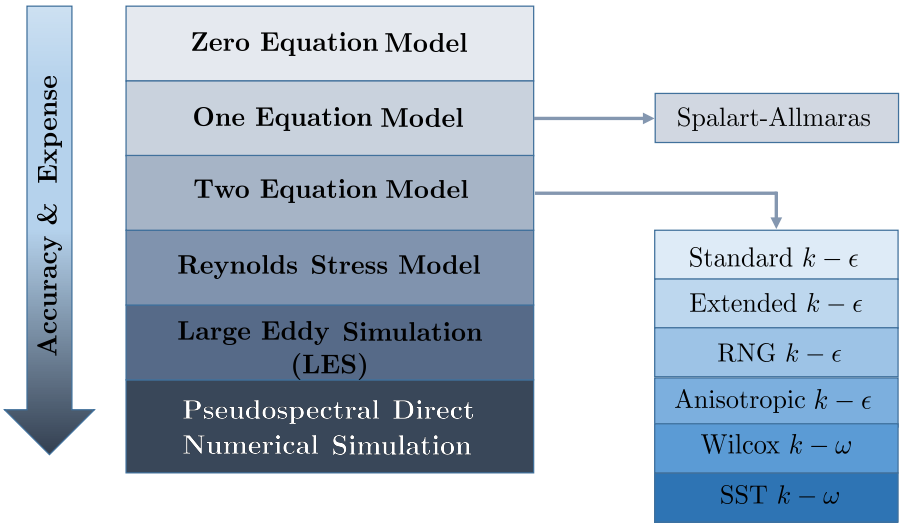

Figure 1.2: Subgrid scale models

Before delving into the main part of our research, it is important to talk briefly about our approach, which is essentially categorized under the class of deterministic movements. However, in addition to the dynamical system

methods used in almost all deterministic studies, here we follow the functional analysis approach adopted by Foias and Constantin in the early 21st century. This method applies functional analysis tools to obtain an alternative way of solving the closure problem instead of applying some concocted model. One might say that this new approach compared to the previous ways of treating the closure problem is analogous to the relation between the pseudospectral method and various LES models. In view of this analogy, this approach can be considered as the first systematic attempt to study turbulence on a firm mathematical basis, an outlook that I believe promises a detailed and rigorous understanding of turbulence in the near future.

Chapter 2

Energy and Enstrophy Relations on the Global Attractor of the 2D Navier–Stokes Equation: Constant Forcing

2.A Introduction

In this chapter we are going to study isotropic homogeneous turbulence for incompressible fluid flows using a functional analysis approach. We consider a governing equation that is a partial differential equation defined on a compact domain in $\mathbb{R}^3$. Regarding the discussion we had in the previous chapter about the difficulties of having a precise physical model for fluid flows using a statistical approach, and the paucity of our knowledge, it is still believed by the majority of researchers that the Navier–Stokes equation is the best available governing equation describing the behaviour of fluid flows. It is

derived by assuming the validity and applicability of the Newtonian fluid model and Stokes assumption. The fact that these fairly nonrestrictive assumptions lead to physically realistic simulations of *laminar* flows motivates us to apply the Navier–Stokes equation to turbulent flows too. This chapter is devoted to using functional analysis methods to obtain deeper knowledge about this equation in particular and turbulence in general.

2.B Definitions and preliminaries

One of the simplest contexts in which to pose the turbulence problem is 2D incompressible homogeneous isotropic turbulent flow in a bounded domain with periodic boundary conditions and no mean velocity and forcing. One close realization of this ideal form of turbulence in laboratories can be thought of a very thin layer of turbulent flow far down the stream of a flow passing over a net of wires. Looking at this ideal form of turbulence deterministically involves using the Navier–Stokes and continuity equations expressed as the following set of integro-differential equations:

$$\begin{aligned}
&\frac{\partial \boldsymbol{u}}{\partial t} - \nu \nabla^2 \boldsymbol{u} + \boldsymbol{u} \cdot \boldsymbol{\nabla} \boldsymbol{u} + \boldsymbol{\nabla}\left(\frac{p}{\rho}\right) = \boldsymbol{F}, \\
&\boldsymbol{\nabla} \cdot \boldsymbol{u} = 0, \\
&\int_\Omega \boldsymbol{u}\, d\boldsymbol{x} = \boldsymbol{0}, \qquad \int_\Omega \boldsymbol{F}\, d\boldsymbol{x} = \boldsymbol{0}, \\
&\boldsymbol{u}(\boldsymbol{x}, 0) = \boldsymbol{u}_0(\boldsymbol{x}),
\end{aligned}$$

with $\Omega = [0, 2\pi] \times [0, 2\pi]$ and periodic boundary conditions on $\partial\Omega$. This problem can be considered in a specific *Hilbert* space (H) with the standard

L^2 inner product

$$(\boldsymbol{u}, \boldsymbol{v}) = \int_\Omega \boldsymbol{u}(\boldsymbol{x}) \cdot \boldsymbol{v}(\boldsymbol{x})\, d\boldsymbol{x}, \quad \text{where} \quad \boldsymbol{a} \cdot \boldsymbol{b} = \sum_i a_i b_i.$$

That Hilbert space is defined as

$$H(\Omega) \doteq \mathrm{cl} \left\{ \boldsymbol{u} \in C^2(\Omega) \cap L^2(\Omega) \mid \boldsymbol{\nabla} \cdot \boldsymbol{u} = 0, \ \int_\Omega \boldsymbol{u}\, d\boldsymbol{x} = 0 \right\}, \tag{2.1}$$

(here $\doteq$ is used to emphasize a definition) with L^2 norm

$$|\boldsymbol{u}| = (\boldsymbol{u}, \boldsymbol{u})^{1/2} = \left(\int_\Omega \boldsymbol{u}(\boldsymbol{x}, t) \cdot \boldsymbol{u}(\boldsymbol{x}, t)\, d\boldsymbol{x} \right)^{1/2}.$$

For $\boldsymbol{u} \in H$, the above problem can be expressed as

$$\frac{d\boldsymbol{u}}{dt} - \nu \nabla^2 \boldsymbol{u} + \boldsymbol{u} \cdot \boldsymbol{\nabla} \boldsymbol{u} + \boldsymbol{\nabla} \left(\frac{p}{\rho} \right) = \boldsymbol{F}, \qquad \boldsymbol{u} \in H(\Omega). \tag{2.2}$$

Let $A \doteq -\mathcal{P}(\nabla^2)$, $\boldsymbol{f} \doteq \mathcal{P}(\boldsymbol{F})$, and define the *bilinear map*

$$\mathcal{B}(\boldsymbol{u}, \boldsymbol{u}) \doteq \mathcal{P} \left(\boldsymbol{u} \cdot \boldsymbol{\nabla} \boldsymbol{u} + \boldsymbol{\nabla} \left(\frac{p}{\rho} \right) \right),$$

where $\mathcal{P}$ is the *Helmholtz–Leray projection operator* to H:

$$\mathcal{P}(\boldsymbol{v}) = \boldsymbol{v} - \boldsymbol{\nabla} \nabla^{-2} \boldsymbol{\nabla} \cdot \boldsymbol{v}, \qquad \forall \boldsymbol{v} \in C^2(\Omega) \cap L^2(\Omega).$$

In terms of these definitions, (2.1) can be written more compactly as

$$\frac{d\boldsymbol{u}}{dt} + \nu A \boldsymbol{u} + \mathcal{B}(\boldsymbol{u}, \boldsymbol{u}) = \boldsymbol{f}. \tag{2.3}$$

2.C Stokes operator A

The operator $A = \mathcal{P}(-\nabla^2)$ is *positive-semidefinite* and *self-adjoint*, with a compact inverse whose eigenvalues for a periodic domain with length L in each direction are

$$\lambda = \left(\frac{2\pi}{L}\right)^2 \boldsymbol{k}\cdot\boldsymbol{k}, \qquad \boldsymbol{k} \in \mathbb{Z}\times\mathbb{Z}\backslash\{\boldsymbol{0}\},$$

and in the case of our domain

$$\lambda = \boldsymbol{k}\cdot\boldsymbol{k}, \qquad \boldsymbol{k} \in \mathbb{Z}\times\mathbb{Z}\backslash\{\boldsymbol{0}\}.$$

The eigenvalues of a positive-definite infinite-dimensional linear operator can be arranged as

$$0 < \lambda_0 < \lambda_1 < \lambda_2 < \cdots, \qquad \lambda_0 = \left(\frac{2\pi}{L}\right)^2$$

and their eigenvectors, $\boldsymbol{w}_i,\ i \in \mathbb{N}_0$, form an orthonormal basis for the Hilbert space H, upon which we can define any quotient power of A as:

$$A^\alpha \boldsymbol{w}_j = \lambda_j^\alpha \boldsymbol{w}_j, \qquad \alpha \in \mathbb{Q}, \quad j \in \mathbb{N}_0.$$

Having the above orthonormal basis, it is possible to define a new space $V^{2\alpha} \subset H$ as

$$V^{2\alpha} = D(A^\alpha) \doteq \left\{ \boldsymbol{u} \in H \mid \sum_{j=0}^{\infty} \lambda_j^{2\alpha} (\boldsymbol{u}, \boldsymbol{w}_j)^2 < \infty \right\}.$$

Among all possible values of α, we are especially interested in the space $V = V^{2(1/2)}$. The motivation comes from the definition of *enstrophy* (which we shall talk about it later on in this chapter), so V is defined to be

$$V = D(A^{1/2}) \doteq \left\{ \boldsymbol{u} \in H \mid \sum_{j=0}^{\infty} \lambda_j (\boldsymbol{u}, \boldsymbol{w}_j)^2 < \infty \right\}.$$

A suitable norm for the elements of V is

$$||\boldsymbol{u}|| = \left|A^{1/2}\right| = \left(\int_\Omega \sum_{i=1}^{2} \frac{\partial \boldsymbol{u}}{\partial x_i} \cdot \frac{\partial \boldsymbol{u}}{\partial x_i} \right)^{1/2} = \left(\sum_{j=0}^{\infty} \lambda_j (\boldsymbol{u}, \boldsymbol{w}_j)^2 \right)^{1/2}.$$

We will soon see that V is the subspace of H with elements possessing finite enstrophy.

2.D Fourier representation and Sobolev inequalities

In a periodic space, it is possible to represent the elements of H using a Fourier series:

$$\boldsymbol{u}(\boldsymbol{x}) = \frac{1}{\sqrt{2\pi}} \sum_{\boldsymbol{k} \in \mathbb{Z}^2} a_{\boldsymbol{k}} e^{i k_0 \boldsymbol{k} \cdot \boldsymbol{x}},$$

where

$k_0^2 = \lambda_0 = 1$	in our domain,
$a_0 = 0$,	because of no mean velocity,
$\boldsymbol{k} \cdot a_{\boldsymbol{k}} = 0$	by incompressibility, and
$a_{\boldsymbol{k}}^* = a_{-\boldsymbol{k}}$,	because $\boldsymbol{u}$ is a real-valued function.

By the *Parseval identity* we have

$$|\boldsymbol{u}|^2 = \sum_{\boldsymbol{k}\in\mathbb{Z}^2} a_{\boldsymbol{k}}\cdot a_{-\boldsymbol{k}} = \sum_{\boldsymbol{k}\in\mathbb{Z}^2} |a_{\boldsymbol{k}}|^2. \tag{2.4}$$

To work with the elements of H, we require some orthogonal projectors. For every $\boldsymbol{u} \in H$, we define

$$\begin{aligned} P_n &= \operatorname{span}\{\boldsymbol{w}_j \mid A\boldsymbol{w}_j = \lambda_j \boldsymbol{w}_j, j \le n\}, \\ Q_n &= I - P_n, \\ R_n &= P_n - P_{n-1}. \end{aligned}$$

It is essential to exploit properties of the bilinear map $\mathcal{B}$ such as incompressibility and periodicity, along with specific properties of the Stokes operator A. Here we only list the most important properties of that bilinear map and the reader who is interested in their proofs is referred to Appendix A for further details. Specifically, we will need *orthogonality in 3D*,

$$(\mathcal{B}(\boldsymbol{u},\boldsymbol{v}),\boldsymbol{w}) = -(\mathcal{B}(\boldsymbol{u},\boldsymbol{w}),\boldsymbol{v}),$$

orthogonality in 2D,

$$(\mathcal{B}(\boldsymbol{u},\boldsymbol{u}), A\boldsymbol{u}) = 0,$$

the *strong form of enstrophy invariance*,

$$(\mathcal{B}(A\boldsymbol{v},\boldsymbol{v}),\boldsymbol{u}) = (\mathcal{B}(\boldsymbol{u},\boldsymbol{v}), A\boldsymbol{v}),$$

and the *2D general identity*,

$$(\mathcal{B}(A\boldsymbol{u},\boldsymbol{u}),\boldsymbol{u})+(\mathcal{B}(\boldsymbol{v},A\boldsymbol{v}),\boldsymbol{u})+(\mathcal{B}(\boldsymbol{v},\boldsymbol{v}),A\boldsymbol{v})=0.$$

Finally, just before going to the next section, we state two important *Sobolev inequalities* that will be used in this and future work. These inequalities, whose relevant proofs and properties are explained in Appendix B, are called the *Agmon inequality* and the *Ladyzhenskaya inequality*:

$$|\boldsymbol{u}|_{L^\infty(\Omega)}\leq C_A|\boldsymbol{u}|^{1/2}|A\boldsymbol{u}|^{1/2}, \qquad \text{Agmon inequality,} \tag{2.5}$$

$$|\boldsymbol{u}|_{L^4(\Omega)}\leq C_L|\boldsymbol{u}|^{1/4}||\boldsymbol{u}||^{3/4}, \qquad \text{Ladyzhenskaya inequality,} \tag{2.6}$$

where the constants C_A and C_L depend only on the space.

2.E Nondimensional Navier–Stokes equation using the Grashof number

As the most important quantities are physical and dynamical, it is reasonable to choose the scales

$$L=\frac{1}{k_0},\quad T=\frac{1}{\nu {k_0}^2},\quad U=\nu k_0,\quad F=\nu^2 {k_0}^3.$$

Now considering the above scales, and denoting the original quantities with primes, the dimensionless quantities can be defined as

$$u = \frac{u'}{U} \Rightarrow u' = u\nu k_0, \qquad t = \frac{t'}{T} \Rightarrow t' = t\nu {k_0}^2, \qquad x = \frac{x'}{L} \Rightarrow x' = xk_0,$$
$$f = \frac{f'}{F} \Rightarrow f' = f\nu^2 {k_0}^3, \qquad \frac{p'}{\rho'} = \nu^2 k_0^3 \left(\frac{p}{\rho}\right), \qquad \boldsymbol{\nabla} = k_0 \boldsymbol{\nabla}'.$$

Using the above scaling, we can then rewrite the Navier–Stokes equation,

$$\frac{\partial \boldsymbol{u}'}{\partial t'} + \boldsymbol{u}' \boldsymbol{\cdot} \boldsymbol{\nabla}' \boldsymbol{u}' = -\boldsymbol{\nabla}' \left(\frac{p'}{\rho'}\right) + \nu \nabla'^2 \boldsymbol{u}' + \boldsymbol{f}', \tag{2.7}$$

as

$$\nu^2 {k_0}^3 \left(\frac{\partial \boldsymbol{u}}{\partial t}\right) + \nu^2 {k_0}^3 \left[u \boldsymbol{\cdot} \boldsymbol{\nabla} \boldsymbol{u} + \boldsymbol{\nabla} \left(\frac{p}{\rho}\right)\right] = \nu^2 {k_0}^3 \nabla^2 \boldsymbol{u} + \nu^2 {k_0}^3 \boldsymbol{f}. \tag{2.8}$$

On taking the incompressibility condition into account, it is possible to represent the pressure gradient in terms of the inertial term using the *Helmholtz–Leray projection operator*:

$$\mathcal{B}(\boldsymbol{u}, \boldsymbol{u}) = \mathcal{P}(\boldsymbol{u} \boldsymbol{\cdot} \boldsymbol{\nabla} \boldsymbol{u}).$$

Thus, regardless of the values of ν and k_0, we will obtain the following dimensionless equation:

$$\frac{\partial \boldsymbol{u}}{\partial t} + \mathcal{B}(\boldsymbol{u}, \boldsymbol{u}) = \nabla^2 \boldsymbol{u} + \boldsymbol{f}. \tag{2.9}$$

On defining the dimensionless *Grashof number*,

$$G = \frac{|\boldsymbol{f}|}{\nu^2 {k_0}^2}, \tag{2.10}$$

it is convenient to introduce the normalized velocity $\boldsymbol{v} \doteq \boldsymbol{u}/G$:

$$G\frac{\partial \boldsymbol{v}}{\partial t} + G^2\mathcal{B}(\boldsymbol{v},\boldsymbol{v}) = G\nabla^2\boldsymbol{v} + \boldsymbol{f}. \tag{2.11}$$

Dividing the both sides of (2.11) by G and denoting $h \doteq \dfrac{\boldsymbol{f}}{G}$, we obtain

$$\frac{\partial \boldsymbol{v}}{\partial t} + G\mathcal{B}(\boldsymbol{v},\boldsymbol{v}) = \nabla^2\boldsymbol{v} + \boldsymbol{h}. \tag{2.12}$$

It is now obvious that without loss of generality, it is possible to take

$$k_0 = 1, \quad \nu = 1.$$

With these values, we see that $G = |\boldsymbol{f}|$, and hence $|\boldsymbol{h}| = 1$.

2.F The Navier–Stokes equation as a dynamical system

Before considering the dynamical behaviour of the Navier–Stokes equation using functional analysis tools, we need to define certain global flow quantities known as the energy, enstrophy, and palinstrophy:

$$\begin{aligned}
E &= \frac{1}{2}|\boldsymbol{u}(t)|^2 && \text{energy,}\\
Z &= \frac{1}{2}\left|A^{1/2}\boldsymbol{u}(t)\right|^2 = \frac{1}{2}||\boldsymbol{u}(t)||^2 && \text{enstrophy,}\\
P &= \frac{1}{2}|A\boldsymbol{u}(t)|^2 && \text{palinstrophy.}
\end{aligned}$$

Just as energy is proportional to the mean-squared velocity, enstrophy is proportional to the mean-squared vorticity and therefore provides a measure of the rotational energy in a flow. It is easily shown that the rate at which energy is dissipated is proportional to the enstrophy. Likewise, the enstrophy is dissipated at a rate proportional to the palinstrophy.

We begin with the incompressible Navier–Stokes equation, given periodic boundary conditions:

$$\frac{\partial \boldsymbol{u}}{\partial t} + \nu A\boldsymbol{u} + \mathcal{B}(\boldsymbol{u}, \boldsymbol{u}) = \boldsymbol{f}, \qquad u \in H. \tag{2.13}$$

Taking the inner product of $\boldsymbol{u}$ (respectively $A\boldsymbol{u}$) with the above equation, we find

$$\frac{1}{2}\frac{d}{dt}|\boldsymbol{u}(t)|^2 + \nu||\boldsymbol{u}(t)||^2 = (\boldsymbol{f}, \boldsymbol{u}(t)), \tag{2.14}$$

$$\frac{1}{2}\frac{d}{dt}||\boldsymbol{u}(t)||^2 + \nu|A\boldsymbol{u}(t)|^2 = (\boldsymbol{f}, A\boldsymbol{u}(t)). \tag{2.15}$$

Applying the *Cauchy–Schwarz inequality* and *Poincaré inequality*, we obtain

$$\text{Cauchy–Schwarz} : (\boldsymbol{f}, \boldsymbol{u}(t)) \leq |\boldsymbol{f}||\boldsymbol{u}(t)|,$$

$$\text{Poincaré} : \quad k_0^2|\boldsymbol{u}(t)| \leq ||\boldsymbol{u}(t)||,$$

leading to

$$-\nu||\boldsymbol{u}||^2 \geq -\nu k_0^2|\boldsymbol{u}|^2.$$

Thus, (2.14) can be written as

$$\frac{d}{dt}|\boldsymbol{u}(t)|^2 \leq -2\nu k_0^2|\boldsymbol{u}(t)|^2 + 2|\boldsymbol{f}|\,|\boldsymbol{u}(t)|. \tag{2.16}$$

Simplifying the above equation will yield

$$\frac{d}{dt}|\boldsymbol{u}(t)| \leq -\nu k_0^2 |\boldsymbol{u}(t)| + |\boldsymbol{f}|, \tag{2.17}$$

which is a first-order differential inequality. If $\boldsymbol{f}$ is constant in time, we can solve the corresponding differential equation obtained by replacing the inequality with an equality to obtain

$$|\boldsymbol{u}(t)| = e^{-\nu k_0^2 t}|\boldsymbol{u}(0)| + \left(\frac{1 - e^{-\nu k_0^2 t}}{\nu k_0^2}\right)|\boldsymbol{f}|.$$

Applying a *Gronwall inequality* to (2.17), we thus find

$$|\boldsymbol{u}(t)| \leq e^{-\nu k_0^2 t}|\boldsymbol{u}(0)| + \left(\frac{1 - e^{-\nu k_0^2 t}}{\nu k_0^2}\right)|\boldsymbol{f}|. \tag{2.18}$$

Now, taking $\alpha \doteq e^{-\nu k_0^2 t}$ and $\beta \doteq \dfrac{|\boldsymbol{f}|}{\nu k_0^2}$, (2.18) can be expressed as

$$|\boldsymbol{u}(t)| \leq \alpha|\boldsymbol{u}(0)| + (1 - \alpha)\beta,$$

which is a segment connecting $|\boldsymbol{u}(0)|$ and β. On squaring both sides and exploiting convexity, we obtain

$$|\boldsymbol{u}(t)|^2 \leq \alpha|\boldsymbol{u}(0)|^2 + (1 - \alpha)\beta^2.$$

Thus we arrive at the following result:

$$|\boldsymbol{u}(t)|^2 \leq e^{-\nu k_0^2 t}|\boldsymbol{u}(0)|^2 + (1 - e^{-\nu k_0^2 t})\left(\frac{|\boldsymbol{f}|}{\nu k_0^2}\right)^2. \tag{2.19}$$

Using the Grashof number, (2.19) can be simplified to

$$|\boldsymbol{u}(t)|^2 \leq e^{-\nu k_0^2 t}|\boldsymbol{u}(0)|^2 + (1 - e^{-\nu k_0^2 t})\nu^2 G^2. \tag{2.20}$$

Applying the same argument to (2.15) will result in the following estimation for $||\boldsymbol{u}(t)||$:

$$||\boldsymbol{u}(t)||^2 \leq e^{-\nu k_0^2 t}||\boldsymbol{u}(0)||^2 + (1 - e^{-\nu k_0^2 t})\nu^2 k_0^2 G^2. \tag{2.21}$$

From (2.21), it can be observed that the closed ball $\mathfrak{B}$ of radius $\nu k_0 G$ in the space V is a bounded absorbing set [Dascaliuc *et al.* 2005]. If we take S to be the solution operator for (2.13) defined by

$$S(t)\boldsymbol{u}_0 = \boldsymbol{u}(t), \qquad \boldsymbol{u}_0 = \boldsymbol{u}(0),$$

where $\boldsymbol{u}(t)$ is the unique solution of (2.13), then by the definition of the absorbing set for the solution of a dynamical system, for any bounded set $\mathfrak{B}'$, there would be a time t_0 such that

$$t_0 = t_0(\mathfrak{B}'), \quad \text{and} \quad S(t)\mathfrak{B}' \subset \mathfrak{B}, \quad \forall t \geq t_0.$$

The global attractor $\mathcal{A}$ is then defined by

$$\mathcal{A} = \bigcap_{t \geq 0} S(t)\mathfrak{B}, \tag{2.22}$$

so $\mathcal{A}$ is the largest bounded, invariant set such that $S(t)\mathcal{A} = \mathcal{A}$ for all $t \geq 0$. Taking into account the definition of a global attractor and the existence of

a closed bounded absorbing set in $V \subset H$, an immediate observation from (2.20) and (2.21) shows that being on the attractor requires the following two conditions:

$$|\boldsymbol{u}| \leq \nu G, \tag{2.23}$$

$$||\boldsymbol{u}|| \leq \nu k_0 G. \tag{2.24}$$

The above observation leads to a suitable normalization for the energy and enstrophy that we use later on for finding bounds in the Z–E plane.

Remark. *The above bounds assure us that on the attractor both the energy and enstrophy are bounded.*

2.G Further estimations using the Navier–Stokes equation

Now that we have obtained the attractor of the Navier–Stokes equation for energy and enstrophy, it is time to proceed to find other useful estimates using the Navier–Stokes equation, together with the bilinear map identities, *Sobolev inequalities*, and other properties of the Stokes operator. These estimations will be used latter on when we want to prove the existence of some specific solutions on the attractor, which will help us find useful bounds on the region where the attractor lives. Beginning with the Navier–Stokes equation

$$\frac{\partial \boldsymbol{u}}{\partial t} + \nu A\boldsymbol{u} + \mathcal{B}(\boldsymbol{u}, \boldsymbol{u}) = \boldsymbol{f},$$

we take its inner product with a general term $A^j\boldsymbol{u}$ to obtain generalized forms for dynamical estimates of the form $\left|A^{j/2}\boldsymbol{u}\right|$. The main motivation for finding such estimates comes from the fact that some of these terms for specific values of j correspond to meaningful and important physical quantities like energy and enstrophy. Taking the inner product, we will obtain

$$\begin{aligned}
&\left(\frac{\partial \boldsymbol{u}}{\partial t}, A^j\boldsymbol{u}\right) + \nu(A\boldsymbol{u}, A^j\boldsymbol{u}) + (\mathcal{B}(\boldsymbol{u},\boldsymbol{u}), A^j\boldsymbol{u}) = (\boldsymbol{f}, A^j\boldsymbol{u}) \Rightarrow \\
&\frac{1}{2}\frac{d}{dt}(A^{j/2}\boldsymbol{u}, A^{j/2}\boldsymbol{u})^2 + \nu(A^{j/2}\boldsymbol{u}, A^{j/2+1}\boldsymbol{u}) + (\mathcal{B}(\boldsymbol{u},\boldsymbol{u}), A^j\boldsymbol{u}) = (A^{j/2}\boldsymbol{f}, A^{j/2}\boldsymbol{u}) \Rightarrow \\
&\frac{1}{2}\frac{d}{dt}\left|A^{j/2}\boldsymbol{u}\right|^2 + \nu(A^{j/2}\boldsymbol{u}, A^{j/2+1}\boldsymbol{u}) + (\mathcal{B}(\boldsymbol{u},\boldsymbol{u}), A^j\boldsymbol{u}) = (A^{j/2}\boldsymbol{f}, A^{j/2}\boldsymbol{u}) \qquad (2.25)
\end{aligned}$$

The above result is meaningful as long as $\left|A^{j/2}\boldsymbol{f}\right|$ exists. This means that $\boldsymbol{f}$ has to be in $D(A^{j/2})$, and so to obtain useful estimates out of (2.25), we need to assume that $\boldsymbol{f} \in D(A^{j/2})$. Having this assumption, for a general $\boldsymbol{f} \in D(A^{j/2})$ ($\boldsymbol{f}$ does not need to be an eigenvector of the operator A), we can define a *generalized eigenvalue* of $\boldsymbol{f}$:

$$\Lambda_j = \frac{\left|A^{j/2}\boldsymbol{f}\right|^2}{\lambda_0^j|\boldsymbol{f}|^2} = \frac{\left|A^{j/2}\boldsymbol{f}\right|^2}{k_0^{2j}|\boldsymbol{f}|^2}.$$

2.G.1 Estimate obtained for $j = 0$

For $j = 0$ we have

$$\frac{1}{2}\frac{d}{dt}|\boldsymbol{u}|^2 + \nu(A\boldsymbol{u}, \boldsymbol{u}) + (\mathcal{B}(\boldsymbol{u},\boldsymbol{u}), \boldsymbol{u}) = (\boldsymbol{f}, \boldsymbol{u}).$$

Having $(\mathcal{B}(\boldsymbol{u},\boldsymbol{u}),\boldsymbol{u}) = 0$ and using the Cauchy–Schwarz inequality for the right-hand side, we obtain

$$\frac{1}{2}\frac{d}{dt}|\boldsymbol{u}|^2 + \nu(A^{1/2}\boldsymbol{u}, A^{1/2}\boldsymbol{u}) \leq |\boldsymbol{f}|\,|\boldsymbol{u}|,$$

or equivalently

$$\frac{1}{2}\frac{d}{dt}|\boldsymbol{u}|^2 + \nu\left|A^{1/2}\boldsymbol{u}\right|^2 \leq |\boldsymbol{f}|\,|\boldsymbol{u}|,$$

where in our norm notation we would have

$$\frac{1}{2}\frac{d}{dt}|\boldsymbol{u}|^2 + \nu||\boldsymbol{u}||^2 \leq |\boldsymbol{f}|\,|\boldsymbol{u}|. \tag{2.26}$$

We observe that this is the same estimate that we found in the previous section for the energy.

2.G.2 Estimate obtained for $j = 1$

For $j = 1$ we have

$$\frac{1}{2}\frac{d}{dt}\left|A^{1/2}\boldsymbol{u}\right|^2 + \nu(A^{1/2}\boldsymbol{u}, A^{3/2}\boldsymbol{u}) + (\mathcal{B}(\boldsymbol{u},\boldsymbol{u}), A\boldsymbol{u}) = (\boldsymbol{f}, A\boldsymbol{u}).$$

This case can lead to different estimates, depending on the use of the self-adjoint property of the Stokes operator A.

Case I

The first one can be obtained using the self-adjoint property, such that $\boldsymbol{f}$ appears on the right-hand side without any factor of $A^{1/2}$. This case can be

expressed as

$$\frac{1}{2}\frac{d}{dt}\left|A^{1/2}\boldsymbol{u}\right|^2+\nu(A^{1/2}\boldsymbol{u},A^{3/2}\boldsymbol{u})+(\mathcal{B}(\boldsymbol{u},\boldsymbol{u}),A\boldsymbol{u})=(\boldsymbol{f},A\boldsymbol{u}).$$

Having $(\mathcal{B}(\boldsymbol{u},\boldsymbol{u}),A\boldsymbol{u})=0$ and using the Cauchy–Schwarz inequality for the right-hand side, we will obtain

$$\frac{1}{2}\frac{d}{dt}\left|A^{1/2}\boldsymbol{u}\right|^2+\nu(A^{1/2}\boldsymbol{u},A^{3/2}\boldsymbol{u})\leq|\boldsymbol{f}|\,|A\boldsymbol{u}|.$$

Using the self-adjoint property one more time for the term $\nu(A^{1/2}\boldsymbol{u},A^{3/2}\boldsymbol{u})$, we obtain

$$\frac{1}{2}\frac{d}{dt}\left|A^{1/2}\boldsymbol{u}\right|^2+\nu|A\boldsymbol{u}|^2\leq|\boldsymbol{f}|\,|A\boldsymbol{u}|,$$

where in our norm notation we would have

$$\frac{1}{2}\frac{d}{dt}||\boldsymbol{u}||^2+\nu|A\boldsymbol{u}|^2\leq|\boldsymbol{f}|\,|A\boldsymbol{u}|. \tag{2.27}$$

Again the reader may observe that this is the same estimate that we obtained in the previous section for the enstrophy. In fact this equation can be used as an alternative way to obtain the upper bound for enstrophy. This alternative method is given in the following lemma, but before getting into the lemma, we need to talk about some observations. The fact that (2.23) implies boundedness of $\boldsymbol{u}$ for all $t\in[0,\infty)$, in view of the compactness of the attractor $\mathcal{A}$ and the completeness of H, leads to some useful results.

The first result is

$$\forall\boldsymbol{u}\in\mathcal{A},\ \exists t_0(\boldsymbol{u})\text{ such that }\sup_t|\boldsymbol{u}(t)|=|\boldsymbol{u}(t_0)|.$$

The second result is obtained using the compactness of $\mathcal{A}$. Since each solution $\boldsymbol{u} \in \mathcal{A}$ attains its maximum at some t, the compactness of $\mathcal{A}$ ensures that $\tilde{\boldsymbol{u}}(\tilde{t}) \doteq \sup_{\boldsymbol{u}}\{\sup_t |\boldsymbol{u}(t)|, \boldsymbol{u} \in \mathcal{A}\}$ is well-defined, which implies

$$|\boldsymbol{u}(t)| \leq \left|\tilde{\boldsymbol{u}}(\tilde{t})\right|, \quad \forall \boldsymbol{u} \in \mathcal{A}, \forall t \geq 0. \tag{2.28}$$

A similar argument for enstrophy leads to

$$||\boldsymbol{u}(t)|| \leq ||\tilde{\boldsymbol{u}}(\tilde{t})||, \quad \forall \boldsymbol{u} \in \mathcal{A}, \forall t \geq 0. \tag{2.29}$$

Having the above results, we are prepared to make use of them in the following lemma.

Lemma 1. *If $\boldsymbol{f}$ is constant with respect to time, then for any $\boldsymbol{u} \in \mathcal{A}$*

$$|\boldsymbol{u}| \leq \nu G, \tag{$\boldsymbol{a}$}$$

$$||\boldsymbol{u}|| \leq \nu k_0 G. \tag{$\boldsymbol{b}$}$$

Proof.

($\boldsymbol{a}$) *Let $\tilde{\boldsymbol{u}}(\tilde{t})$ be the solution that maximizes energy. So because $|\boldsymbol{u}|^2$ is an analytic function of t, we expect to have*

$$\frac{d}{dt}|\tilde{\boldsymbol{u}}|^2\Big|_{t=\tilde{t}} = 0 \overset{(2.26)}{\Rightarrow} ||\tilde{\boldsymbol{u}}(\tilde{t})||^2 \leq \frac{|\boldsymbol{f}|\left|\tilde{\boldsymbol{u}}(\tilde{t})\right|}{\nu}.$$

Using the Poincaré inequality yields

$$k_0^2\big|\tilde{\boldsymbol{u}}(\tilde{t})\big|^2 \le ||\tilde{\boldsymbol{u}}(\tilde{t})||^2 \le \frac{|\boldsymbol{f}|\big|\tilde{\boldsymbol{u}}(\tilde{t})\big|}{\nu}$$
$$\Rightarrow \big|\tilde{\boldsymbol{u}}(\tilde{t})\big| \le \frac{|\boldsymbol{f}|}{k_0^2\nu}.$$

So by (2.28) and the definition of the Grashof number, we find

$$|\boldsymbol{u}(t)| \le \big|\tilde{\boldsymbol{u}}(\tilde{t})\big| \le \frac{|\boldsymbol{f}|}{k_0^2\nu} = G\nu, \quad \forall t.$$

(*b*) *Similar to part* **(*a*)**, *let* $\tilde{\boldsymbol{u}}(\tilde{t})$ *be the solution that maximizes enstrophy. Because* $||\boldsymbol{u}||^2$ *is an analytic function of* t, *we expect to have*

$$\frac{d}{dt}||\tilde{\boldsymbol{u}}||^2\Big|_{t=\tilde{t}} = 0 \overset{(2.27)}{\Rightarrow} \big|A\tilde{\boldsymbol{u}}(\tilde{t})\big| \le \frac{|\boldsymbol{f}|}{\nu}.$$

On the other hand,

$$||\boldsymbol{u}||^2 = \int_\Omega A^{1/2}\boldsymbol{u}\cdot A^{1/2}\boldsymbol{u}\,d\boldsymbol{x} = \int_\Omega \boldsymbol{u}\cdot A\boldsymbol{u}\,d\boldsymbol{x} \le \int_\Omega |\boldsymbol{u}\cdot A\boldsymbol{u}|\,d\boldsymbol{x}$$
$$\overset{\text{Cauchy-Schwarz}}{\le} \left(\int_\Omega |\boldsymbol{u}|^2\,d\boldsymbol{x}\right)^{1/2}\left(\int_\Omega |A\boldsymbol{u}|^2\,d\boldsymbol{x}\right)^{1/2} = |\boldsymbol{u}|\,|A\boldsymbol{u}|.$$

So in view of (2.29) we would have

$$||\boldsymbol{u}(t)||^2 \le ||\tilde{\boldsymbol{u}}(\tilde{t})||^2 \le \big|\tilde{\boldsymbol{u}}(\tilde{t})\big|\big|A\tilde{\boldsymbol{u}}(\tilde{t})\big| = \big|\tilde{\boldsymbol{u}}(\tilde{t})\big|\frac{|\boldsymbol{f}|}{\nu} \le G|\boldsymbol{f}| = \nu^2 k_0^2 G^2, \quad \forall t.$$

■

Case II

In this case, we try to retain the term $A^{1/2}\boldsymbol{f}$ on the right-hand side:

$$\frac{1}{2}\frac{d}{dt}\left|A^{1/2}\boldsymbol{u}\right|^2 + \nu(A^{1/2}\boldsymbol{u}, A^{3/2}\boldsymbol{u}) + (\mathcal{B}(\boldsymbol{u},\boldsymbol{u}), A\boldsymbol{u}) = (A^{1/2}\boldsymbol{f}, A^{1/2}\boldsymbol{u}).$$

Applying the same argument as used for **Case I**, we obtain

$$\frac{1}{2}\frac{d}{dt}||\boldsymbol{u}||^2 + \nu|A\boldsymbol{u}|^2 \leq \left|A^{1/2}\boldsymbol{f}\right| ||\boldsymbol{u}||.$$

Using the definition of a *generalized eigenvalue*, the above equation can be written as

$$\frac{1}{2}\frac{d}{dt}||\boldsymbol{u}||^2 + \nu|A\boldsymbol{u}|^2 \leq k_0\Lambda_1^{1/2}|\boldsymbol{f}| \, ||\boldsymbol{u}||,$$

using the Grashof number, the final form of our estimate for **Case II** would be

$$\frac{1}{2}\frac{d}{dt}||\boldsymbol{u}||^2 + \nu|A\boldsymbol{u}|^2 \leq G\nu^2 k_0^3\Lambda_1^{1/2}||\boldsymbol{u}||. \tag{2.30}$$

However, the above equation does not yield a sharper upper bound than what we have already obtained.

2.G.3 Estimate obtained for $j = 2$

This estimation is really important as it includes a new term involving the bilinear map that cannot be simplified using any of the identities that we have proven for the bilinear map in Appendix A. As a result, we need to estimate this new term in a separate manner, following section 1.E of Appendix A.

For $j = 2$, using (2.25) leads to

$$\frac{1}{2}\frac{d}{dt}|A\boldsymbol{u}|^2 + \nu(A\boldsymbol{u}, A^{5/2}\boldsymbol{u}) + (\mathcal{B}(\boldsymbol{u},\boldsymbol{u}), A^2\boldsymbol{u}) = (A\boldsymbol{f}, A\boldsymbol{u}),$$

where the self-adjoint property yields

$$\frac{1}{2}\frac{d}{dt}|A\boldsymbol{u}|^2 + \nu(A^{3/2}\boldsymbol{u}, A^{3/2}\boldsymbol{u}) + (\mathcal{B}(\boldsymbol{u},\boldsymbol{u}), A^2\boldsymbol{u}) = (A\boldsymbol{f}, A\boldsymbol{u}).$$

On the other hand the self-adjoint property for the bilinear and forcing terms yields

$$\begin{aligned}(\mathcal{B}(\boldsymbol{u},\boldsymbol{u}), A^2\boldsymbol{u}) &= -(\mathcal{B}(A\boldsymbol{u},\boldsymbol{u}), A\boldsymbol{u}),\\ (A\boldsymbol{f}, A\boldsymbol{u}) &= (A^{1/2}\boldsymbol{f}, A^{3/2}\boldsymbol{u}).\end{aligned}$$

Thus, we can write

$$\frac{1}{2}\frac{d}{dt}|A\boldsymbol{u}|^2 + \nu(A^{3/2}\boldsymbol{u}, A^{3/2}\boldsymbol{u}) - (\mathcal{B}(A\boldsymbol{u},\boldsymbol{u}), A\boldsymbol{u}) = (A^{1/2}\boldsymbol{f}, A^{3/2}\boldsymbol{u}).$$

Now, using the estimate (A.15) for the term containing the bilinear map derived in Appendix A, we obtain

$$\begin{aligned}\frac{1}{2}\frac{d}{dt}|A\boldsymbol{u}|^2 + \nu\left|A^{3/2}\boldsymbol{u}\right| &= (A^{1/2}\boldsymbol{f}, A^{3/2}\boldsymbol{u}) + (\mathcal{B}(A\boldsymbol{u},\boldsymbol{u}), A\boldsymbol{u})\\ &\le \left|(A^{1/2}\boldsymbol{f}, A^{3/2}\boldsymbol{u})\right| + |(\mathcal{B}(A\boldsymbol{u},\boldsymbol{u}), A\boldsymbol{u})|\\ &\le \left|A^{1/2}\boldsymbol{f}\right|^{1/2}\left|A^{3/2}\boldsymbol{u}\right|^{1/2} + c_L|A\boldsymbol{u}|\left|A^{1/2}\boldsymbol{u}\right|\left|A^{3/2}\boldsymbol{u}\right|,\end{aligned}$$

where in our norm notation,

$$\frac{1}{2}\frac{d}{dt}|A\boldsymbol{u}|^2 + \nu\left|A^{3/2}\boldsymbol{u}\right|^2 \leq ||\boldsymbol{f}||\left|A^{3/2}\boldsymbol{u}\right| + c_L||\boldsymbol{u}||\,|A\boldsymbol{u}|\left|A^{3/2}\boldsymbol{u}\right|.$$

Using the definition of a generalized eigenvalue, we find

$$\frac{1}{2}\frac{d}{dt}|A\boldsymbol{u}|^2 + \nu\left|A^{3/2}\boldsymbol{u}\right|^2 \leq G\nu^2 k_0^3 \Lambda_1^{1/2}\left|A^{3/2}\boldsymbol{u}\right|^{1/2} + c_L||\boldsymbol{u}||\,|A\boldsymbol{u}|\left|A^{3/2}\boldsymbol{u}\right|. \quad (2.31)$$

An argument similar to the one used to obtain (2.30) can be applied to the solution $\tilde{\boldsymbol{u}}$ that maximizes palinstrophy. Again because palinstrophy is an analytic function of t, we expect

$$\frac{d}{dt}|A\tilde{\boldsymbol{u}}(t)|^2\Big|_{t=\tilde{t}} = 0,$$

from which we see that

$$\begin{aligned}
&\nu\left|A^{3/2}\tilde{\boldsymbol{u}}\right|^2 \leq G\nu^2 k_0^3 \Lambda_1^{1/2}\left|A^{3/2}\tilde{\boldsymbol{u}}\right| + c_L\,|A\tilde{\boldsymbol{u}}|\,||\tilde{\boldsymbol{u}}||\left|A^{3/2}\tilde{\boldsymbol{u}}\right| \Rightarrow \\
&\nu\left|A^{3/2}\tilde{\boldsymbol{u}}\right| \leq G\nu^2 k_0^3 \Lambda_1^{1/2} + c_L\,||\tilde{\boldsymbol{u}}||\,|A\tilde{\boldsymbol{u}}| \overset{||\tilde{\boldsymbol{u}}|| \leq G\nu k_0}{\Rightarrow} \\
&\nu\left|A^{3/2}\tilde{\boldsymbol{u}}\right| \leq G\nu^2 k_0^3 \Lambda_1^{1/2} + c_L G\nu k_0 |A\tilde{\boldsymbol{u}}|.
\end{aligned}$$

On the other hand, we have

$$\begin{aligned}
|A\boldsymbol{u}|^2 &= \int_\Omega A\boldsymbol{u}\cdot A\boldsymbol{u}\,d\boldsymbol{x} = \int_\Omega A^{1/2}\boldsymbol{u}\cdot A^{3/2}\boldsymbol{u}\,d\boldsymbol{x} \leq \int_\Omega \left|A^{1/2}\boldsymbol{u}\cdot A^{3/2}\boldsymbol{u}\right| d\boldsymbol{x} \\
&\overset{\text{Cauchy-Schwarz}}{\leq} \left(\int_\Omega \left|A^{1/2}\boldsymbol{u}\right|^2 d\boldsymbol{x}\right)^{1/2}\left(\int_\Omega \left|A^{3/2}\boldsymbol{u}\right|^2 d\boldsymbol{x}\right)^{1/2} \\
&\leq ||\boldsymbol{u}||\left|A^{3/2}\boldsymbol{u}\right|, \qquad \forall \boldsymbol{u} \in \mathcal{A}.
\end{aligned}$$

So, for all $\boldsymbol{u} \in \mathcal{A}$, we will obtain

$$|A\boldsymbol{u}|^2 \leq ||\boldsymbol{u}|| \left|A^{3/2}\boldsymbol{u}\right| \Rightarrow |A\tilde{\boldsymbol{u}}|^2 \leq ||\tilde{\boldsymbol{u}}|| \left|A^{3/2}\tilde{\boldsymbol{u}}\right| \overset{||\tilde{\boldsymbol{u}}|| \leq G\nu k_0}{\Rightarrow}$$
$$\nu|A\tilde{\boldsymbol{u}}|^2 \leq G^2\nu^3 k_0^4 \Lambda_1^{1/2} + c_L G^2 \nu^2 k_0^2 |A\tilde{\boldsymbol{u}}|.$$

Using the *Young inequality* for the rightmost term yields

$$\nu|A\tilde{\boldsymbol{u}}|^2 \leq G^2\nu^3 k_0^4 \Lambda_1^{1/2} + \frac{1}{2\nu}(c_L G^2 \nu^2 k_0^2)^2 |A\tilde{\boldsymbol{u}}|^2 \Rightarrow$$
$$\frac{\nu}{2}|A\tilde{\boldsymbol{u}}|^2 \leq G^2\nu^3 k_0^4 \Lambda_1^{1/2} + \frac{1}{2\nu} c_L^2 (G\nu k_0)^4.$$

In addition, we know that

$$|A\boldsymbol{u}|^2 \leq |A\tilde{\boldsymbol{u}}|^2 \leq ||\tilde{\boldsymbol{u}}|| \left|A^{3/2}\tilde{\boldsymbol{u}}\right|, \qquad \forall \boldsymbol{u} \in \mathcal{A},$$

so we can write

$$\begin{aligned} |A\boldsymbol{u}|^2 \leq |A\tilde{\boldsymbol{u}}|^2 &\leq 2G^2\nu^2 k_0^4 \Lambda_1^{1/2} + c_L^2 G^4 \nu^2 k_0^4 \\ &\leq G^2\nu^2 k_0^4 \underbrace{(c_L^2 G^2 + 2\Lambda_1^{1/2})}_{\Gamma_0} = G^2\nu^2 k_0^4 \Gamma_0. \end{aligned}$$

This proves the following theorem of Dascaliuc *et al.* [2005].

Theorem 1. *If $f \in D(A^{1/2})$ then for all $\boldsymbol{u} \in \mathcal{A}$ we have*

$$|A\boldsymbol{u}|^2 \leq G^2\nu^2 k_0^4 \Gamma_0,$$

where $\Gamma_0 = c_L^2 G^2 + 2\Lambda_1^{1/2}$.

Similarly, Dascaliuc *et al.* [2005] proved

Theorem 2. *If $f \in D(A)$ then for all $\boldsymbol{u} \in \mathcal{A}$ we have*

$$\left|A^{3/2}\boldsymbol{u}\right|^2 \leq G^2\nu^2 k_0^6 \Gamma_1,$$

where $\Gamma_1 = 2(\Lambda_2^{1/2}\Gamma_0^{1/2} 2c_L^2 G^2 \Gamma_0)$.

2.H Relation between Z and E

Now that we have some useful estimates for terms of the form $A^{j/2}\boldsymbol{u}$, we can go further and find useful relations between Z and E. First, it is will helpful to introduce a new quantity and a related theorem.

Definition. *For all $\boldsymbol{u} \in \mathcal{A}\backslash\{\mathbf{0}\} \cap V\backslash\{\mathbf{0}\}$, let*

$$\chi(\boldsymbol{u}) = \frac{||\boldsymbol{u}||^2}{|\boldsymbol{u}|} = \frac{2Z}{\sqrt{2E}}.$$

Theorem 3. *The quotient $\chi(\boldsymbol{u})$ attains its absolute maximum on $\mathcal{A}\backslash\{\mathbf{0}\}$. Moreover, if $\mathbf{0} \in \mathcal{A}$, then*

$$\chi(\boldsymbol{u}) \leq \nu^{2/3} k_0^2 G^{2/3} \Gamma_1^{1/3} |\boldsymbol{u}|^{1/3}, \quad \boldsymbol{u} \in \mathcal{A}\backslash\{\mathbf{0}\},$$

where Γ_1 is given in Theorem 2.

Proof. *See Dascaliuc et al. [2005].* ■

Remark. *Let $\boldsymbol{u}(t)$ be a solution such that $\boldsymbol{u}(t) \neq 0$ on some interval $(t_1, t_2]$,*

then the function $\chi(t) = \dfrac{||\boldsymbol{u}||^2}{|\boldsymbol{u}|}$ *satisfies*

$$\frac{d\chi}{dt} = \frac{\frac{d||\boldsymbol{u}||^2}{dt}|\boldsymbol{u}| - ||\boldsymbol{u}||^2\frac{d|\boldsymbol{u}|}{dt}}{|\boldsymbol{u}|^2} = \frac{2\big[(\boldsymbol{f}, A\boldsymbol{u}) - \nu|A\boldsymbol{u}|^2\big]}{|\boldsymbol{u}|} - \frac{||\boldsymbol{u}||^2[(\boldsymbol{f}, \boldsymbol{u}) - \nu||\boldsymbol{u}||^2]}{|\boldsymbol{u}|^3}. \tag{2.32}$$

Using the definition

$$\lambda = \lambda(t) = \frac{\chi(t)}{|\boldsymbol{u}|} = \frac{||\boldsymbol{u}||^2}{|\boldsymbol{u}|^2},$$

we can rewrite (2.32) as

$$|\boldsymbol{u}|\frac{d\chi}{dt} = -2\nu|(A-\lambda)\boldsymbol{u}|^2 + 2(\boldsymbol{f}, (A-\lambda)\boldsymbol{u}) + \lambda(\boldsymbol{f}, \boldsymbol{u}) - \nu\lambda^2|\boldsymbol{u}|^2. \tag{2.33}$$

By introducing

$$\boldsymbol{f}_{\boldsymbol{u}}^{\perp} = \boldsymbol{f} - \frac{(\boldsymbol{f}, \boldsymbol{u})\boldsymbol{u}}{|\boldsymbol{u}|^2},$$

then (2.32) can be rewritten as

$$\begin{aligned} |\boldsymbol{u}|\frac{d\chi}{dt} &= -2\nu|(A-\lambda)\boldsymbol{u}|^2 + 2(\boldsymbol{f}_{\boldsymbol{u}}^{\perp}, (A-\lambda)\boldsymbol{u}) + \lambda(\boldsymbol{f}, \boldsymbol{u}) - \nu\lambda^2|\boldsymbol{u}|^2 \\ &= -2\nu\left|(A-\lambda)\boldsymbol{u} - \frac{\boldsymbol{f}_{\boldsymbol{u}}^{\perp}}{2\nu}\right|^2 + \frac{\left|\boldsymbol{f}_{\boldsymbol{u}}^{\perp}\right|^2}{2\nu} + \lambda(\boldsymbol{f}, \boldsymbol{u}) - \nu\lambda^2|\boldsymbol{u}|^2. \end{aligned} \tag{2.34}$$

Defining

$$\begin{aligned} \boldsymbol{v} &= (A-\lambda)\boldsymbol{u} - \frac{\boldsymbol{f}_{\boldsymbol{u}}^{\perp}}{2\nu}, \\ \sigma &= \frac{(\boldsymbol{f}, \boldsymbol{u})\boldsymbol{u}}{|\boldsymbol{f}||\boldsymbol{u}|}, \end{aligned}$$

we can represent (2.34) as

$$
\begin{aligned}
|\boldsymbol{u}|\frac{d\chi}{dt} &= -2\nu\left|(A-\lambda)\boldsymbol{u} - \frac{\boldsymbol{f}_{\boldsymbol{u}}^{\perp}}{2\nu}\right|^2 + \frac{\left|\boldsymbol{f}_{\boldsymbol{u}}^{\perp}\right|^2}{2\nu} + \lambda(\boldsymbol{f},\boldsymbol{u}) - \nu\lambda^2|\boldsymbol{u}|^2 \\
&= -2\nu|\boldsymbol{v}|^2 + \frac{|\boldsymbol{f}|^2}{2\nu}(1-\sigma^2) - \nu\chi^2 + \chi\sigma|\boldsymbol{f}| \quad \Rightarrow \\
|\boldsymbol{u}|\frac{d}{dt}\left(\frac{|\boldsymbol{f}|}{\nu} - \chi\right) &= 2\nu|\boldsymbol{v}|^2 + \nu\chi^2 - \frac{|\boldsymbol{f}|^2}{2\nu}(1-\sigma^2) - \chi\sigma|\boldsymbol{f}| \\
&= 2\nu|\boldsymbol{v}|^2 + \nu\left(\frac{|\boldsymbol{f}|}{\nu} - \chi\right)^2 - \frac{|\boldsymbol{f}|^2}{\nu} + 2\chi|\boldsymbol{f}| \\
&\quad - \frac{|\boldsymbol{f}|^2}{2\nu}(1-\sigma^2) - \chi\sigma|\boldsymbol{f}| \\
&= 2\nu|\boldsymbol{v}|^2 + \nu\left(\frac{|\boldsymbol{f}|}{\nu} - \chi\right)^2 - (2-\sigma)|\boldsymbol{f}|\left(\frac{|\boldsymbol{f}|}{\nu} - \chi\right) \\
&\quad + (2-\sigma)\frac{|\boldsymbol{f}|^2}{\nu} - (3-\sigma^2)\frac{|\boldsymbol{f}|^2}{2\nu} \\
&= 2\nu|\boldsymbol{v}|^2 + \nu\left(\frac{|\boldsymbol{f}|}{\nu} - \chi\right)^2 - (2-\sigma)|\boldsymbol{f}|\left(\frac{|\boldsymbol{f}|}{\nu} - \chi\right) \\
&\quad + (1-\sigma)\frac{|\boldsymbol{f}|^2}{2\nu}.
\end{aligned}
$$

Again, introducing

$$
\begin{aligned}
\phi &= 2\nu|\boldsymbol{v}|^2 + \nu\left(\frac{|\boldsymbol{f}|}{\nu} - \chi\right)^2 + (1-\sigma^2)\frac{|\boldsymbol{f}|^2}{2\nu} \\
\psi &= (2-\sigma)|\boldsymbol{f}| \quad \Rightarrow \quad \psi \geq |\boldsymbol{f}|,
\end{aligned} \tag{2.35}
$$

results in

$$
\frac{d}{dt}\left(\frac{|\boldsymbol{f}|}{\nu} - \chi\right) = \frac{\phi}{|\boldsymbol{u}|} - \frac{\psi}{|\boldsymbol{u}|}\left(\frac{|\boldsymbol{f}|}{\nu} - \chi\right),
$$

whose solution can be easily obtained for $t_0 \leq t,\ t, t_0 \in (t_1, t_2]$*:*

$$\left(\frac{|\boldsymbol{f}|}{\nu} - \chi\right) = \left(\frac{|\boldsymbol{f}|}{\nu} - \chi(t_0)\right) \exp\left(-\int_{t_0}^{t} \frac{\psi}{|\boldsymbol{u}|}\, dt\right) + \int_{t_0}^{t} \frac{\phi}{|\boldsymbol{u}|} \exp\left(-\int_{\tau}^{t} \frac{\psi}{|\boldsymbol{u}|}\, dt\right) d\tau. \tag{2.36}$$

2.I Bounds in the Z–E plane

In this section we are going to represent some bounds on the attractor in the Z–E plane using some functional inequalities and the dynamical behaviour of the Navier–Stokes equation represented in the previous section. One useful and important bound is obtained from the Poincaré inequality:

$$k_0^2 |\boldsymbol{u}|^2 \leq ||\boldsymbol{u}||^2 \quad \Rightarrow \quad E \leq Z.$$

As we have observed, the above inequality will impose a lower bound on the attractor in the Z–E plane. A less trivial upper bound relies on the following theorem, which plays a key role for finding the upper bound.

Theorem 4. *For all* $\boldsymbol{u} \in \mathcal{A}$*,*

$$||\boldsymbol{u}||^2 \leq \frac{|\boldsymbol{f}|}{\nu} |\boldsymbol{u}|. \tag{2.37}$$

In the case $||\boldsymbol{u}_0||^2 \leq \dfrac{|\boldsymbol{f}|}{\nu} |\boldsymbol{u}_0|$ *for* $\boldsymbol{u}_0 \in \mathcal{A} \backslash \{\boldsymbol{0}\}$*, it follows that* $\boldsymbol{u}_0$ *is a stationary solution and there exists* $n_0 \in \mathbb{N}$ *such that*

$$\boldsymbol{f} = R_{n_0} \boldsymbol{f}, \quad \boldsymbol{u}_0 = \frac{\boldsymbol{f}}{\nu \lambda_{n_0}}.$$

Moreover, in this case $\mathbf{0} \notin \mathcal{A}$ *and for all* $\boldsymbol{u} \in \mathcal{A}\backslash\{\boldsymbol{u}_0\}$

$$||\boldsymbol{u}||^2 \leq \lambda_{n_0}|\boldsymbol{u}|, \quad ||\boldsymbol{u}||^2 \leq \frac{|\boldsymbol{f}|}{\nu}|\boldsymbol{u}| = G\nu\lambda_0|\boldsymbol{u}|. \tag{2.38}$$

Proof. *Here we will just present the proof of (2.37) as it will be used for the rest of our work in the following chapter, and so for the remaining parts of the theorem, the reader is referred to Dascaliuc et al. [2005]. Let* $\boldsymbol{u}_0 \in \mathcal{A}$*. If* $\boldsymbol{u}_0 = 0$*, then it is clear that (2.37) holds. Now if* $\boldsymbol{u}_0 \neq 0$*, let* $u(t)$ *be the solution for* $\boldsymbol{u}(0) = \boldsymbol{u}_0$*. Then there are two cases to consider:*

- ***Case 1***

  Suppose that we have

  $$\inf_{t\in(-\infty,0]} |\boldsymbol{u}(t)| = u' > 0.$$

  This together with the boundedness of enstrophy for all values of t_0 *implies that* $\dfrac{|\boldsymbol{f}|}{\nu} - \chi(t_0)$ *is bounded for all* $t \in (-\infty, 0]$*. Also, based on the (2.35), we obtain*

  $$\lim_{t_0\to-\infty} \exp\left(-\int_\tau^t \frac{\psi}{|\boldsymbol{u}|}\,dt\right) \leq \lim_{t_0\to-\infty} \exp\left(-\frac{|\boldsymbol{f}|}{u'}(t-t_0)\right) = 0.$$

  Now if we take $t = 0$ *and* $t_0 \to -\infty$*, then (2.36) results in*

  $$\frac{|\boldsymbol{f}|}{\nu} - \chi(0) \geq 0.$$

  Then (2.36) will immediately yield

  $$\frac{|\boldsymbol{f}|}{\nu} - \chi(t) \geq 0,$$

and thus (2.37) holds.

- ***Case 2***

  Suppose that

$$\inf_{t\in(-\infty,0]} |\boldsymbol{u}(t)| = 0.$$

  Then $\mathbf{0} \in \mathcal{A}$ *and, by the definition of the infimum, there must exist a* $t_0 \in (-\infty, 0]$ *such that*

$$|\boldsymbol{u}(t_0)|^{1/3} \leq \frac{|\boldsymbol{f}|}{\nu^{5/3} k_0^2 G^{2/3} \Gamma_1^{1/3}},$$

  where Γ_1 *is defined in Theorem 2. So from Theorem 3, (2.37) follows and so for all* $\boldsymbol{u} \in \mathcal{A}$*, we have*

$$||\boldsymbol{u}||^2 \leq \frac{|\boldsymbol{f}|}{\nu} |\boldsymbol{u}|.$$

■

The above theorem implies that the attractor is located inside the bounded region shown in Figure 2.1.

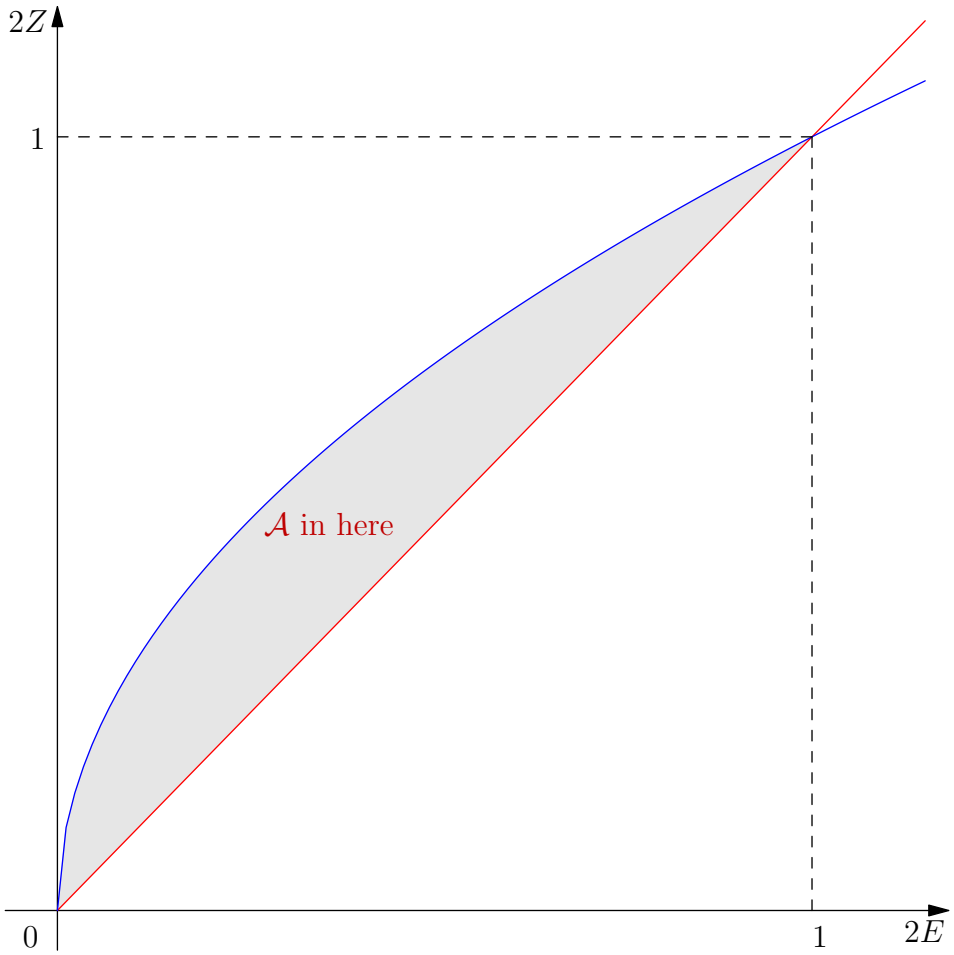

Figure 2.1: Bounds in the Z–E plane

Chapter 3

Energy and Enstrophy Relations on the Global Attractor of the 2D Navier–Stokes Equation: Random Forcing

3.A Introduction

In the previous chapter we presented a functional analysis of the Navier–Stokes equation assuming a constant (with respect to time) forcing applied to the fluid. In this chapter we are going to extend our analysis to random forcing. Random forcing is a more realistic way of injecting energy into a turbulent system than constant forcing. One of the important types of random forcing, called *white-noise forcing*, can be readily implemented numerically, an advantage that we will exploit in the numerical work of this study. Before starting our analysis, it is required to talk briefly about the nature and importance

of this particular kind of random forcing.

3.B The importance of homogeneous Gaussian (white-noise) force

White-noise forcing is a Gaussian random force that is homogeneous in space, with a Gaussian probability density function. This kind of forcing is extremely important in studying incompressible homogeneous isotropic turbulence because of the following two reasons:

- In view of the typical forcing encountered in experiments, white-noise forcing is much more realistic than the constant forcing treated in the previous chapter.
- By applying the theorem of Novikov [1964], we are able to obtain an explicit relation between the magnitude of the white-noise forcing and the energy and enstrophy injection rates. This is a remarkable result that makes it possible to have an estimate of the rate of the enstrophy injected into the fluid domain.

3.C Preliminaries

Generalizing the analysis of the previous chapter to account for random forcing requires a new norm. Among various possibilities for defining a new norm, what we are going to select will depend on the approach that we want to take for solving the problem. One one hand, we want to exploit as much as possible the analysis we applied in the previous chapter and on the other hand, we want

to exploit the randomness of the random forcing and the applicability of the Novikov theorem for white-noise forcing.

If we adopt the validity of the *ergodic theorem*, it is reasonable to use the notion of ensemble average in our new norm, combined with the L^2 norm used in the previous chapter. One can come up with the following definition for the extended norm (adopted for the rest of our analysis) as a reasonable definition:

$$|\boldsymbol{f}|_{\tilde{\omega}} \doteq \left(\int_{\Omega} \left\langle |\boldsymbol{f}|^2 \right\rangle \, d\boldsymbol{x} \right)^{1/2},$$

where $\tilde{\omega}$ indicates that this norm applies to the set of all random-valued functions. For a random variable α, with the probability density function P, we define the ensemble average

$$\langle \alpha \rangle = \int_{-\infty}^{\infty} \alpha \left(\frac{dP}{d\zeta} \right) d\zeta.$$

As we want to define our problem in a Hilbert space to exploit all the suitable properties of the Stokes operator A, the above norm must be a norm coming from an inner product on that Hilbert space. So although the above definition defines a norm, the essential point in extending our analysis is coming up with a suitable inner product on the Hilbert space H of random-valued functions.

3.C.1 Extended inner-product for random-valued functions in H

As an extension to the inner product we applied in the previous chapter, we define the inner product

$$(\boldsymbol{u},\boldsymbol{v})_{\tilde{\omega}} \doteq \int_{\Omega} \langle \boldsymbol{u}\cdot\boldsymbol{v} \rangle \, d\boldsymbol{x} = \int_{\Omega} \left(\int_{-\infty}^{\infty} \boldsymbol{u}\cdot\boldsymbol{v} \, \frac{dP}{d\zeta} d\zeta \right) d\boldsymbol{x}.$$

Adopting the above extended inner product, the definitions of energy, enstrophy, and palinstophy are unchanged, consistent with our previous analysis. So as the first step, we need to prove that the above definition is indeed an inner product, whose resulting norm is exactly the extended norm defined earlier.

Lemma 2. *Let $\mathcal{F}$ be the space of all homogeneous Gaussian $C^2(\Omega,t;\tilde{\omega}) \cap L^2(\Omega,t;\tilde{\omega})$ random-valued functions from $\Omega \times \mathbb{R}$ to $\mathbb{R}^2$. Then the following definition defines an inner-product on $\mathcal{F}$:*

$$(\boldsymbol{f},\boldsymbol{g})_{\tilde{\omega}} \doteq \int_{\Omega} \langle \boldsymbol{f}\cdot\boldsymbol{g} \rangle \, d\boldsymbol{x} = \int_{\Omega} \left(\int_{-\infty}^{\infty} \boldsymbol{f}\cdot\boldsymbol{g} \, \frac{dP}{d\zeta} d\zeta \right) d\boldsymbol{x}$$

Proof.

The required linearity, homogeneity, and positive-definiteness all follow directly from the definition. ■

Now that we have defined our extended inner product and the resulting norm, for the sake of simplicity, we are going to use $|\cdot|$ instead of $|\cdot|_{\tilde{\omega}}$.

3.C.2 Novikov theorem

As stated above, the Novikov theorem is going to play an essential role in the implementation of white-noise forcing. The Novikov theorem reads:

Theorem 5 (Novikov 1964)**.** *Let* $\boldsymbol{v} = (v_1, v_2, \cdots, v_n)$ *be a vector-valued centered Gaussian random variable and let* f *be a differentiable function of* n *variables, then assuming all averages exists,*

$$\langle v_i f(v_1, v_2, \cdots, v_n)\rangle = \Gamma_{ij} \left\langle \frac{\partial f}{\partial v_j} \right\rangle,$$

where $\Gamma_{ij} = \langle v_i v_j \rangle$.

Proof. *See Frisch [1995].* ■

Being equipped with the extended inner product and norm, we have enough functional analysis tools to begin our extension.

3.D The Navier–Stokes equation with random forcing as a dynamical system

In this section we consider the Navier–Stokes equation driven by a white-noise force in preparation for the numerical simulation results that will use this type of random forcing in the next chapter. However it is crucial to mention here that the rest of the analysis done in this chapter is completely valid for and applicable to a general random forcing.

Similar to the approach that we followed in the last chapter, we begin with

the Navier–Stokes equation

$$\frac{\partial \boldsymbol{u}}{\partial t} + \nu A\boldsymbol{u} + \mathcal{B}(\boldsymbol{u},\boldsymbol{u}) = \boldsymbol{f},$$

recalling that throughout this chapter, $\boldsymbol{f}$ is a general random force. A particular random force of interest to us is an isotropic Gaussian white-noise solenoidal force with the following Fourier transform $\boldsymbol{f}_{\boldsymbol{k}}$:

$$\boldsymbol{f}_{\boldsymbol{k}}(t) = F_{\boldsymbol{k}}\left(\mathbf{1} - \frac{\boldsymbol{k}\boldsymbol{k}}{k^2}\right)\cdot\boldsymbol{\xi}_{\boldsymbol{k}}(t), \quad \boldsymbol{k}\cdot\boldsymbol{f}_{\boldsymbol{k}} = 0,$$

where $F_{\boldsymbol{k}}$ is a real number and $\boldsymbol{\xi}_{\boldsymbol{k}}(t)$ is a unit central real Gaussian random 2D vector that satisfies $\langle \boldsymbol{\xi}_{\boldsymbol{k}}(t)\boldsymbol{\xi}_{\boldsymbol{k}'}(t')\rangle = \delta_{\boldsymbol{k}\boldsymbol{k}'}\mathbf{1}\delta(t-t')$. This implies

$$\begin{aligned}\langle \boldsymbol{f}_{\boldsymbol{k}}(t)\cdot\boldsymbol{f}_{\boldsymbol{k}'}(t')\rangle &= F_{\boldsymbol{k}}F_{\boldsymbol{k}'}\left(\delta_{ij} - \frac{k_i k_j}{k^2}\right)\langle \xi_{\boldsymbol{k}j}(t)\xi_{\boldsymbol{k}'j'}(t')\rangle\left(\delta_{j'i} - \frac{k'_{j'}k'_i}{k'^2}\right)\\ &= F_{\boldsymbol{k}}^2\delta_{\boldsymbol{k},\boldsymbol{k}'}\delta(t-t')\left(\mathbf{1} - \frac{\boldsymbol{k}\boldsymbol{k}}{k^2}\right) : \left(\mathbf{1} - \frac{\boldsymbol{k}\boldsymbol{k}}{k^2}\right) = F_{\boldsymbol{k}}^2\delta_{\boldsymbol{k},\boldsymbol{k}'}\delta(t-t').\end{aligned}$$

Integration of the energy equation leads to

$$\boldsymbol{u}_{\boldsymbol{k}}(t) = \boldsymbol{u}_{\boldsymbol{k}'}(t') + \int_{t'}^{t} A_{\boldsymbol{k}}[\boldsymbol{u}(\tau)]d\tau + \int_{t'}^{t}\boldsymbol{f}_{\boldsymbol{k}}(\tau)d\tau,$$

where $A_{\boldsymbol{k}}$ is an unknown functional of the velocity field such that $\dfrac{\delta A_{\boldsymbol{k}}[\boldsymbol{u}(\tau)]}{\delta \boldsymbol{f}_{\boldsymbol{k}'}(t')}$ is bounded. The nonlinear Green's function is then

$$\frac{\delta \boldsymbol{u}_{\boldsymbol{k}}(t)}{\delta \boldsymbol{f}_{\boldsymbol{k}'}(t')} = \int_{t'}^{t}\frac{\delta A_{\boldsymbol{k}}[\boldsymbol{u}(\tau)]}{\delta \boldsymbol{f}_{\boldsymbol{k}'}(t')}d\tau + \int_{t'}^{t}\delta_{\boldsymbol{k}\boldsymbol{k}'}\mathbf{1}\delta(\tau-t')d\tau = \int_{t'}^{t}\frac{\delta A_{\boldsymbol{k}}[\boldsymbol{u}(\tau)]}{\delta \boldsymbol{f}_{\boldsymbol{k}'}(t')}d\tau + \delta_{\boldsymbol{k}\boldsymbol{k}'}\mathbf{1}H(t-t'),$$

where H is the Heaviside unit step function. The Novikov theorem then allows

the energy injection rate ϵ for white-noise forcing to be computed exactly:

$$\begin{aligned}\epsilon = (\boldsymbol{f}(\boldsymbol{x},t),\boldsymbol{u}(\boldsymbol{x},t)) &= \int_\Omega \langle \boldsymbol{f}(\boldsymbol{x},t)\cdot\boldsymbol{u}(\boldsymbol{x},t)\rangle\, d\boldsymbol{x} = \mathrm{Re}\sum_{\boldsymbol{k}} \langle \boldsymbol{f}_{\boldsymbol{k}}(t)\cdot\boldsymbol{u}^*_{\boldsymbol{k}}(t)\rangle \\ &= \mathrm{Re}\sum_{\boldsymbol{k},\boldsymbol{k}'}\int \langle \boldsymbol{f}_{\boldsymbol{k}}(t)\boldsymbol{f}^*_{\boldsymbol{k}'}(t')\rangle : \left\langle \frac{\delta \boldsymbol{u}^*_{\boldsymbol{k}}(t)}{\delta \boldsymbol{f}^*_{\boldsymbol{k}'}(t')}\right\rangle dt' \\ &= \sum_{\boldsymbol{k}} F^2_{\boldsymbol{k}}\left(\mathbf{1}-\frac{\boldsymbol{k}\boldsymbol{k}}{k^2}\right) : \left(\mathbf{1}-\frac{\boldsymbol{k}\boldsymbol{k}}{k^2}\right) H(0) \\ &= \frac{1}{2}\sum_{\boldsymbol{k}} F^2_{\boldsymbol{k}},\end{aligned}$$

since $H(0) = \dfrac{1}{2}$.

As we observed in the previous chapter, analyzing the set of ordinary differential equations obtained on taking the inner product of $A^j\boldsymbol{u}$ with the Navier–Stokes equation is a promising approach. Thus we are going to follow this approach here, using our new extended norm and inner product. We will again require all of the bilinear map identities and estimates used earlier and also the same Sobolev inequalities. Here we must note that adopting the new norm and inner product, all the bilinear map identities and Sobolov inequalities are still valid. On taking the inner product of the Navier–Stokes equation with $A^j\boldsymbol{u}$, we will obtain dynamical estimates for general terms of the form $\left|A^{j/2}\boldsymbol{u}\right|$:

$$\begin{aligned}&\left(\frac{\partial \boldsymbol{u}}{\partial t}, A^j\boldsymbol{u}\right) + \nu(A\boldsymbol{u}, A^j\boldsymbol{u}) + (\mathcal{B}(\boldsymbol{u},\boldsymbol{u}), A^j\boldsymbol{u}) = (\boldsymbol{f}, A^j\boldsymbol{u}) \Rightarrow \\ &\frac{1}{2}\frac{d}{dt}(A^{j/2}\boldsymbol{u}, A^{j/2}\boldsymbol{u})^2 + \nu(A^{j/2}\boldsymbol{u}, A^{j/2+1}\boldsymbol{u}) + (\mathcal{B}(\boldsymbol{u},\boldsymbol{u}), A^j\boldsymbol{u}) = (A^{j/2}\boldsymbol{f}, A^{j/2}\boldsymbol{u}) \Rightarrow \\ &\frac{1}{2}\frac{d}{dt}\left|A^{j/2}\boldsymbol{u}\right|^2 + \nu(A^{j/2}\boldsymbol{u}, A^{j/2+1}\boldsymbol{u}) + (\mathcal{B}(\boldsymbol{u},\boldsymbol{u}), A^j\boldsymbol{u}) = (A^{j/2}\boldsymbol{f}, A^{j/2}\boldsymbol{u}). \qquad (3.1)\end{aligned}$$

3.D.1 Estimate obtained for $j = 0$

For $j = 0$ we have

$$\frac{1}{2}\frac{d}{dt}|\boldsymbol{u}|^2 + \nu(A\boldsymbol{u}, \boldsymbol{u}) + (\mathcal{B}(\boldsymbol{u}, \boldsymbol{u}), \boldsymbol{u}) = (\boldsymbol{f}, \boldsymbol{u}).$$

Having $(\mathcal{B}(\boldsymbol{u}, \boldsymbol{u}), \boldsymbol{u}) = 0$, and using the Novikov theorem, we obtain

$$\frac{1}{2}\frac{d}{dt}|\boldsymbol{u}|^2 + \nu(A^{1/2}\boldsymbol{u}, A^{1/2}\boldsymbol{u}) = \epsilon,$$

or equivalently,

$$\frac{1}{2}\frac{d}{dt}|\boldsymbol{u}|^2 + \nu\left|A^{1/2}\boldsymbol{u}\right|^2 = \epsilon,$$

where ϵ is the energy injection rate. Thus in our norm notation we have

$$\frac{1}{2}\frac{d}{dt}|\boldsymbol{u}|^2 + \nu||\boldsymbol{u}||^2 = \epsilon.$$

Using the Poincaré inequality results in

$$\begin{aligned}
&\frac{1}{2}\frac{d}{dt}|\boldsymbol{u}|^2 \leq \epsilon - \nu k_0^2|\boldsymbol{u}|^2 \overset{\text{Gronwall ineqality}}{\Rightarrow} \\
&|\boldsymbol{u}(t)|^2 \leq e^{-2\nu k_0^2 t}|\boldsymbol{u}(0)|^2 + \left(\frac{1 - e^{-2\nu k_0^2 t}}{\nu k_0^2}\right)\epsilon.
\end{aligned}$$

So for every $\boldsymbol{u} \in \mathcal{A}$, we would expect to have

$$|\boldsymbol{u}(t)|^2 \leq \frac{\epsilon}{\nu k_0^2}. \tag{3.2}$$

3.D.2 Estimate obtained for $j = 1$

For $j = 1$ we have

$$\frac{1}{2}\frac{d}{dt}\left|A^{1/2}\boldsymbol{u}\right|^2 + \nu(A^{1/2}\boldsymbol{u}, A^{3/2}\boldsymbol{u}) + (\mathcal{B}(\boldsymbol{u},\boldsymbol{u}), A\boldsymbol{u}) = (\boldsymbol{f}, A\boldsymbol{u}).$$

This case can lead to different estimates, depending on the use of the self-adjoint property of the Stokes operator A.

Case I

The first one can be obtained using the self-adjoint property such that $\boldsymbol{f}$ appears on the right-hand side without any factor of $A^{1/2}$. This case can be expressed as

$$\frac{1}{2}\frac{d}{dt}\left|A^{1/2}\boldsymbol{u}\right|^2 + \nu(A^{1/2}\boldsymbol{u}, A^{3/2}\boldsymbol{u}) + (\mathcal{B}(\boldsymbol{u},\boldsymbol{u}), A\boldsymbol{u}) = (\boldsymbol{f}, A\boldsymbol{u}).$$

Having $(\mathcal{B}(\boldsymbol{u},\boldsymbol{u}), A\boldsymbol{u}) = 0$ and using the Cauchy–Schwarz inequality for the right-hand side, we will obtain

$$\frac{1}{2}\frac{d}{dt}\left|A^{1/2}\boldsymbol{u}\right|^2 + \nu(A^{1/2}\boldsymbol{u}, A^{3/2}\boldsymbol{u}) \leq |\boldsymbol{f}||A\boldsymbol{u}|.$$

Using the self-adjoint property one more time for the term $\nu(A^{1/2}\boldsymbol{u}, A^{3/2}\boldsymbol{u})$, we obtain

$$\frac{1}{2}\frac{d}{dt}\left|A^{1/2}\boldsymbol{u}\right|^2 + \nu|A\boldsymbol{u}|^2 \leq |\boldsymbol{f}|\,|A\boldsymbol{u}|,$$

where in our norm notation we would have

$$\frac{1}{2}\frac{d}{dt}||\boldsymbol{u}||^2 + \nu|A\boldsymbol{u}|^2 \leq |\boldsymbol{f}|\,|A\boldsymbol{u}|. \tag{3.3}$$

From the above result, it is clear that this estimate does not exploit the Novikov theorem and so it would not be fruitful.

Case II

In this case, we try to keep the term $A^{1/2}\boldsymbol{f}$ appearing on the right-hand side

$$\frac{1}{2}\frac{d}{dt}\left|A^{1/2}\boldsymbol{u}\right|^2 + \nu(A^{1/2}\boldsymbol{u}, A^{3/2}\boldsymbol{u}) + (\mathcal{B}(\boldsymbol{u},\boldsymbol{u}), A\boldsymbol{u}) = (A^{1/2}\boldsymbol{f}, A^{1/2}\boldsymbol{u}).$$

Applying the same argument that we used for **Case I**, the Novikov theorem helps us obtain

$$\frac{1}{2}\frac{d}{dt}||\boldsymbol{u}||^2 + \nu|A\boldsymbol{u}|^2 = \eta,$$

where η in the enstrophy injection rate. Again with the help of the Poincaré inequality we obtain

$$\frac{1}{2}\frac{d}{dt}||\boldsymbol{u}||^2 \leq \eta - \nu k_0^2||\boldsymbol{u}||^2 \overset{\text{Gronwall inequality}}{\Rightarrow}$$
$$||\boldsymbol{u}(t)||^2 \leq e^{-2\nu k_0^2 t}||\boldsymbol{u}(0)||^2 + \left(\frac{1-e^{-2\nu k_0^2 t}}{\nu k_0^2}\right)\eta.$$

In analogy with the energy estimate, we would expect for every $\boldsymbol{u} \in \mathcal{A}$ that

$$||\boldsymbol{u}(t)||^2 \leq \frac{\eta}{\nu k_0^2}. \tag{3.4}$$

3.D.3 Estimate obtained for $j = 2$

For $j = 2$, using (3.1) results in

$$\frac{1}{2}\frac{d}{dt}|A\boldsymbol{u}|^2 + \nu(A\boldsymbol{u}, A^{5/2}\boldsymbol{u}) + (\mathcal{B}(\boldsymbol{u},\boldsymbol{u}), A^2\boldsymbol{u}) = (A\boldsymbol{f}, A\boldsymbol{u}),$$

where the self-adjoint property yields

$$\frac{1}{2}\frac{d}{dt}|A\boldsymbol{u}|^2 + \nu(A^{3/2}\boldsymbol{u}, A^{3/2}\boldsymbol{u}) + (\mathcal{B}(\boldsymbol{u},\boldsymbol{u}), A^2\boldsymbol{u}) = (A\boldsymbol{f}, A\boldsymbol{u}).$$

In view of the Novikov theorem, we will obtain

$$\frac{1}{2}\frac{d}{dt}|A\boldsymbol{u}|^2 + \nu(A^{3/2}\boldsymbol{u}, A^{3/2}\boldsymbol{u}) + (\mathcal{B}(\boldsymbol{u},\boldsymbol{u}), A^2\boldsymbol{u}) = \eta.$$

Using the upper bound we found for $(\mathcal{B}(\boldsymbol{u},\boldsymbol{u}), A^2\boldsymbol{u})$, one finds

$$\begin{aligned}\frac{1}{2}\frac{d}{dt}|A\boldsymbol{u}|^2 + \nu\big|A^{3/2}\boldsymbol{u}\big| &= \eta + (\mathcal{B}(A\boldsymbol{u}, A\boldsymbol{u}), \boldsymbol{u}) \\ &\leq \eta + |(\mathcal{B}(A\boldsymbol{u}, A\boldsymbol{u}), \boldsymbol{u})| \\ &\leq \eta + c_L|A\boldsymbol{u}|\big|A^{1/2}\boldsymbol{u}\big|\big|A^{3/2}\boldsymbol{u}\big|,\end{aligned}$$

where in our norm notation,

$$\frac{1}{2}\frac{d}{dt}|A\boldsymbol{u}|^2 + \nu\big|A^{3/2}\boldsymbol{u}\big|^2 \leq \eta + c_L||\boldsymbol{u}||\,|A\boldsymbol{u}|\big|A^{3/2}\boldsymbol{u}\big|.$$

3.E An upper bound in the Z–E plane for a random forcing

Let $\boldsymbol{u}(t)$ be a solution such that $\boldsymbol{u}(t) \neq 0$ on some interval $(t_1, t_2]$. Then the function $\chi(t) = \dfrac{||\boldsymbol{u}||^2}{|\boldsymbol{u}|}$ satisfies

$$\frac{d\chi}{dt} = \frac{\dfrac{d||\boldsymbol{u}||^2}{dt}|\boldsymbol{u}| - ||\boldsymbol{u}||^2\dfrac{d|\boldsymbol{u}|}{dt}}{|\boldsymbol{u}|^2} = \frac{2[(\boldsymbol{f}, A\boldsymbol{u}) - \nu|A\boldsymbol{u}|^2]}{|\boldsymbol{u}|} - \frac{||\boldsymbol{u}||^2[(\boldsymbol{f},\boldsymbol{u}) - \nu||\boldsymbol{u}||^2]}{|\boldsymbol{u}|^3}. \tag{3.5}$$

Using the definition

$$\lambda = \lambda(t) = \frac{\chi(t)}{|\boldsymbol{u}|} = \frac{||\boldsymbol{u}||^2}{|\boldsymbol{u}|^2},$$

we see that (3.5) can be written as

$$|\boldsymbol{u}|\frac{d\chi}{dt} = -2\nu|A\boldsymbol{u}|^2 + 2(\boldsymbol{f}, A\boldsymbol{u}) - \lambda(\boldsymbol{f}, \boldsymbol{u}) + \underbrace{\nu\lambda||\boldsymbol{u}||^2}_{\nu\lambda^2|\boldsymbol{u}|^2}. \tag{3.6}$$

On introducing $\boldsymbol{v} = (A - \lambda)\boldsymbol{u} - \dfrac{\boldsymbol{f}}{2\nu}$, then

$$\begin{aligned}
|\boldsymbol{v}|^2 &= \left|(A-\lambda)\boldsymbol{u} - \frac{\boldsymbol{f}}{2\nu}\right|^2 \quad \Rightarrow \\
|\boldsymbol{v}|^2 &= |A\boldsymbol{u}|^2 - 2\lambda||\boldsymbol{u}||^2 - \frac{1}{\nu}(f, A\boldsymbol{u}) + \frac{\lambda}{\nu}(\boldsymbol{f}, \boldsymbol{u}) + \lambda^2|\boldsymbol{u}|^2 + \frac{|\boldsymbol{f}|^2}{4\nu^2} \quad \Rightarrow \\
-2\nu|\boldsymbol{v}|^2 &= -2\nu|A\boldsymbol{u}|^2 + 4\nu\lambda||\boldsymbol{u}||^2 + 2(f, A\boldsymbol{u}) - 2\lambda(\boldsymbol{f}, \boldsymbol{u}) - 2\nu\lambda^2|\boldsymbol{u}|^2 - \frac{|\boldsymbol{f}|^2}{2\nu} \\
&= \underbrace{\left(2(\boldsymbol{f}, A\boldsymbol{u}) - 2\nu|A\boldsymbol{u}|^2\right) - \lambda(f, u) + \nu\lambda||\boldsymbol{u}||^2}_{|\boldsymbol{u}|\frac{d\chi}{dt}} + \underbrace{\nu\lambda||\boldsymbol{u}||^2}_{\nu\chi^2} \\
&\quad - \lambda(f, \boldsymbol{u}) - \frac{|\boldsymbol{f}|^2}{2\nu}.
\end{aligned}$$

So we will obtain

$$-|\boldsymbol{u}|\frac{d\chi}{dt} = 2\nu|\boldsymbol{v}|^2 + \nu\chi^2 - \epsilon\lambda - \frac{|\boldsymbol{f}|^2}{2\nu}.$$

On introducing a real constant α whose value will be determined later, we may write

$$|\boldsymbol{u}|\frac{d}{dt}(\alpha-\chi) = 2\nu|\boldsymbol{v}|^2 + \nu(\alpha-\chi)^2 - \nu\alpha^2 + 2\nu\alpha\chi - \epsilon\lambda - \frac{|\boldsymbol{f}|^2}{2\nu} \quad \overset{\chi=\lambda|\boldsymbol{u}|}{\Rightarrow}$$
$$= 2\nu|\boldsymbol{v}|^2 + \nu(\alpha-\chi)^2 - \nu\alpha^2 + \left(2\nu\alpha - \frac{\epsilon}{|\boldsymbol{u}|}\right)\chi - \frac{|\boldsymbol{f}|^2}{2\nu}.$$

The above result can be rewritten in the following form

$$|\boldsymbol{u}|\frac{d}{dt}(\alpha-\chi) = 2\nu|\boldsymbol{v}|^2 + \nu(\alpha-\chi)^2 - \beta(\alpha-\chi) + \alpha\beta - \nu\alpha^2 - \frac{|\boldsymbol{f}|^2}{2\nu}$$
$$= 2\nu|\boldsymbol{v}|^2 + \nu(\alpha-\chi)^2 - \beta(\alpha-\chi) + \nu\alpha^2 - \frac{\epsilon\alpha}{|\boldsymbol{u}|} - \frac{|\boldsymbol{f}|^2}{2\nu},$$

where $\beta = 2\nu\alpha - \dfrac{\epsilon}{|\boldsymbol{u}|}$. Thus, if α is such that

$$\beta = 2\nu\alpha - \frac{\epsilon}{|\boldsymbol{u}|} > 0 \quad \text{and} \quad \nu\alpha^2 - \frac{\epsilon\alpha}{|\boldsymbol{u}|} - \frac{|\boldsymbol{f}|^2}{2\nu} > 0, \tag{3.7}$$

we can introduce

$$\phi \doteq 2\nu|\boldsymbol{v}|^2 + \nu(\alpha-\chi)^2 + \alpha\beta - \nu\alpha^2 - \frac{|\boldsymbol{f}|^2}{2\nu} > 0$$

to express the above first-order differential equation as

$$|\boldsymbol{u}|\frac{d}{dt}(\alpha-\chi) + \beta(\alpha-\chi) = \phi. \tag{3.8}$$

The solution to this equation is

$$\alpha - \chi(t) = (\alpha - \chi(t_0))\exp\left(-\int_{t_0}^{t}\frac{\beta}{|\boldsymbol{u}|}\,dt\right) + \int_{t_0}^{t}\frac{\phi}{|\boldsymbol{u}|}\exp\left(-\int_{t_0}^{t}\frac{\beta}{|\boldsymbol{u}|}\,dt\right)d\tau.$$

Taking $t_0 \to -\infty$, and $t = 0$, results in $(\alpha - \chi(0)) \geq 0$. Now taking $t_0 = 0$, and $t \to \infty$, one finds that $\alpha - \chi(t) \geq 0$ for all $t \in (-\infty, \infty)$. Thus

$$\chi \leq \alpha \quad \Rightarrow \quad ||\boldsymbol{u}||^2 \leq \alpha |\boldsymbol{u}|. \tag{3.9}$$

To get the above result we need to check the conditions (3.7). Working on these inequalities, one can show

$$\begin{aligned}
\nu\alpha^2 - \frac{\epsilon\alpha}{|\boldsymbol{u}|} - \frac{|\boldsymbol{f}|^2}{2\nu} = 0 \Rightarrow \alpha_{1,2} = \frac{\frac{\epsilon}{|\boldsymbol{u}|} \pm \sqrt{\frac{\epsilon^2}{|\boldsymbol{u}|^2} + 2|\boldsymbol{f}|^2}}{2\nu} \Rightarrow \begin{cases} \alpha_1 < 0, \\ \alpha_2 \geq \dfrac{\epsilon}{\nu|\boldsymbol{u}|}, \end{cases} \\
\Rightarrow \nu\alpha^2 - \frac{\epsilon\alpha}{|\boldsymbol{u}|} - \frac{|\boldsymbol{f}|^2}{2\nu} > 0 \iff \alpha \geq \frac{\epsilon}{\nu|\boldsymbol{u}|} \text{ or } \alpha \leq 0 \\
\Rightarrow \beta = 2\nu\alpha - \frac{\epsilon}{|\boldsymbol{u}|} > 0.
\end{aligned} \tag{3.10}$$

On the other hand, using (3.2) and applying the *Cauchy–Schwarz inequality* and the *Novikov theorem* leads to

$$\begin{cases} |\boldsymbol{u}(t)|^2 \leq \dfrac{\epsilon}{\nu k_0^2} \quad \Rightarrow \quad k_0\sqrt{\nu\epsilon} \leq \dfrac{\epsilon}{|\boldsymbol{u}|}, \\ \\ \epsilon = (\boldsymbol{f}, \boldsymbol{u}) \leq |\boldsymbol{f}||\boldsymbol{u}|, \end{cases} \qquad \Rightarrow \quad k_0\sqrt{\nu\epsilon} \leq |\boldsymbol{f}|, \tag{3.11}$$

and consequently we will find that

$$\alpha \geq \frac{\epsilon}{\nu|\boldsymbol{u}|} \geq k_0\sqrt{\frac{\epsilon}{\nu}}.$$

So if we take $\alpha = k_0\sqrt{\frac{\epsilon}{\nu}}$, then using (3.9) will result in an extremely important bound in the Z–E plane:

$$||\boldsymbol{u}||^2 \leq k_0\sqrt{\frac{\epsilon}{\nu}}|\boldsymbol{u}|. \tag{3.12}$$

It is convenient to use the lower bound for $|\boldsymbol{f}|$ found in (3.11) to define a *Grashof number* for white-noise forcing:

$$G = \frac{|\boldsymbol{f}|}{\nu^2 k_0^2} \Rightarrow G = \frac{\sqrt{\nu\epsilon}}{\nu^2 k_0},$$

in terms of which,

$$\begin{aligned} \boldsymbol{v}(t) = \frac{\boldsymbol{u}(t)}{G\nu} \quad &\Rightarrow \\ ||\boldsymbol{u}||^2 \leq k_0\sqrt{\frac{\epsilon}{\nu}}|\boldsymbol{u}| \quad &\Rightarrow \quad G^2\nu^2||\boldsymbol{v}||^2 \leq k_0\sqrt{\frac{\epsilon}{\nu}}G\nu|\boldsymbol{v}| \quad \Rightarrow \\ ||\boldsymbol{v}||^2 \leq \frac{k_0}{G\nu}\sqrt{\frac{\epsilon}{\nu}}|\boldsymbol{v}| \quad &\Rightarrow \quad ||\boldsymbol{v}||^2 \leq k_0^2|\boldsymbol{v}|. \end{aligned} \tag{3.13}$$

Result (3.12) can be expressed in the following theorem.

Theorem 6. *For all $\boldsymbol{u} \in \mathcal{A}$ driven by a random forcing injecting energy at a rate ϵ,*

$$||\boldsymbol{u}||^2 \leq k_0\sqrt{\frac{\epsilon}{\nu}}\,|\boldsymbol{u}|.$$

The above result for random forcing has the same form as the upper bound found by Dascaliuc *et al.* [2005] for constant forcing, thus elucidating the relation between these two types of forcing.

3.F Optimization of the upper bound in the Z–E plane for random forcing

Let $\boldsymbol{u}(t)$ be a solution such that $\boldsymbol{u}(t) \neq 0$ on some interval $(t_1, t_2]$. Then the function $\chi(t) = \dfrac{||\boldsymbol{u}||^2}{|\boldsymbol{u}|}$ satisfies

$$\frac{d\chi}{dt} = \frac{\frac{d||\boldsymbol{u}||^2}{dt}|\boldsymbol{u}| - ||\boldsymbol{u}||^2\frac{d|\boldsymbol{u}|}{dt}}{|\boldsymbol{u}|^2} = \frac{2[(\boldsymbol{f}, A\boldsymbol{u}) - \nu|A\boldsymbol{u}|^2]}{|\boldsymbol{u}|} - \frac{||\boldsymbol{u}||^2[(\boldsymbol{f}, \boldsymbol{u}) - \nu||\boldsymbol{u}||^2]}{|\boldsymbol{u}|^3}. \tag{3.14}$$

Using the definition

$$\lambda = \lambda(t) = \frac{\chi(t)}{|\boldsymbol{u}|} = \frac{||\boldsymbol{u}||^2}{|\boldsymbol{u}|^2},$$

we see that (3.14) can be written as

$$|\boldsymbol{u}|\frac{d\chi}{dt} = -2\nu|A\boldsymbol{u}|^2 + 2(\boldsymbol{f}, A\boldsymbol{u}) - \lambda(\boldsymbol{f}, \boldsymbol{u}) + \underbrace{\nu\lambda||\boldsymbol{u}||^2}_{\nu\lambda^2|\boldsymbol{u}|^2}. \tag{3.15}$$

On introducing $\boldsymbol{v} = (A - \gamma\lambda)\boldsymbol{u} - \dfrac{\boldsymbol{f}}{2\nu}$, we see that

$$
\begin{aligned}
|\boldsymbol{v}|^2 &= \left|(A - \gamma\lambda)\boldsymbol{u} - \frac{\boldsymbol{f}}{2\nu}\right|^2 \quad \Rightarrow \\
|\boldsymbol{v}|^2 &= |A\boldsymbol{u}|^2 - 2\gamma\lambda||\boldsymbol{u}||^2 - \frac{1}{\nu}(f, A\boldsymbol{u}) + \frac{\gamma\lambda}{\nu}(\boldsymbol{f}, \boldsymbol{u}) + \gamma^2\lambda^2|\boldsymbol{u}|^2 + \frac{|\boldsymbol{f}|^2}{4\nu^2} \quad \Rightarrow \\
-2\nu|\boldsymbol{v}|^2 &= -2\nu|A\boldsymbol{u}|^2 + 4\nu\gamma\lambda||\boldsymbol{u}||^2 + 2(f, A\boldsymbol{u}) - 2\gamma\lambda(\boldsymbol{f}, \boldsymbol{u}) - 2\nu\gamma^2\lambda^2|\boldsymbol{u}|^2 \\
&\quad - \frac{|\boldsymbol{f}|^2}{2\nu} \quad \Rightarrow \\
-2\nu|\boldsymbol{v}|^2 &= \underbrace{\big(2(\boldsymbol{f}, A\boldsymbol{u}) - 2\nu|A\boldsymbol{u}|^2\big) - \lambda(f, u) + \nu\lambda^2|\boldsymbol{u}|^2}_{|\boldsymbol{u}|\dfrac{d\chi}{dt}} \\
&\quad + (4\gamma - 2\gamma^2 - 1)\nu\lambda||\boldsymbol{u}||^2 - (2\gamma - 1)\lambda(f, \boldsymbol{u}) - \frac{|\boldsymbol{f}|^2}{2\nu}.
\end{aligned}
$$

Thus, we will obtain

$$
-|\boldsymbol{u}|\frac{d\chi}{dt} = 2\nu|\boldsymbol{v}|^2 + \underbrace{(4\gamma - 2\gamma^2 - 1)}_{\sigma}\nu\lambda||\boldsymbol{u}||^2 - \underbrace{(2\gamma - 1)}_{\tau}\lambda(f, \boldsymbol{u}) - \frac{|\boldsymbol{f}|^2}{2\nu}.
$$

In order to apply the same argument that we used for the nonoptimized bound, at first we have to find the values of γ such that

$$
\begin{cases}
\sigma = -2\gamma^2 + 4\gamma - 1 > 0 & \Rightarrow 1 - \dfrac{\sqrt{2}}{2} < \gamma < 1 + \dfrac{\sqrt{2}}{2}, \quad \sigma_{\max} = \sigma\big|_{\tau=1} = 1, \\
\tau = 2\gamma - 1 > 0 & \Rightarrow \quad \dfrac{1}{2} < \gamma,
\end{cases}
$$

which implies that

$$
\frac{1}{2} < \gamma < 1 + \frac{\sqrt{2}}{2} \quad \Rightarrow \quad 0 \le \sigma \le 1. \tag{3.16}
$$

Again on introducing a real constant α whose value will be determined later, we may write

$$|\boldsymbol{u}|\frac{d}{dt}(\alpha-\chi) = 2\nu|\boldsymbol{v}|^2 + \nu\sigma(\alpha-\chi)^2 - \nu\sigma\alpha^2 + 2\nu\sigma\alpha\chi - \tau\epsilon\lambda - \frac{|\boldsymbol{f}|^2}{2\nu} \quad \overset{\chi=\lambda|\boldsymbol{u}|}{\Rightarrow}$$
$$= 2\nu|\boldsymbol{v}|^2 + \nu\sigma(\alpha-\chi)^2 - \nu\sigma\alpha^2 + \left(2\nu\sigma\alpha - \frac{\tau\epsilon}{|\boldsymbol{u}|}\right)\chi - \frac{|\boldsymbol{f}|^2}{2\nu}.$$

Defining $\beta = 2\nu\sigma\alpha - \dfrac{\tau\epsilon}{|\boldsymbol{u}|}$, the above result can be rewritten in the following form

$$|\boldsymbol{u}|\frac{d}{dt}(\alpha-\chi) = 2\nu|\boldsymbol{v}|^2 + \nu\sigma(\alpha-\chi)^2 - \beta(\alpha-\chi) + \alpha\beta - \nu\sigma\alpha^2 - \frac{|\boldsymbol{f}|^2}{2\nu}$$
$$= 2\nu|\boldsymbol{v}|^2 + \nu\sigma(\alpha-\chi)^2 - \beta(\alpha-\chi) + \nu\sigma\alpha^2 - \frac{\tau\sigma\epsilon\alpha}{|\boldsymbol{u}|} - \frac{|\boldsymbol{f}|^2}{2\nu}.$$

Thus, if α is such that

$$\nu\sigma\alpha^2 - \frac{\tau\sigma\epsilon\alpha}{|\boldsymbol{u}|} - \frac{|\boldsymbol{f}|^2}{2\nu} > 0 \quad \text{and} \quad \beta = 2\nu\sigma\alpha - \frac{\tau\epsilon}{|\boldsymbol{u}|} > 0, \tag{3.17}$$

and we redefine

$$\phi \doteq 2\nu|\boldsymbol{v}|^2 + \nu\sigma(\alpha-\chi)^2 + \nu\sigma\alpha^2 - \frac{\tau\sigma\epsilon\alpha}{|\boldsymbol{u}|} - \frac{|\boldsymbol{f}|^2}{2\nu} > 0,$$

the argument in Section 3.E leads again to the implication

$$\chi \le \alpha \quad \Rightarrow \quad ||\boldsymbol{u}||^2 \le \alpha|\boldsymbol{u}|. \tag{3.18}$$

So to get the above result we need to check the conditions (3.17). Working on

the inequalities, one can show

$$\nu\sigma\alpha^2 - \frac{\tau\sigma\epsilon\alpha}{|\boldsymbol{u}|} - \frac{|\boldsymbol{f}|^2}{2\nu} = 0 \Rightarrow \alpha = \begin{cases} \alpha_1 < 0, \\ \alpha_2 \geq \dfrac{\tau\epsilon}{2\nu|\boldsymbol{u}|} \end{cases}$$

$$\Rightarrow \nu\sigma\alpha^2 - \frac{\tau\sigma\epsilon\alpha}{|\boldsymbol{u}|} - \frac{|\boldsymbol{f}|^2}{2\nu} > 0 \iff \alpha \geq \frac{\tau\epsilon}{2\nu|\boldsymbol{u}|}$$

$$\Rightarrow \beta = 2\nu\sigma\alpha - \frac{\tau\epsilon}{|\boldsymbol{u}|} > 0 \Rightarrow \sigma > 1,$$

which is not admissible in view of (3.16). Thus $\sigma = \sigma_{\max} = 1$, which in turn implies that τ has to be equal 1, and so the upper bound that we obtained in the previous section is the tightest bound that we are able to find exploiting the argument used in the previous section. The upper bound (3.13) and the Poincaré inequality characterize the region in the E–Z plane where the projection of the global attractor of the 2D incompressible homogeneous isotropic turbulence will be located. These bounds together with the attractors obtained by the numerical simulations are illustrated in Chapter 5.

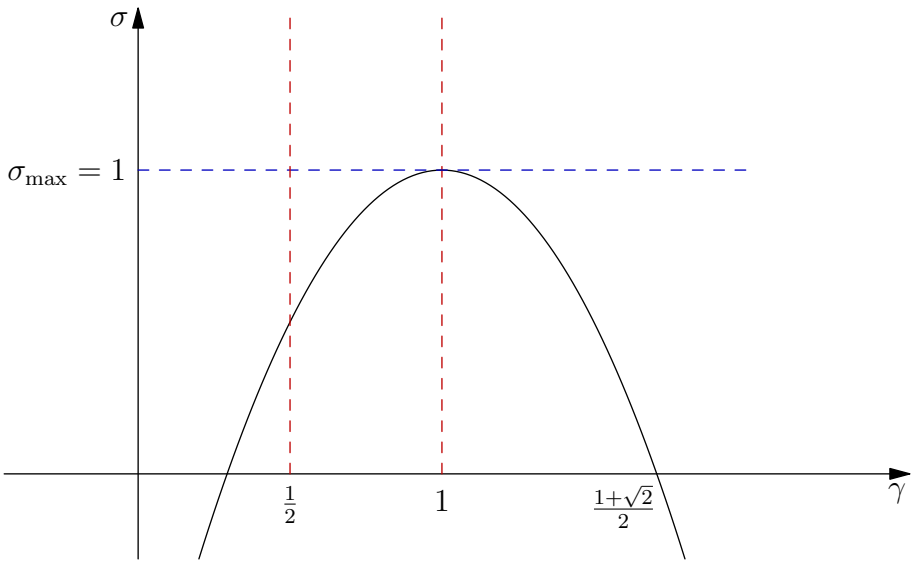

Figure 3.1: $\sigma(\gamma)$

Chapter 4

Direct Numerical Simulation of 2D & 3D Incompressible Turbulence Flows

4.A Introduction

In this chapter we explain the set of governing equations and the method we use to obtain numerical solutions of the 2D Navier–Stokes equation. We use the pseudospectral code `PROTODNS` for direct numerical simulation (DNS) of two-dimensional incompressible homogeneous turbulent flow with periodic boundary conditions in Fourier space, available at https://github.com/dealias/dns/tree/master/protodns. Here we mention that as can be inferred from its name, `PROTODNS` is the simpler version of an efficient and complete code called `DNS`. So the main reason for having `PROTODNS` is essentially for educational purposes, as it does not exploit many possible implementation optimizations that can speed up the simulation process. The reader who is interested in

the most advanced, efficient, and complete version of this code, can refer to the full 2D code at available at https://github.com/dealias/dns/tree/master/2d.

4.B Governing equations

We start our work with the set of governing equations for incompressible turbulent flows: the Navier–Stokes equation for momentum and the incompressibility condition,

$$\begin{cases} \dfrac{\partial \boldsymbol{u}}{\partial t} + \boldsymbol{u} \cdot \boldsymbol{\nabla} \boldsymbol{u} = -\boldsymbol{\nabla} p + \nu \nabla^2 \boldsymbol{u} + \boldsymbol{F}, \\ \\ \boldsymbol{\nabla} \cdot \boldsymbol{u} = 0. \end{cases} \tag{4.1}$$

However, there is another possible set of equations, the *vorticity* representation, which is equivalent to (4.1) but is sometimes more convenient:

$$\begin{cases} \dfrac{\partial \boldsymbol{\omega}}{\partial t} + (\boldsymbol{u} \cdot \boldsymbol{\nabla}) \boldsymbol{\omega} = (\boldsymbol{\omega} \cdot \boldsymbol{\nabla}) \boldsymbol{u} + \nu \nabla^2 \boldsymbol{\omega} + \boldsymbol{\nabla} \times \boldsymbol{F}, \\ \\ \boldsymbol{\nabla} \cdot \boldsymbol{u} = 0. \end{cases} \tag{4.2}$$

The main advantage of using the vorticity equation instead of the momentum equation is the fact that the vorticity equation does not involve a pressure term. Taking into account that our problem is two dimensional, it is possible to make use of the *stream function* ψ, and so for the case of 2D incompressible

turbulent flow in the x–y plane, we would have

$$\begin{cases} \boldsymbol{u} = u(x,y)\hat{\boldsymbol{x}} + v(x,y)\hat{\boldsymbol{y}}, & \\ & \Rightarrow \boldsymbol{\nabla}\cdot\boldsymbol{u} = 0. \\ u = -\dfrac{\partial\psi}{\partial y}, \quad v = \dfrac{\partial\psi}{\partial x} & \end{cases} \tag{4.3}$$

Since $\boldsymbol{\omega} = \boldsymbol{\nabla}\times\boldsymbol{u}$, we find

$$\boldsymbol{\omega} = \left(\frac{\partial v}{\partial x} - \frac{\partial u}{\partial y}\right)\hat{\boldsymbol{z}}, \tag{4.4}$$

which in fact shows that in the case of 2D incompressible flow, $\boldsymbol{\omega}$ is a vector whose direction is always perpendicular to the velocity vector, so what is important is just the length of the vorticity vector. Thus, we can look at the vorticity as an scalar function. Now using the equation (4.3) in (4.4), we will have

$$\boldsymbol{\omega} = (\nabla^2\psi)\hat{\boldsymbol{z}}, \tag{4.5}$$

while we can write

$$\boldsymbol{u} = \frac{\partial\psi}{\partial y}\hat{\boldsymbol{x}} + \frac{\partial\psi}{\partial x}\hat{\boldsymbol{y}} = \hat{\boldsymbol{z}}\times\boldsymbol{\nabla}\psi. \tag{4.6}$$

So using equations (4.5), (4.6), we can represent the velocity vector with respect to the stream function as $\boldsymbol{u} = \hat{\boldsymbol{z}}\times\boldsymbol{\nabla}(\nabla^{-2}\omega)$. As we mentioned above, because in 2D flow, the vorticity is always perpendicular to the velocity vector, so the first term on the right-hand side of the vorticity equation vanishes:

$$\frac{\partial\omega}{\partial t} + (\boldsymbol{u}\cdot\boldsymbol{\nabla})\omega = \nu\nabla^2\omega + f. \tag{4.7}$$

Expanding the second term in the equation (4.7), we will obtain

$$\frac{\partial \omega}{\partial t} + (\hat{\boldsymbol{z}} \times \boldsymbol{\nabla}(\nabla^{-2}\omega) \cdot \boldsymbol{\nabla})\omega = \nu \nabla^2 \omega + f. \tag{4.8}$$

Taking the inverse discrete Fourier transform of this equation, we find

$$\frac{\partial \omega_{\boldsymbol{k}}}{\partial t} + \sum_{\boldsymbol{p}} \frac{(\hat{\boldsymbol{z}} \times \boldsymbol{p}) \cdot \boldsymbol{k}}{p^2} \omega_{\boldsymbol{p}} \omega_{\boldsymbol{k}-\boldsymbol{p}} = -\nu k^2 \omega_{\boldsymbol{k}} + f_{\boldsymbol{k}}. \tag{4.9}$$

Although equation (4.9) is obtained as the governing equation in Fourier space that must be solved numerically, that representation is not used in practice. Instead, we represent the equation (4.9) in the following form:

$$\frac{\partial \omega_{\boldsymbol{k}}}{\partial t} + \mathcal{F}\{(\boldsymbol{u} \cdot \boldsymbol{\nabla})\omega\} = -\nu k^2 \omega_{\boldsymbol{k}} + f_{\boldsymbol{k}}. \tag{4.10}$$

The values of u and v are then derived from the scalar ω.

4.C Numerical simulation

4.C.1 The domain of simulation

Now that we have our governing equation (4.10) in Fourier space, we need a numerical scheme to solve that equation. First, we need to characterize the simulation domain. As we mentioned before, because our intention is direct numerical simulation of homogeneous isotropic turbulence, so we have to avoid having walls (or at least stay far away from walls). This allows us to use periodic boundary conditions. Considering this point, our schematic domain is shown in Figure 4.1.

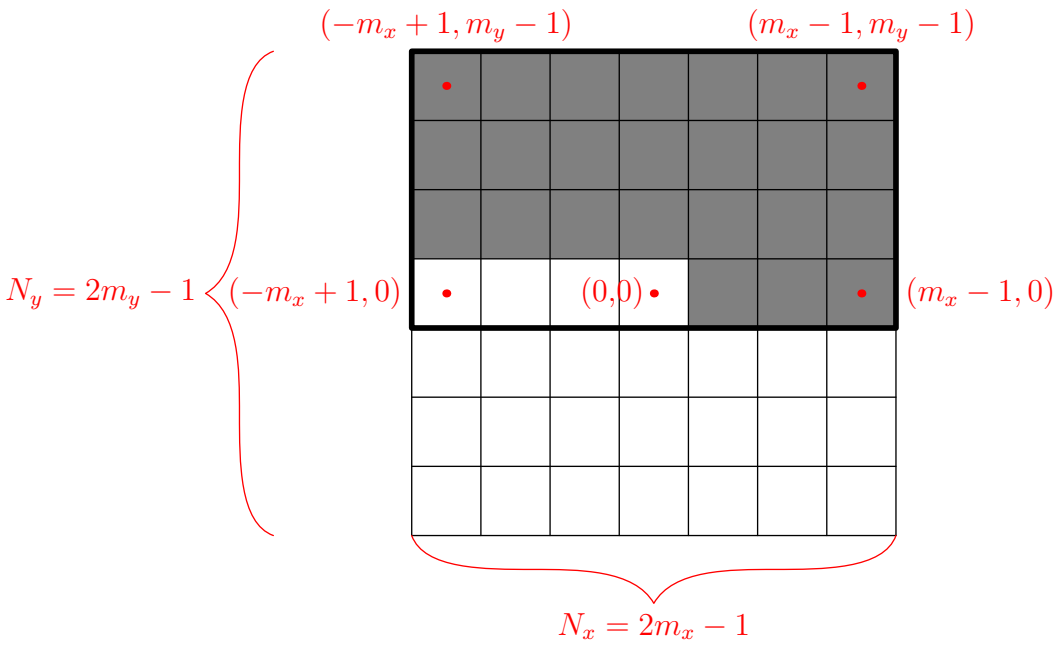

Figure 4.1: Domain of simulation

4.C.2 Solution algorithm

We now represent the numerical scheme for solving our governing equation. As stated in the previous section, the governing equation is:

$$\frac{\partial \omega_{\boldsymbol{k}}}{\partial t} + \mathcal{F}\{\boldsymbol{u} \cdot \boldsymbol{\nabla}\omega\} = -\nu k^2 \omega_{\boldsymbol{k}} + f_{\boldsymbol{k}}. \tag{4.11}$$

This equation can be written as an evolution equation for ω by taking all the terms except the time derivative of ω to the right-hand side:

$$\frac{\partial \omega_{\boldsymbol{k}}}{\partial t} = -\mathcal{F}\left\{u\frac{\partial \omega}{\partial x} + v\frac{\partial \omega}{\partial y}\right\} - \nu k^2 \omega_{\boldsymbol{k}} + f_{\boldsymbol{k}}. \tag{4.12}$$

The numerical solution steps are:

1. Initialize $\omega_{\boldsymbol{k}}$ in Fourier space.

2. Calculate the velocity components u and v based on ω.

3. Take the inverse discrete fast Fourier transform (FFT^{-1}) of u, v $\dfrac{\partial \omega}{\partial x}$, and $\dfrac{\partial \omega}{\partial y}$ to go to physical space.

4. Calculate the multiplicative terms appearing in the inertial term in physical space.

5. Take the discrete fast Fourier transform (FFT) of the advection term to get back to Fourier space.

6. Update the values of ω by marching one step in time.

7. Calculate the values of energy, enstrophy, and palinstrophy.

8. Go to Step 2.

The flowchart of the above numerical algorithm is shown in Figure 4.2.

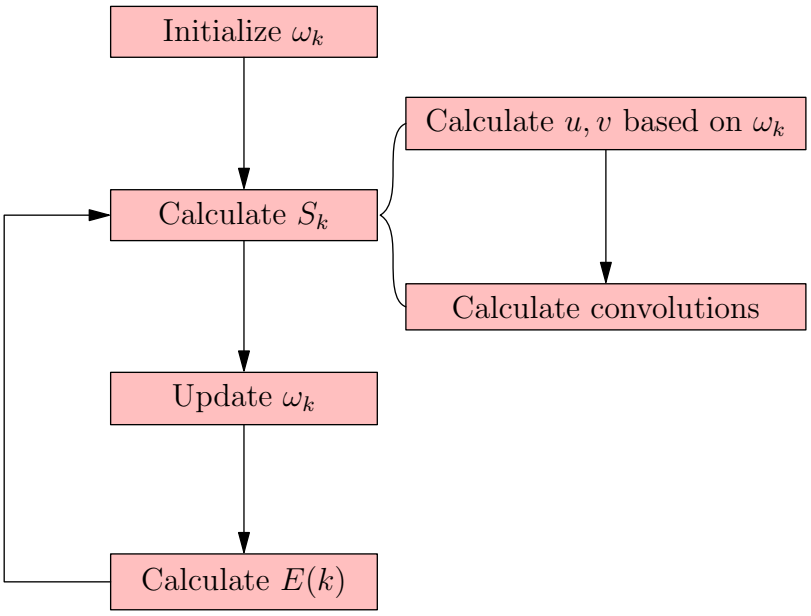

Figure 4.2: Solution algorithm

4.D Governing equations revisited

Counting the number of FFTs required for the numerical solution of (4.12), it can be observed that there are 5 FFTs (four inverse FFTs for u, v, $\frac{\partial \omega}{\partial x}$, and $\frac{\partial \omega}{\partial y}$, and one forward transform of the resulting advection term). Now, we can ask if it is possible to reduce the number of FFTs required in the numerical solution, since they are the most expensive part of calculation?

The answer is positive if we rewrite the governing equation more intelligently using some sort of symmetries available by using incompressibility. This was done both for 2D and 3D cases by Basdevant [1983], however it seems that it has not been well appreciated since then. This approach will reduce the number of required FFTs from five to four. Regarding the fact that taking fast Fourier transforms (both forward or backward) is the most expensive part of the calculation, it can be easily understood that this new representation of governing equations can significantly speed up the solution. In the following we will represent the argument proposed by Basdevant [1983] for the three-dimensional case, as well as the corresponding two-dimensional one.

4.D.1 3D case

Let us begin with our governing equations (4.1):

$$\begin{cases} \dfrac{\partial \boldsymbol{u}}{\partial t} + \boldsymbol{u} \cdot \boldsymbol{\nabla} \boldsymbol{u} = -\boldsymbol{\nabla} p + \nu \nabla^2 \boldsymbol{u} + \boldsymbol{F}, \\ \\ \boldsymbol{\nabla} \cdot \boldsymbol{u} = 0. \end{cases} \tag{4.13}$$

Expanding the above equation for the first component the velocity vector, we have:

$$\frac{\partial u}{\partial t} + u\frac{\partial u}{\partial x} + v\frac{\partial u}{\partial y} + w\frac{\partial u}{\partial z} = -\boldsymbol{\nabla} p + \nu\nabla^2 u + \boldsymbol{F}. \tag{4.14}$$

Using incompressibility, we can rewrite the (4.14) as what follows:

$$\frac{\partial u}{\partial t} + \frac{\partial uu}{\partial x} + \frac{\partial uv}{\partial y} + \frac{\partial uw}{\partial z} = -\boldsymbol{\nabla} p + \nu\nabla^2 u + \boldsymbol{F}. \tag{4.15}$$

This motivates us to define a symmetric tensor $D_{ij} = u_i u_j$, where $(u_1, u_2, u_3) \doteq (u, v, w)$, and now changing to index notation, we can rewrite the (4.1) in the following compact form:

$$\frac{\partial u_i}{\partial t} + \frac{\partial D_{ij}}{\partial x_j} = -\frac{\partial p}{\partial x_i} + \nu\frac{\partial^2 u_i}{\partial x_j \partial x_j} + F_i. \tag{4.16}$$

Now, as we intend to solve our equations in Fourier space, we need to take the Fourier transform of the above equation, the same process mentioned for (4.12), so by the definition of the symmetric tensor D_{ij}, we have to take three inverse FFTs for velocity components, and then calculate six independent components of the tensor D_{ij}, and afterwards take their FFT transforms to get back to Fourier space. So, it can be easily observed that the naive method requires 9 FFTs. However Basdevant [1983] showed that this number can be reduced to eight. This is done by defining a diagonal tensor, $E_{ij} = \delta_{ij} P_{jk} e_k$, where the matrix P is the corresponding permutation matrix for $1 \to 2 \to 3 \to 1$, and $e_k = u_k^2$. Using this tensor, we can rewrite (4.16) as the following form:

$$\frac{\partial u_i}{\partial t} + \frac{\partial (D_{ij} - E_{ij})}{\partial x_j} = -\frac{\partial (p + u_j u_j)}{\partial x_i} + \nu\frac{\partial^2 u_i}{\partial x_j \partial x_j} + F_i. \tag{4.17}$$

Looking thoroughly at the above equation, it can be noticed that instead of six independent components that we had for D_{ij}, in $D_{ij} - E_{ij}$ any of the diagonal components can be calculated as the negative of the addition of the other two diagonal components, so $D_{ij} - E_{ij}$ has just five independent terms, which consequently requires five FFTs. This means that our governing equation can be solved using just eight FFTs. (A careful reader may notice that the new term added to the right-hand side of the equation, $u_j u_j$, does not involve any extra FFT).

4.D.2 2D case

In two dimensions, we begin with the inertial term in the vorticity equation:

$$\boldsymbol{u} \cdot \boldsymbol{\nabla}\omega = u\frac{\partial \omega}{\partial x} + v\frac{\partial \omega}{\partial y}. \tag{4.18}$$

Using incompressibility, we can rewrite the inertial term S:

$$S \doteq u\frac{\partial \omega}{\partial x} + v\frac{\partial \omega}{\partial y} = \frac{\partial (u\omega)}{\partial x} + \frac{\partial (v\omega)}{\partial y}. \tag{4.19}$$

On the other hand, $\omega = \dfrac{\partial v}{\partial x} - \dfrac{\partial u}{\partial y}$, so we can rewrite the inertial term as follows

$$S = \frac{\partial(u\omega)}{\partial x} + \frac{\partial(v\omega)}{\partial y} = \frac{\partial}{\partial x}\left(u\frac{\partial v}{\partial x} - u\frac{\partial u}{\partial y}\right) + \frac{\partial}{\partial y}\left(v\frac{\partial v}{\partial x} - v\frac{\partial u}{\partial y}\right) \tag{4.20}$$

$$= \frac{\partial}{\partial x}\left(u\frac{\partial(uv)}{\partial x} - v\frac{\partial u}{\partial x} - \frac{1}{2}\frac{\partial u^2}{\partial y}\right) + \frac{\partial}{\partial y}\left(\frac{1}{2}\frac{\partial v^2}{\partial x} - \frac{\partial(uv)}{\partial y} - u\frac{\partial v}{\partial y}\right)$$

$$= \frac{\partial^2(uv)}{\partial x^2} - \frac{1}{2}\frac{\partial^2 u^2}{\partial x \partial y} - \frac{\partial}{\partial x}\left(v\frac{\partial u}{\partial x}\right) + \frac{1}{2}\frac{\partial^2 v^2}{\partial x \partial y} - \frac{\partial^2(uv)}{\partial y^2} + \frac{\partial}{\partial y}\left(u\frac{\partial v}{\partial y}\right)$$

$$= \left(\frac{\partial^2}{\partial x^2} - \frac{\partial^2}{\partial y^2}\right)(uv) + \frac{1}{2}\frac{\partial^2}{\partial x \partial y}\left(v^2 - u^2\right) + \frac{\partial}{\partial y}\left(u\frac{\partial v}{\partial y}\right) - \frac{\partial}{\partial x}\left(v\frac{\partial u}{\partial x}\right). \tag{4.21}$$

Using incompressibility again for the last two terms on the right-hand side, we obtain

$$S = \left(\frac{\partial^2}{\partial x^2} - \frac{\partial^2}{\partial y^2}\right)(uv) + \frac{\partial^2}{\partial x \partial y}\left(v^2 - u^2\right), \tag{4.22}$$

so the vorticity equation in Fourier space can be written

$$\frac{\partial \omega_{\boldsymbol{k}}}{\partial t} = -\mathcal{F}\left\{\left(\frac{\partial^2}{\partial x^2} - \frac{\partial^2}{\partial y^2}\right)(uv) + \frac{\partial^2}{\partial x \partial y}\left(v^2 - u^2\right)\right\} - \nu k^2 \omega_{\boldsymbol{k}} + f_{\boldsymbol{k}}. \tag{4.23}$$

Two transforms are required to compute u and v in physical space, from which the quantities uv and $v^2 - u^2$ can then be calculated and transformed back to Fourier space with two additional transforms. The advective term in 2D can thus be calculated with four FFTs.

Chapter 5

Numerical Simulations and Results

In this chapter we report on the results of numerical simulations of 2D homogeneous isotropic incompressible turbulence with white-noise forcing done with one of the fastest direct numerical simulation (DNS) codes available at the time of this work, publically available at https://github.com/dealias/dns. It is a well-known fact that DNS simulations are by far the most expensive simulations in the field of fluid mechanics and especially turbulence. So this numerical method cannot be used for practical applications, unless either the domain of the simulation is small or a heuristic subgrid scale model is employed. We recall that one of the main assumptions behind almost all theoretical analysis of incompressible homogeneous isotropic turbulence is that the Reynolds number $R_e \to \infty$. Approach this limit requires an extremely refined grid, which is fundamentally the main obstacle towards numerically simulating turbulence. The reader must therefore bear in mind that simulations based on the DNS method are just approximations for the

ideal simulation, which will likely remain infeasible until at least the mid-21st century.

5.A An overview of the DNS code

All the simulations whose main results will be shown later on in this chapter have been done using one of most advanced and probably the fastest DNS code available at the time of this work. The code, which is called `DNS`, was written by Professor John C. Bowman at the University of Alberta. Under the hood, the code, written in C++, is quite complicated. It is comprised of a kernel called `TRIAD` containing an advanced differential equation solver that receives a discretized form of any differential equation (ODE & PDE). This packages also contains a set of different numerical integrators and exploits the `FFTW++` library for calculating implicit dealiased convolutions [Bowman & Roberts 2011], along with many other features. A general overview of the `DNS` software is represented in Figure 5.1. The reader who is interested in learning more about `DNS` is referred to `https://github.com/dealias/dns/tree/master/2d`.

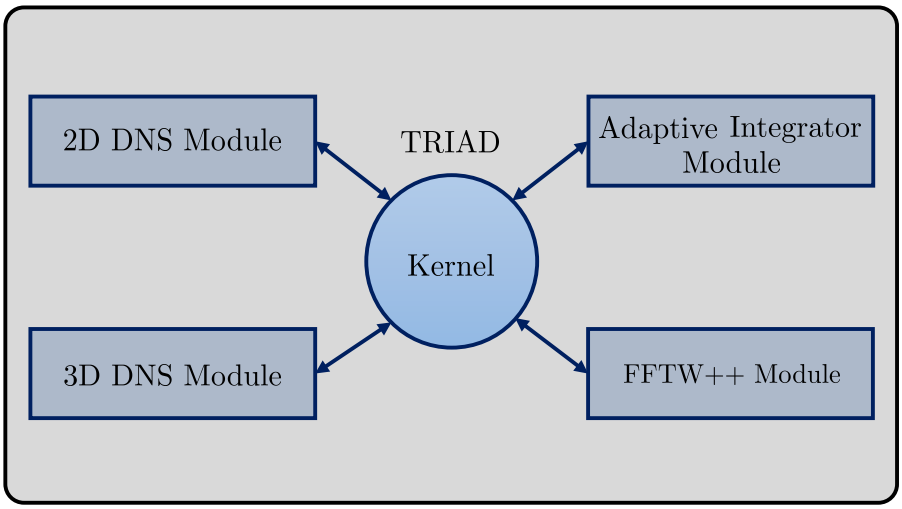

Figure 5.1: DNS overview

The software DNS is an advanced pseudospectral direct numerical simulation code that exploits implicit dealiasing and advanced computer memory management, like padding and memory alignment to attain its extreme performance. Besides applying many technical features, it makes use of the argument of Basdevant [1983] to minimize the number of FFTs required for simulating two and three-dimensional turbulence. It is worth noting here that a simplified version of the DNS code called PROTODNS has also been developed for educational purposes: https://github.com/dealias/dns/tree/master/protodns.

5.B Numerical simulations

The numerical method, algorithm, and implementation utilized in DNS and all relevant topics are explained in detail in Chapter 4. Before demonstrating the numerical simulation, it is vital to talk briefly about some numerical considerations applied to the simulations. As we mentioned in Chapter 1,

by the work of Kraichnan in 1969, the 2D variant of Kolmogorov theory involves both a direct cascade of enstrophy and an inverse cascade of energy. This means that energy goes to the low wavenumbers (large scales) and will eventually pile up at the large scales. In the real physical world, one of the places where 2D turbulence happens under some special circumstances is believed to be in high altitude layers of the atmosphere. It is believed that for this case of 2D turbulence, the energy cascading to the large scales is taken out by some external physical mechanisms like atmospheric gravity waves. If this is the case, how can that be implemented in numerical simulations? The answer is basically by adding some sort of artificial damping to the Navier–Stokes equation. Although there are different approaches toward applying this idea like hyper-viscosity, constant large-scale friction, etc., a common impact of all these methods is the fact that they will change the Navier–Stokes equation into another equation. This implies that one does not actually solve the true Navier–Stokes equation when these energy extracting mechanisms are implemented.

Although it also has the capability of solving the true Navier–Stokes equation, the `DNS` code can optionally apply some sort of artificial energy extracting method. A large-scale linear friction term proportional to a coefficient ν_L can be included, somewhat in analogy to the molecular viscosity term of the Navier–Stokes equation, proportional to ν_H. This capability of the `DNS` code makes it possible to track down the dominant effect of this extra term on the global attractor, an investigation that has not previously been performed. This investigation could open many new doors into the long controversial debate about the possible effects of such artificial energy damping methods.

In the following demonstrated numerical results, the choice $\nu_L = 0$ indicates

the solution of the true Navier–Stokes equation (truncated at a high wavenumber, corresponding to the given resolution).

5.B.1 White-noise forcing

In this section, the numerical results obtained from simulating the 2D homogeneous isotropic incompressible turbulence with white-noise forcing and periodic boundary conditions are demonstrated. The implementation of the white-noise forcing is limited to an annulus in the Fourier lattice domain, as shown in the Figure 5.2.

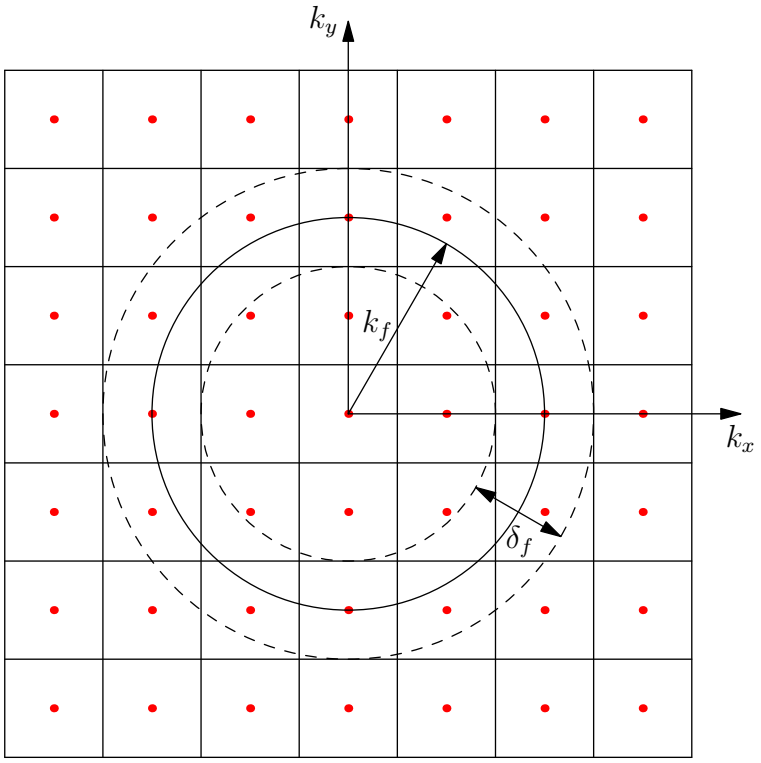

Figure 5.2: Banded forcing region on the Fourier lattice.

5.B.2 Attractor in the Z–E plane

In the rest of this section we present pseudospectral simulation results for the two-dimensional forced-dissipative scalar vorticity equation

$$\frac{\partial \omega}{\partial t} + (\hat{\boldsymbol{z}} \times \boldsymbol{\nabla} \nabla^{-2} \omega \cdot \boldsymbol{\nabla}) \omega = \nu_H \nabla^2 \omega - H(k_L - k) \nu_L \omega + f, \tag{5.1}$$

where H is the Heaviside unit step function.

Upon expressing the nonlinearity as

$$S = (\hat{\boldsymbol{z}} \times \boldsymbol{\nabla} \nabla^{-2} \omega \cdot \boldsymbol{\nabla}) \omega,$$

and Fourier transforming, the enstrophy spectrum $Z(k) = k^2 E(k)$ is seen to satisfy a balance equation of the form

$$\frac{\partial}{\partial t} Z(k) + 2(\nu_H k^2 + \nu_L H(k_L - k)) Z(k) = 2T(k) + G(k),$$

where $T(k)$ and $G(k)$ represent angular sums of $\mathrm{Re}\,\langle S_{\boldsymbol{k}} \omega_{\boldsymbol{k}}^* \rangle$ and $\mathrm{Re}\,\langle f_{\boldsymbol{k}} \omega_{\boldsymbol{k}}^* \rangle$, respectively. Following Kraichnan [1959], it is convenient to define the *nonlinear enstrophy transfer* $\Pi(k)$, which measures the cumulative nonlinear transfer of enstrophy into $[k, \infty)$:

$$\Pi(k) = 2 \int_k^\infty T(p)\, dp.$$

On integrating from k to ∞, we find

$$\frac{d}{dt} \int_k^\infty Z(p)\, dp = \Pi(k) - \eta(k),$$

where $\eta(k) \doteq 2 \displaystyle\int_k^\infty (\nu_H p^2 + \nu_L H(k_L - k)) Z(p)\, dp - \int_k^\infty G(p)\, dp$ is the total

enstrophy transfer, via dissipation and forcing, out of wavenumbers higher than k. A positive (negative) value for $\Pi(k)$ represents a flow of enstrophy to wavenumbers higher (lower) than k. When $\nu = f_{\boldsymbol{k}} = 0$, enstrophy conservation implies that

$$0 = \frac{d}{dt}\int_0^\infty Z(p)\,dp = 2\int_0^\infty T(p)\,dp,$$

so that

$$\Pi(k) = 2\int_k^\infty T(p)\,dp = -2\int_0^k T(p)\,dp. \tag{5.2}$$

We note that $\Pi(0) = \Pi(\infty) = 0$. Moreover, in a steady state, $\Pi(k) = \eta(k)$; this provides an excellent numerical diagnostic for validating a steady state.

We evolve the simulations starting from anisotropic Hermitian initial conditions of the form

$$\boldsymbol{\omega}(k_x, k_y)(0) = \sqrt{\frac{\sqrt{k_x^2 + k_y^2} + i(k_x + k_y)}{\alpha + \beta k^2}},$$

which corresponds to an initial energy spectrum

$$E(k) = \frac{\pi k}{\alpha + \beta k^2}$$

and total energy $E = \int E(k)\,dk = \frac{1}{2}\sum_k \omega_{\boldsymbol{k}}^2/k^2$.

In Figures 5.3 and 5.4 the vorticity fields are shown for two numerical simulations of (5.1) with identical values of η, k_f, δ_f, α, β, and ν_H, but different values of ν_L. Figure 5.3 demonstrates the effect of applying an artificial energy damping mechanism at large scales, with $\nu_L = 0.15$ and $k_L = 3.5$, whereas Figure 5.4 depicts the vorticity field for the pure Navier–Stokes equation considered in the theoretical analysis of this work, where $\nu_L = 0$. Figures 5.5 and 5.6 illustrate the Z–E evolution for these simulations, respectively. Each dot represents 1000 variable time steps of mean duration 0.003 and 0.0005,

respectively. Comparing these results highlights the dramatic impact that the *hypoviscosity* term $\nu_L\omega$ in (5.1) has on the turbulent dynamics. Instead of approaching the projected global attractor that we have found for (2.3), the solutions are absorbed into the region characterized by the two pink lines in Figure 5.5 that denote the slopes $k_f + \frac{1}{2}\delta_f$ and $k_f - \frac{1}{2}\delta_f$, respectively. In contrast, once the hypoviscous term is removed, we observe in Fig. 5.6 an outstanding agreement of the numerical simulation and the predicted projection of the global attractor on the Z–E plane.

Figures 5.7 and 5.8 demonstrate the energy spectrums corresponding to these simulations. As is seen in Figure 5.7, the application of an energy damping mechanism at large scales tends to flatten the large-scale energy spectrum, while in Figure 5.8, the absence of this mechanism is reflected as a steeper slope for the energy spectrum at large scales. Figures 5.9 and 5.10 represent the energy and enstrophy transfers for the corresponding simulations. The coincidence of these graphs (which is expected theoretically) is an indication of being in a quasisteady state, where both the enstrophy injection and dissipation rates are nearly in balance.

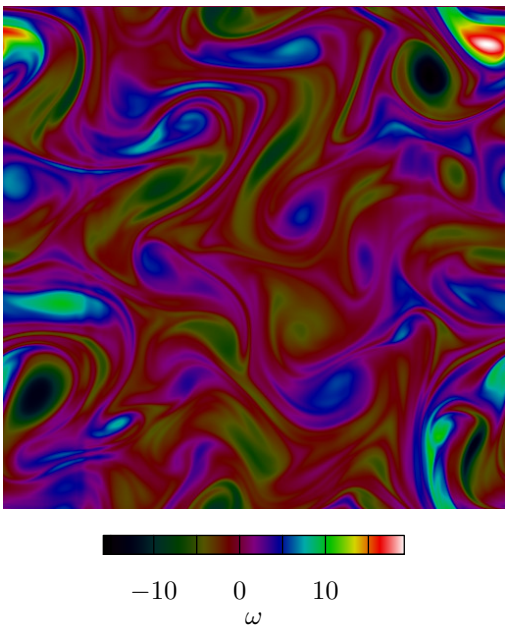

Figure 5.3: Vorticity field for white-noise forcing computed with 511×511 dealiased modes using $\eta = 1$, $k_f = 4$, $\delta_f = 1$, $k_L = 3.5$, $\nu_H = 0.0005$, $\nu_L = 0.15$, $\alpha = 10^4$, and $\beta = 10^4$.

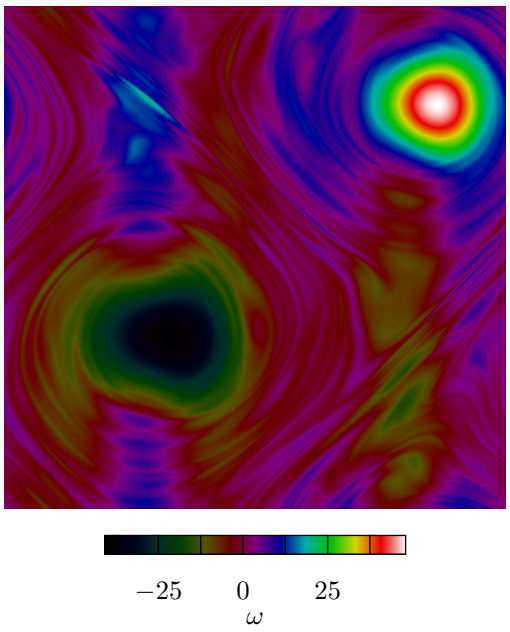

Figure 5.4: Vorticity field for white-noise forcing computed with 511×511 dealiased modes using $\eta = 1$, $k_f = 4$, $\delta_f = 1$, $\nu_H = 0.0005$, $\nu_L = 0$, $\alpha = 10^4$, and $\beta = 10^4$.

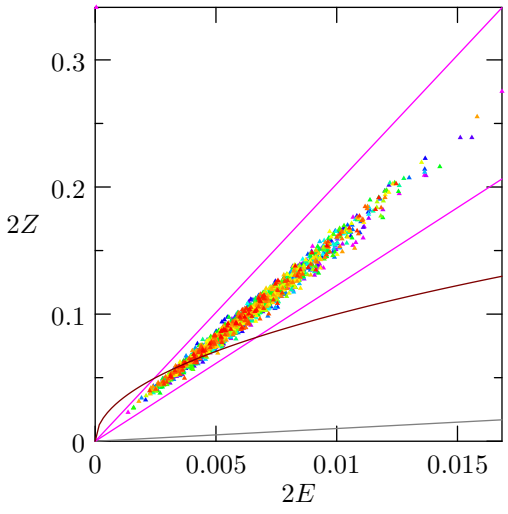

Figure 5.5: Enstrophy vs. energy for the simulation shown in Fig. 5.3.

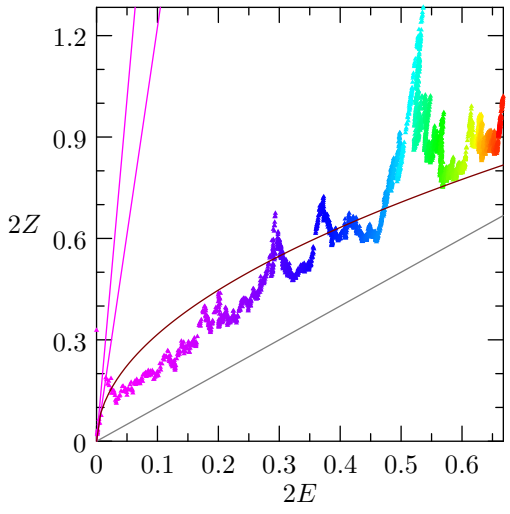

Figure 5.6: Enstrophy vs. energy for the simulation shown in Fig. 5.4.

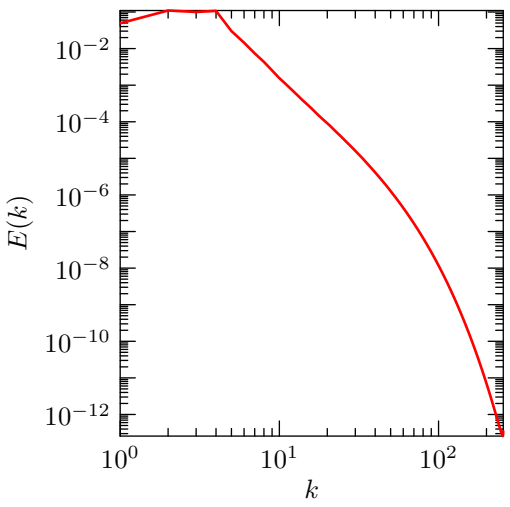

Figure 5.7: The energy spectrum for the simulation shown in Fig. 5.3.

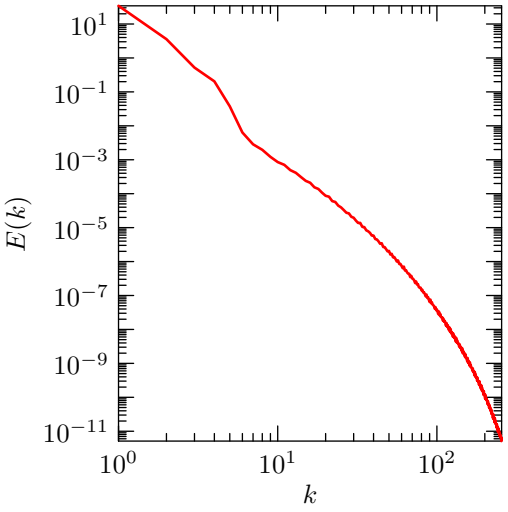

Figure 5.8: The energy spectrum for the simulation shown in Fig. 5.4.

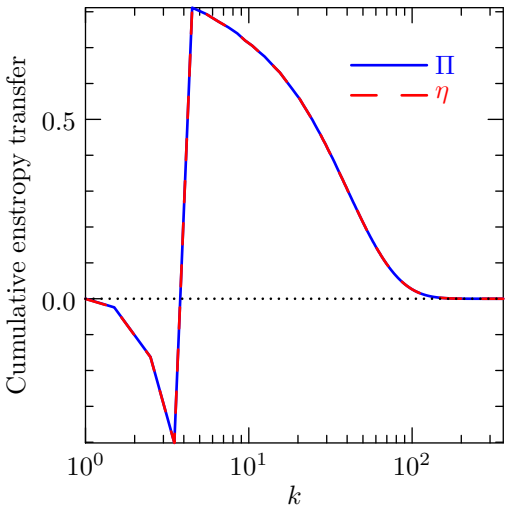

Figure 5.9: The enstrophy transfer for the simulation shown in Fig. 5.3.

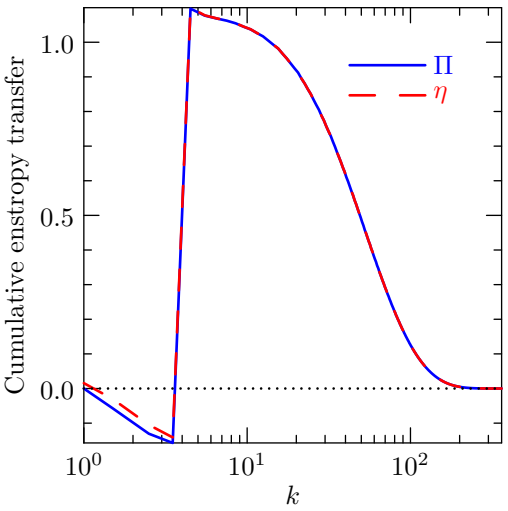

Figure 5.10: The enstrophy transfer for the simulation shown in Fig. 5.4.

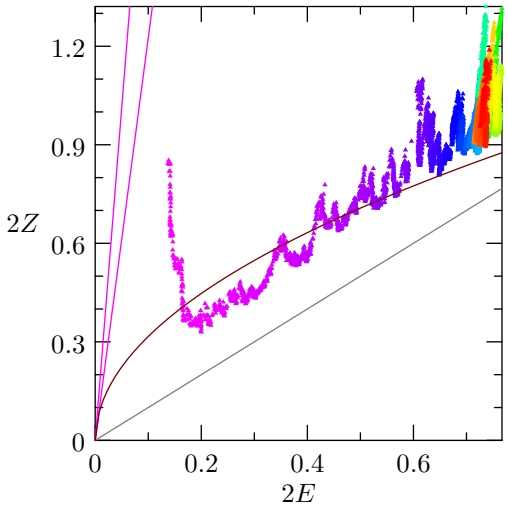

Figure 5.11: Enstrophy vs. energy for white-noise forcing computed with 255×255 dealiased modes using $\eta = 1$, $k_f = 4$, $\delta_f = 1$, $\nu_H = 0.0005$, $\nu_L = 0$, $\alpha = 1$, and $\beta = 1$.

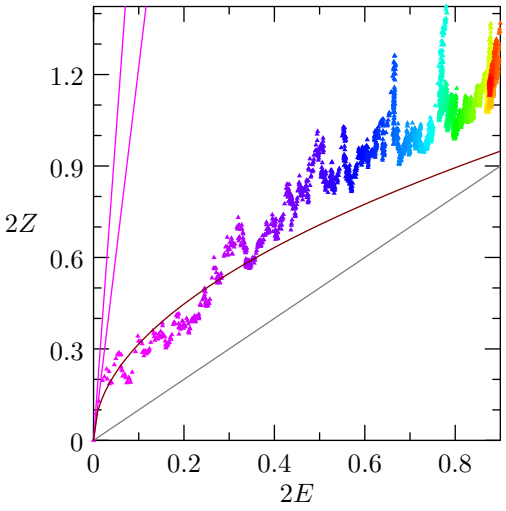

Figure 5.12: Enstrophy vs. energy for white-noise forcing computed with 255×255 dealiased modes using $\eta = 10^{12}$, $k_f = 4$, $\delta_f = 1$, $\nu_H = 5$, $\nu_L = 0$, $\alpha = 1$, and $\beta = 1$.

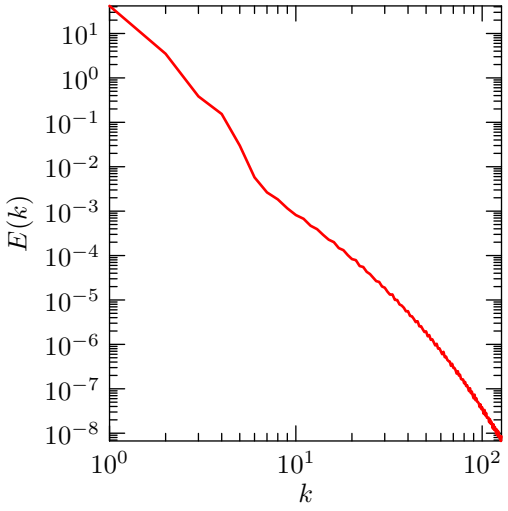

Figure 5.13: The energy spectrum for the simulation shown in Fig. 5.11.

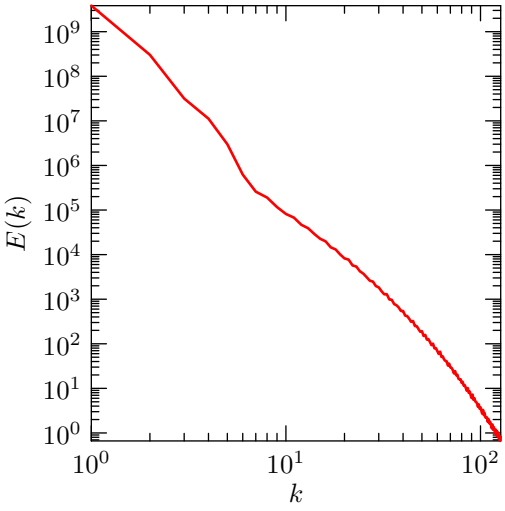

Figure 5.14: The energy spectrum for the simulation shown in Fig. 5.12.

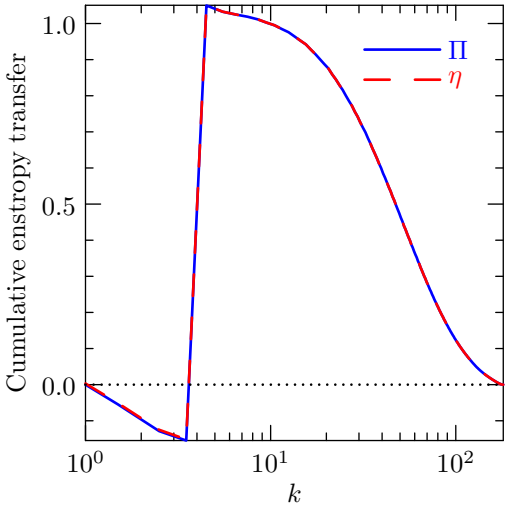

Figure 5.15: The enstrophy transfer for the simulation shown in Fig. 5.11.

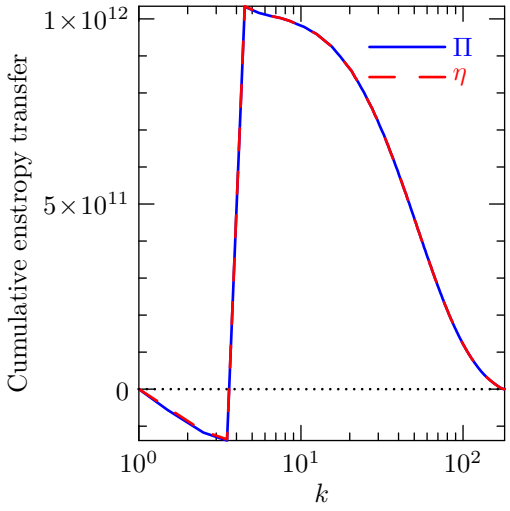

Figure 5.16: The enstrophy transfer for the simulation shown in Fig. 5.12.

To test the sensitivity of these results with respect to resolution and initial conditions, we repeated the simulation shown in Figure 5.3 with a larger initial condition and a lower 255×255 resolution. The corresponding energy spectrum and cumulative enstrophy transfer graphs are shown in Figures 5.13 and 5.15. The projection of the solution onto the Z–E plane is shown in Figure 5.11, where for illustration purposes, the evolution of the first $100,000$ timesteps is omitted. Finally, Figure 5.12 illustrates the projection of the global attractor for $\eta = 10^{12}$ and $\nu_H = 5$, with a 255×255 resolution. Here we need to address one issue regarding the very large values of the parameters in this simulation. This issue pertains to the finite floating-point representation used on digital computers, which can result in a loss of precision. Due to the sensitivity of turbulence to the initial conditions, this issue could well cause significant discrepancies between numerical and analytical results. Nevertheless, Figure 5.12 demonstrates the robustness of the numerical simulation

and the global attractor. Figures 5.14 and 5.16 depict the energy spectrum and transfer graphs for this simulation.

In the preceding results, we have observed excellent agreement between the theoretical predictions and high accuracy numerical simulations based on the pseudospectral method. One observes the attraction of the solutions to the global attractor, whose projection lies in the region characterized by the upper and lower bounds. We also established the robustness of the numerical simulation with respect to changes in the resolution and initial conditions. In other simulations not shown here, we addressed the consistency and robustness of the numerical results with respect to changes in k_f and δ_f.

Chapter 6

Conclusions

6.A Main results of this work

The most important achievement of this work is the extension of the bounds in the Z–E plane obtained by Dascaluic, Foias, and Jolly [2005, 2010] for 2D incompressible homogenous isotropic turbulence, under the assumption of constant forcing, to the more realistic case of random forcing. This valuable result has a few consequences, some of which should be followed up in future work. For example:

1. The analytical bounds for random forcing provide a means to evaluate various heuristic turbulent subgrid models by characterizing the behaviour of the global attractor under these models.

2. The bounds should assist one in studying artificial energy damping mechanisms designed to remove the energy that cascades upscale before it piles up and reflects off the largest scale, back towards smaller scales.

3. With these tools, it should now be possible to study the relation between

a specific white-noise forcing and a constant forcing by examining their effect on the global attractor, which may lead to an explicit relation for the energy and enstrophy injection rates for constant forcing.

6.B Future works and improvements

It is sometimes said the only well-understood fact about turbulence is that there is so much about turbulence to learn, with many open questions. In this section we try to address some of the issues that require further research and are relevant to the present work. The list here is by no means exhaustive. As the reader might have noticed, the field of turbulence is connected to many areas of mathematics, and so we can look at these open areas from two separate point of view: analytic problems and numerical difficulties.

6.B.1 Theoretical and analytic difficulties

The complexity of turbulence is such that even the simplest case, the two-dimensional homogeneous isotropic incompressible turbulence with periodic boundary conditions, is still far from the point of thorough understanding.

An important extension of this work is the analysis of a more practical example of turbulence (e.g. anisotropic turbulence), with more realistic boundary conditions. The reader may observe that even under the assumption of isotropic homogeneous incompressible turbulence, if we want to consider realistic laboratory boundary conditions, there is no guarantee that the bilinear map identities will remain valid. Furthur functional analysis could lead to major improvements in the field of turbulence, especially for understanding turbulent behaviour near boundaries, for which there is currently no rigorous mathematical

theory.

In contrast to the case of white-noise forcing, in the case of a constant forcing, there is no a valid theory that can estimate the enstrophy and energy injection with respect to the forcing magnitude. This makes it almost impossible to compare analytic results obtained for constant forcing with experiments, even though it might seem to be easier to deal with constant forcing than other alternatives.

6.B.2 Numerical deficiencies and problems

Another field involving turbulence that has many difficulties on its own is the world of numerical simulations. From the lack of computational resources to numerical discretization error to the problem of finite floating-point precision, one must confront many issues. In the following, we are going to list some of the most important numerical simulation issues specifically for the case of two-dimensional turbulence.

1. Every numerical simulation has to deal with finite-floating point precision, which leads to a constraint on refining the numerical lattice. This is a well-known problem in numerical simulations like turbulence that are very sensitive to and dependent on having a well-refined lattice.

2. In pseudospectral simulation of high Reynolds number turbulence, refining the grid down to the Kolmogorov dissipation scale k_d, is almost impossible due to memory limitations, computation time, and even machine precision. To have a more tangible feeling for the time required to model high Reynolds number with the pseudospectral method, running on the most

advanced available parallel computers, all the way to the Kolmogorov dissipation scale, a realistic speculation would be millions of years.

For engineering applications, it is essential to somehow tackle this deficiency. There is a common approach called subgrid modelling, where one strives to obtain a reasonable model of the damping effect of neglected small scales on larger scales. This makes it possible to avoid the use of a highly refined grid, significantly speeding up the simulation. Although these heuristic models are not based on a firm mathematical foundation, they are the best one can currently do as far as obtaining a crude realization of turbulence using current technology and computational resources.

3. Finally, one of the main important problems for simulating 2D turbulence is the artificial large-scale damping (*hypoviscosity*) introduced in most numerical studies. This work raises serious questions about the impact of these artificial energy damping mechanisms on turbulent behaviour. Perhaps an awareness of constraints on the global attractor can direct researchers in devising less interfering artificial energy damping models.

Now that we have been acquainted with some of the main obstacles along the way to understanding turbulence, we have a fairly clear picture about the directions in which future research and improvements should be guided. Except for the first problem, which is a matter of technology and time, solving the other two difficulties will require much effort and perseverance. Realistic subgrid models could arise out of a tight interaction between mathematics and physics, leading to a deep understanding of the possible effects of the various artificial damping mechanisms in current simulations of turbulence.

Appendix A

Bilinear Maps

A *bilinear map* $\mathcal{B} : V \times V \to V$ over a vector space V is a function that is linear in each argument separately. That is, for all $\boldsymbol{u}$, $\boldsymbol{v}$, $\boldsymbol{w} \in V$, and scalars λ:

$$\mathcal{B}(\boldsymbol{u}+\boldsymbol{v},\boldsymbol{w}) = \mathcal{B}(\boldsymbol{u},\boldsymbol{w}) + \mathcal{B}(\boldsymbol{v},\boldsymbol{w}) \quad \text{and} \quad \mathcal{B}(\lambda\boldsymbol{u},\boldsymbol{v}) = \lambda\mathcal{B}(\boldsymbol{u},\boldsymbol{v}),$$
$$\mathcal{B}(\boldsymbol{u},\boldsymbol{v}+\boldsymbol{w}) = \mathcal{B}(\boldsymbol{u},\boldsymbol{v}) + \mathcal{B}(\boldsymbol{u},\boldsymbol{w}) \quad \text{and} \quad \mathcal{B}(\boldsymbol{u},\lambda\boldsymbol{v}) = \lambda\mathcal{B}(\boldsymbol{u},\boldsymbol{v}).$$

The main purpose of the definition of the bilinear term is to represent the Navier–Stokes equation in a more compact form. We recall the two-dimensional incompressible homogeneous Navier–Stokes equation on the domain $\Omega = \Omega_2 \doteq [0, 2\pi]^2$, with periodic boundary conditions on $\partial\Omega$, formulated as

$$\begin{aligned}
&\frac{\partial \boldsymbol{u}}{\partial t} - \nu\nabla^2\boldsymbol{u} + \boldsymbol{u}\cdot\boldsymbol{\nabla}\boldsymbol{u} + \boldsymbol{\nabla}\left(\frac{p}{\rho}\right) = \boldsymbol{F},\\
&\boldsymbol{\nabla}\cdot\boldsymbol{u} = 0,\\
&\int_\Omega \boldsymbol{u}\, d\boldsymbol{x} = \boldsymbol{0}, \qquad \int_\Omega \boldsymbol{F}\, d\boldsymbol{x} = \boldsymbol{0},\\
&\boldsymbol{u}(\boldsymbol{x},0) = \boldsymbol{u}_0(\boldsymbol{x}).
\end{aligned}$$

We consider this problem in the *Hilbert* space

$$H(\Omega) \doteq \mathrm{cl}\left\{ \boldsymbol{u} \in C^2(\Omega) \cap L^2(\Omega) \mid \boldsymbol{\nabla}\cdot\boldsymbol{u} = 0,\ \int_\Omega \boldsymbol{u}\, d\boldsymbol{x} = \boldsymbol{0} \right\},$$

with the standard inner product

$$(\boldsymbol{u}, \boldsymbol{v}) = \int_\Omega \boldsymbol{u}(\boldsymbol{x})\cdot\boldsymbol{v}(\boldsymbol{x})\, d\boldsymbol{x}, \quad \text{where} \quad \boldsymbol{a}\cdot\boldsymbol{b} = \sum_i a_i b_i.$$

Although our analysis will be limited to Ω_2, later on in this section we will see that some of our identities can be extended to $\Omega_3 = [0, 2\pi]^3$, so in general let us consider a velocity vector field

$$\boldsymbol{u} : \Omega_3 \times \mathbb{R} \longrightarrow \mathbb{R}^3, \qquad \boldsymbol{\nabla}\cdot\boldsymbol{u} = 0.$$

It is convenient to rewrite the nondimensional incompressible Navier–Stokes equation (with $\rho = 1$) as

$$\frac{\partial \boldsymbol{u}}{\partial t} + \boldsymbol{u}\cdot\boldsymbol{\nabla}\boldsymbol{u} = -\boldsymbol{\nabla}p - \nu\nabla^2\boldsymbol{u} + \boldsymbol{f}$$

in terms of the positive semi-definite operator $A = -\nabla^2$ and bilinear map $\mathcal{B}(\boldsymbol{u}, \boldsymbol{u}) = \mathcal{P}(\boldsymbol{u}\cdot\boldsymbol{\nabla}\boldsymbol{u} + \boldsymbol{\nabla}p)$:

$$\frac{\partial \boldsymbol{u}}{\partial t} + \nu A\boldsymbol{u} + \mathcal{B}(\boldsymbol{u}, \boldsymbol{u}) = \boldsymbol{f}, \tag{A.1}$$

where $\mathcal{P}$ is the *Helmholtz–Leray projection operator* to H defined as

$$\mathcal{P}(\boldsymbol{v}) = \boldsymbol{v} - \boldsymbol{\nabla}\nabla^{-2}\boldsymbol{\nabla}\cdot\boldsymbol{v}, \qquad \forall \boldsymbol{v} \in H.$$

The bilinear map, $\mathcal{B}(\boldsymbol{u},\boldsymbol{u})$, involves a few important identities in the case of two and three-dimensional incompressible fluid flows. Here, we are going to prove some of the important identities of bilinear map, especially in the case of 2D flow, which were used in previous chapters.

1.A Orthogonality in three-dimensional incompressible flows

In the case of three-dimensional incompressible flow, the bilinear map represents the following useful identity

$$(\mathcal{B}(\boldsymbol{u},\boldsymbol{v}),\boldsymbol{w}) = -(\mathcal{B}(\boldsymbol{u},\boldsymbol{w}),\boldsymbol{v}), \quad \forall\ \boldsymbol{u},\boldsymbol{v},\boldsymbol{w} \in H(\Omega_3). \tag{A.2}$$

Having the incompressibility condition for $\boldsymbol{u},\boldsymbol{v}$, and $\boldsymbol{w}$, we can write

$$\begin{aligned}(\mathcal{B}(\boldsymbol{u},\boldsymbol{v}),\boldsymbol{w}) &= \int_\Omega \mathcal{B}(\boldsymbol{u},\boldsymbol{v})\cdot\boldsymbol{w}\, d\boldsymbol{x} = \int_\Omega \left(u_i\frac{\partial v_j}{\partial x_i} + \frac{\partial p}{\partial x_j}\right) w_j\, d\boldsymbol{x} \\ &= \underbrace{\int_\Omega u_i\frac{\partial v_j}{\partial x_i} w_j\, d\boldsymbol{x}}_{I} + \underbrace{\int_\Omega \frac{\partial p}{\partial x_j} w_j\, d\boldsymbol{x}}_{J},\end{aligned} \tag{A.3}$$

so we have

$$\begin{aligned}I &= \int_\Omega \frac{\partial(u_i v_j w_j)}{\partial x_i}\, d\boldsymbol{x} - \int_\Omega \frac{\partial u_i}{\partial x_i} v_j w_j\, d\boldsymbol{x} - \int_\Omega u_i\frac{\partial w_j}{\partial x_i} v_j\, d\boldsymbol{x} \\ &= \int_{\partial\Omega} u_i v_j w_j\, \hat{n}_i\, ds - \int_\Omega u_i\frac{\partial w_j}{\partial x_i} v_j\, d\boldsymbol{x} \\ &= -\int_\Omega u_i\frac{\partial w_j}{\partial x_i} v_j\, d\boldsymbol{x},\end{aligned}$$

and similarly

$$J = \int_\Omega \frac{\partial(pw_j)}{\partial x_j}\, d\boldsymbol{x} - \int_\Omega p\frac{\partial w_j}{\partial x_j}\, d\boldsymbol{x} = \int_{\partial\Omega} (pw_j)\hat{n}_j\, ds = 0,$$

where the integrals on the boundary $\partial\Omega$ vanish because of periodicity. So, (A.3) can be written as

$$(\mathcal{B}(\boldsymbol{u},\boldsymbol{v}),\boldsymbol{w}) = I + J = -\int_\Omega u_i \frac{\partial w_j}{\partial x_i} v_j\, d\boldsymbol{x} - \int_\Omega \frac{\partial p}{\partial x_j} v_j\, d\boldsymbol{x} \tag{A.4}$$

$$= -\int_\Omega \mathcal{B}(\boldsymbol{u},\boldsymbol{w})\cdot\boldsymbol{v}\, d\boldsymbol{x} = -(\mathcal{B}(\boldsymbol{u},\boldsymbol{w}),\boldsymbol{v}). \tag{A.5}$$

1.B Orthogonality in two-dimensional incompressible flows

For two-dimensional incompressible flows there are a few important identities that we are going to talk about in this and the following sections. The orthogonality identity reads

$$(\mathcal{B}(\boldsymbol{u},\boldsymbol{u}), A\boldsymbol{u}) = 0, \quad \text{where} \quad A = -\nabla^2.$$

The proof is based on some important vector calculus identities:

$$\boldsymbol{\nabla}\cdot(\boldsymbol{A}\times\boldsymbol{B}) = \boldsymbol{B}\cdot(\boldsymbol{\nabla}\times\boldsymbol{A}) - \boldsymbol{A}\cdot(\boldsymbol{\nabla}\times\boldsymbol{B}), \tag{A.5 i}$$

$$\boldsymbol{\nabla}\times(\boldsymbol{\nabla}\times\boldsymbol{A}) = \boldsymbol{\nabla}(\boldsymbol{\nabla}\cdot\boldsymbol{A}) - \nabla^2\boldsymbol{A}, \tag{A.5 ii}$$

$$\boldsymbol{\nabla}(\boldsymbol{A}\cdot\boldsymbol{B}) = (\boldsymbol{A}\cdot\boldsymbol{\nabla})\boldsymbol{B} + (\boldsymbol{B}\cdot\boldsymbol{\nabla})\boldsymbol{A} + \boldsymbol{A}\times(\boldsymbol{\nabla}\times\boldsymbol{B}) + \boldsymbol{B}\times(\boldsymbol{\nabla}\times\boldsymbol{A}) \tag{A.5 ii}$$

$$\overset{\boldsymbol{A}=\boldsymbol{B}}{\Rightarrow} \quad \frac{1}{2}\boldsymbol{\nabla}A^2 = (\boldsymbol{A}\cdot\boldsymbol{\nabla})\boldsymbol{A} + \boldsymbol{A}\times(\boldsymbol{\nabla}\times\boldsymbol{A}). \tag{A.5 iii}$$

For $\boldsymbol{A} = \boldsymbol{B} = \boldsymbol{u}$ in (A.5 i) and (A.5 iii), by invoking the incompressibility condition $\boldsymbol{\nabla}\cdot\boldsymbol{u} = 0$, vorticity $\boldsymbol{\omega} = \boldsymbol{\nabla}\times\boldsymbol{u}$, and taking the curl of both sides of (A.5 iii), the above identities become

$$\boldsymbol{\nabla}\cdot(\boldsymbol{A}\times\boldsymbol{B}) = \boldsymbol{B}\cdot(\boldsymbol{\nabla}\times\boldsymbol{A}) - \boldsymbol{A}\cdot(\boldsymbol{\nabla}\times\boldsymbol{B}), \tag{A.6 i}$$

$$\boldsymbol{\nabla}\times\boldsymbol{\omega} = -\nabla^2\boldsymbol{u}, \tag{A.6 ii}$$

$$\boldsymbol{\nabla}\times(\boldsymbol{u}\cdot\boldsymbol{\nabla}\boldsymbol{u}) = \boldsymbol{u}\cdot\boldsymbol{\nabla}\boldsymbol{\omega} - \boldsymbol{\omega}\cdot\boldsymbol{\nabla}\boldsymbol{u}. \tag{A.6 iii}$$

Since $\boldsymbol{\nabla}\times\boldsymbol{\nabla}p = 0$ and, for two-dimensional flows, $\boldsymbol{\omega}\cdot\boldsymbol{\nabla}\boldsymbol{u} = 0$, the curl of the nonlinearity $\boldsymbol{S} \doteq \mathcal{B}(\boldsymbol{u},\boldsymbol{u}) = \boldsymbol{u}\cdot\boldsymbol{\nabla}\boldsymbol{u} + \boldsymbol{\nabla}p$ in the Navier–Stokes equation may be rewritten using (A.6 iii) as $\boldsymbol{\nabla}\times\boldsymbol{S} = \boldsymbol{\nabla}\times(\boldsymbol{u}\cdot\boldsymbol{\nabla}\boldsymbol{u}) = \boldsymbol{u}\cdot\boldsymbol{\nabla}\boldsymbol{\omega}$. Using the inner product and the above identities, we find

$$\begin{aligned}
(\mathcal{B}(\boldsymbol{u},\boldsymbol{u}), A\boldsymbol{u}) &= \int_\Omega -\boldsymbol{S}\cdot\nabla^2\boldsymbol{u}\,d\boldsymbol{x} = \int_\Omega \boldsymbol{S}\cdot(\boldsymbol{\nabla}\times\boldsymbol{\omega})\,d\boldsymbol{x} \\
&= \int_\Omega \boldsymbol{\nabla}\cdot(\boldsymbol{\omega}\times\boldsymbol{S})\,d\boldsymbol{x} + \int_\Omega \boldsymbol{\omega}\cdot(\boldsymbol{\nabla}\times\boldsymbol{S})\,d\boldsymbol{x} \\
&= \int_{\partial\Omega} (\boldsymbol{\omega}\times\boldsymbol{S})\cdot\hat{\boldsymbol{n}}\,ds + \int_\Omega \boldsymbol{\omega}\cdot(\boldsymbol{u}\cdot\boldsymbol{\nabla}\boldsymbol{\omega})\,d\boldsymbol{x} \\
&= 0 + \int_\Omega \boldsymbol{u}\cdot\boldsymbol{\nabla}\left(\frac{\omega^2}{2}\right) d\boldsymbol{x} \\
&= \int_{\partial\Omega} \left(\frac{\omega^2}{2}\boldsymbol{u}\right)\cdot\hat{\boldsymbol{n}}\,ds - \int_\Omega \left(\frac{\omega^2}{2}\right)\boldsymbol{\nabla}\cdot\boldsymbol{u}\,d\boldsymbol{x} \\
&= 0 - 0 = 0,
\end{aligned} \tag{A.7}$$

where the integrals on the boundary $\partial\Omega$ vanish because of periodicity.

1.C Strong form of enstrophy invariance

Another useful identity for the bilinear map in two-dimensional incompressible flows is called the *strong form of enstrophy invariance*:

$$(\mathcal{B}(A\boldsymbol{v},\boldsymbol{v}),\boldsymbol{u}) = (\mathcal{B}(\boldsymbol{u},\boldsymbol{v}),A\boldsymbol{v}). \tag{A.8}$$

The proof given here is is more elegant than the proof given by Dascaliuc *et al.* [2010], as it is based on explicit fluid dynamical quantities and vector calculus identities. We first prove the identity

$$(\mathcal{B}(\boldsymbol{u},A\boldsymbol{v}),\boldsymbol{v}) = (\mathcal{B}(A\boldsymbol{v},\boldsymbol{u}),\boldsymbol{v}). \tag{A.9}$$

We can write

$$\begin{aligned}(\mathcal{B}(\boldsymbol{u},A\boldsymbol{v}),\boldsymbol{v}) - (\mathcal{B}(A\boldsymbol{v},\boldsymbol{u}),\boldsymbol{v}) &= ([\mathcal{B}(\boldsymbol{u},A\boldsymbol{v}) - \mathcal{B}(A\boldsymbol{v},A\boldsymbol{u})],\boldsymbol{v}) \\ &= \int_\Omega (\boldsymbol{u}\cdot\boldsymbol{\nabla}(A\boldsymbol{v}) - A\boldsymbol{v}\cdot\boldsymbol{\nabla}\boldsymbol{u}) + \boldsymbol{\nabla}(p-p')\cdot\boldsymbol{v}\,d\boldsymbol{x} \\ &= \int_\Omega \underbrace{(\boldsymbol{m}\cdot\boldsymbol{\nabla}\boldsymbol{n} - \boldsymbol{n}\cdot\boldsymbol{\nabla}\boldsymbol{m})\cdot\boldsymbol{v}}_{I}\,d\boldsymbol{x} + \int_\Omega \underbrace{\boldsymbol{\nabla}p_1\cdot\boldsymbol{v}}_{J}\,d\boldsymbol{x},\end{aligned}$$

where $\boldsymbol{m} = \boldsymbol{u}$, $\boldsymbol{n} = A\boldsymbol{v}$, and $p_1 = (p - p')$. Using the vector calculus identity

$$\boldsymbol{\nabla}\times(\boldsymbol{n}\times\boldsymbol{m}) = \boldsymbol{n}(\boldsymbol{\nabla}\cdot\boldsymbol{m}) - \boldsymbol{m}(\boldsymbol{\nabla}\cdot\boldsymbol{n}) + (\boldsymbol{m}\cdot\boldsymbol{\nabla})\boldsymbol{n} - (\boldsymbol{n}\cdot\boldsymbol{\nabla})\boldsymbol{m},$$

I can be written as

$$\begin{aligned}(\boldsymbol{m}\cdot\boldsymbol{\nabla}\boldsymbol{n}-\boldsymbol{n}\cdot\boldsymbol{\nabla}\boldsymbol{m})\cdot\boldsymbol{u} &= [\boldsymbol{\nabla}\times(\boldsymbol{n}\times\boldsymbol{m})-(\boldsymbol{\nabla}\cdot\boldsymbol{m})\boldsymbol{n}+(\boldsymbol{\nabla}\cdot\boldsymbol{n})\boldsymbol{m}]\cdot\boldsymbol{v}\\ &= [\boldsymbol{\nabla}\times(\boldsymbol{u}\times A\boldsymbol{v})-(\boldsymbol{\nabla}\cdot A\boldsymbol{v})\boldsymbol{u}+(\boldsymbol{\nabla}\cdot\boldsymbol{u})A\boldsymbol{v}]\cdot\boldsymbol{v}\\ &= (\boldsymbol{\nabla}\times(\boldsymbol{u}\times A\boldsymbol{v}))\cdot\boldsymbol{v}+0+0=(\boldsymbol{\nabla}\times(\boldsymbol{u}\times A\boldsymbol{v}))\cdot\boldsymbol{v},\end{aligned}$$

and J becomes

$$\int_\Omega \boldsymbol{\nabla}p_1\cdot\boldsymbol{u}\,d\boldsymbol{x}\overset{\boldsymbol{\nabla}\cdot\boldsymbol{u}=0}{=}\int_\Omega\boldsymbol{\nabla}\cdot(p_1\boldsymbol{u})\,d\boldsymbol{x}=\int_{\partial\Omega}p_1\boldsymbol{u}\cdot\hat{\boldsymbol{n}}\,ds=0,$$

where the last integral vanishes because of periodic boundary conditions. So we would have

$$\begin{aligned}((\mathcal{B}(\boldsymbol{u},A\boldsymbol{v})-\mathcal{B}(A\boldsymbol{v},\boldsymbol{u})),\boldsymbol{v}) &= \int_\Omega \boldsymbol{v}\cdot\boldsymbol{\nabla}\times(\underbrace{\boldsymbol{u}\times A\boldsymbol{v}}_{\boldsymbol{S}})\,d\boldsymbol{x}\\ &= \int_\Omega\boldsymbol{\nabla}\cdot(\boldsymbol{S}\times\boldsymbol{v})\,d\boldsymbol{x}+\int_\Omega\boldsymbol{S}\cdot\boldsymbol{\nabla}\times\boldsymbol{v}\,d\boldsymbol{x}\\ &= \int_{\partial\Omega}(\boldsymbol{S}\times\boldsymbol{v})\cdot\hat{\boldsymbol{n}}\,ds+\int_\Omega\boldsymbol{\omega}\cdot\boldsymbol{S}\,d\boldsymbol{x}\\ &= 0+\int_\Omega\boldsymbol{\omega}\cdot(\boldsymbol{u}\times A\boldsymbol{v})\,d\boldsymbol{x}\\ &= -\int_\Omega\boldsymbol{u}\cdot(\boldsymbol{\omega}\times A\boldsymbol{u})\,d\boldsymbol{x}\\ &= -\int_\Omega\boldsymbol{u}\cdot(\boldsymbol{\omega}\times(\boldsymbol{\nabla}\times\boldsymbol{\omega}))\,d\boldsymbol{x}.\end{aligned}$$

Using the fact that $\boldsymbol{\omega}\times(\boldsymbol{\nabla}\times\boldsymbol{\omega}) = \frac{1}{2}\boldsymbol{\nabla}\boldsymbol{\omega}^2 - \boldsymbol{\omega}\cdot\boldsymbol{\nabla}\boldsymbol{\omega}$, and since in the two-dimensional case $\boldsymbol{\omega}\cdot\boldsymbol{\nabla}\boldsymbol{\omega} = \mathbf{0}$, we obtain

$$\begin{aligned}((\mathcal{B}(\boldsymbol{u}, A\boldsymbol{v}) - \mathcal{B}(A\boldsymbol{v}, \boldsymbol{u})), \boldsymbol{v}) &= -\int_\Omega \boldsymbol{u}\cdot(\boldsymbol{\omega}\times(\boldsymbol{\nabla}\times\boldsymbol{\omega}))\, d\boldsymbol{x} = -\int_\Omega \boldsymbol{u}\cdot\left(\frac{1}{2}\boldsymbol{\nabla}\omega^2\right) d\boldsymbol{x} \\ &= -\int_\Omega \boldsymbol{u}\cdot\left(\frac{1}{2}\boldsymbol{\nabla}\omega^2\right) d\boldsymbol{x} = -\int_\Omega \boldsymbol{u}\cdot\left(\frac{1}{2}\boldsymbol{\nabla}\omega^2\right) d\boldsymbol{x} \\ &= -\int_\Omega \boldsymbol{\nabla}\cdot\left(\frac{\boldsymbol{u}\omega^2}{2}\right) d\boldsymbol{x} = -\int_{\partial\Omega} \left(\frac{\boldsymbol{u}\omega^2}{2}\right)\cdot\hat{\boldsymbol{n}}\, ds \\ &= 0,\end{aligned}$$

and so (A.9) follows. Having this identity, we can write

$$(\mathcal{B}(A\boldsymbol{v}, \boldsymbol{v}), \boldsymbol{u}) \overset{(A.2)}{=} -(\mathcal{B}(A\boldsymbol{v}, \boldsymbol{u}), \boldsymbol{v}) \overset{(A.9)}{=} -(\mathcal{B}(\boldsymbol{u}, A\boldsymbol{v}), \boldsymbol{v}) \overset{(A.2)}{=} (\mathcal{B}(\boldsymbol{u}, \boldsymbol{v}), A\boldsymbol{v}),$$

which proves (A.8).

1.D General identity in two-dimensional incompressible flow

Using the above identities it is possible to show that

$$\underbrace{(\mathcal{B}(\boldsymbol{v}, \boldsymbol{v}), A\boldsymbol{u})}_{I} + \underbrace{(\mathcal{B}(\boldsymbol{v}, \boldsymbol{u}), A\boldsymbol{v})}_{II} + \underbrace{(\mathcal{B}(\boldsymbol{u}, \boldsymbol{v}), A\boldsymbol{v})}_{III} = 0. \tag{A.10}$$

As in the previous section there is another proof given by Foias *et al.* [2002], and although their proof is much more concise, it is completely based on the functional analysis properties of the bilinear map. In contrast, the following proof is based on vector calculus identities, which are more insightful, especially

for physically oriented readers. We begin with the term I:

$$\begin{aligned}(\mathcal{B}(\boldsymbol{v},\boldsymbol{v}),A\boldsymbol{u}) &= \int_\Omega (\boldsymbol{v}\cdot\boldsymbol{\nabla}\boldsymbol{v}+\boldsymbol{\nabla}p)\cdot(-\nabla^2\boldsymbol{u})\,d\boldsymbol{x}\\ &= \int_\Omega (\boldsymbol{v}\cdot\boldsymbol{\nabla}\boldsymbol{v})\cdot(-\nabla^2\boldsymbol{u})\,d\boldsymbol{x} - \int_\Omega \boldsymbol{\nabla}p\cdot\nabla^2\boldsymbol{u}\,d\boldsymbol{x}\\ &= \int_\Omega (\boldsymbol{v}\cdot\boldsymbol{\nabla}\boldsymbol{v})\cdot(-\nabla^2\boldsymbol{u})\,d\boldsymbol{x}.\end{aligned}$$

Let $\boldsymbol{\omega}=\boldsymbol{\nabla}\times\boldsymbol{u}$, so that $-\nabla^2\boldsymbol{u}=\boldsymbol{\nabla}\times\boldsymbol{\omega}$, and consequently we would obtain

$$\begin{aligned}(\mathcal{B}(\boldsymbol{v},\boldsymbol{v}),A\boldsymbol{u}) &= \int_\Omega (\boldsymbol{v}\cdot\boldsymbol{\nabla}\boldsymbol{v})\cdot\boldsymbol{\nabla}\times\boldsymbol{\omega}\,d\boldsymbol{x}\\ &= \int_\Omega \boldsymbol{\nabla}\cdot(\boldsymbol{\omega}\times(\boldsymbol{v}\cdot\boldsymbol{\nabla}\boldsymbol{v}))\,d\boldsymbol{x} + \int_\Omega \boldsymbol{\omega}\cdot\boldsymbol{\nabla}\times(\boldsymbol{v}\cdot\boldsymbol{\nabla}\boldsymbol{v})\,d\boldsymbol{x}\\ &= \int_{\partial\Omega} \boldsymbol{\omega}\times(\boldsymbol{v}\cdot\boldsymbol{\nabla}\boldsymbol{v})\cdot\hat{\boldsymbol{n}}\,ds + \int_\Omega \boldsymbol{\omega}\cdot\boldsymbol{\nabla}\times(\boldsymbol{v}\cdot\boldsymbol{\nabla}\boldsymbol{v})\,d\boldsymbol{x}\\ &= 0 + \int_\Omega \boldsymbol{\omega}\cdot\underbrace{\boldsymbol{\nabla}\times(\boldsymbol{v}\cdot\boldsymbol{\nabla}\boldsymbol{v})}_{\boldsymbol{S}}\,d\boldsymbol{x} = \int_\Omega \boldsymbol{S}\cdot(\boldsymbol{\nabla}\times\boldsymbol{u})\,d\boldsymbol{x}\\ &= \int_\Omega \boldsymbol{\nabla}\cdot(\boldsymbol{u}\times\boldsymbol{S})\,d\boldsymbol{x} + \int_\Omega \boldsymbol{u}\cdot\boldsymbol{\nabla}\times\boldsymbol{S}\,d\boldsymbol{x}\\ &= \int_{\partial\Omega} (\boldsymbol{u}\times\boldsymbol{S})\cdot\hat{\boldsymbol{n}}\,ds + \int_\Omega \boldsymbol{u}\cdot\boldsymbol{\nabla}\times\boldsymbol{S}\,d\boldsymbol{x}\\ &= 0 + \int_\Omega \boldsymbol{u}\cdot\boldsymbol{\nabla}\times\boldsymbol{S}\,d\boldsymbol{x} = \int_\Omega \boldsymbol{u}\cdot\boldsymbol{\nabla}\times\boldsymbol{S}\,d\boldsymbol{x}.\end{aligned}$$

On the other hand we have

$$\boldsymbol{S}=\boldsymbol{\nabla}\times(\boldsymbol{v}\cdot\boldsymbol{\nabla}\boldsymbol{v})=\boldsymbol{\nabla}\times\left(\boldsymbol{\nabla}\frac{v^2}{2}\right)-\boldsymbol{\nabla}\times(\boldsymbol{v}\times(\boldsymbol{\nabla}\times\boldsymbol{v}))=-\boldsymbol{\nabla}\times(\boldsymbol{v}\times(\underbrace{\boldsymbol{\nabla}\times\boldsymbol{v}}_{\boldsymbol{w}})).$$

But

$$\begin{aligned}\boldsymbol{S} = -\boldsymbol{\nabla}\times(\boldsymbol{v}\times\boldsymbol{w}) &= -[\boldsymbol{v}(\boldsymbol{\nabla}\cdot\boldsymbol{w}) - \boldsymbol{w}(\boldsymbol{\nabla}\cdot\boldsymbol{v}) + (\boldsymbol{w}\cdot\boldsymbol{\nabla})\boldsymbol{v} - (\boldsymbol{v}\cdot\boldsymbol{\nabla})\boldsymbol{w}] \\ &= -0 + 0 - 0 + (\boldsymbol{v}\cdot\boldsymbol{\nabla})\boldsymbol{w} \\ &= (\boldsymbol{v}\cdot\boldsymbol{\nabla})\boldsymbol{w}.\end{aligned}$$

Now using (A.5 ii) and considering the fact that $(\boldsymbol{w}\cdot\boldsymbol{\nabla})\boldsymbol{v} = 0$, we can write

$$\begin{aligned}\boldsymbol{S} = (\boldsymbol{v}\cdot\boldsymbol{\nabla})\boldsymbol{w} &= \boldsymbol{\nabla}(\boldsymbol{v}\cdot\boldsymbol{w}) - \boldsymbol{w}\cdot\boldsymbol{\nabla}\boldsymbol{v} - \boldsymbol{v}\times(\boldsymbol{\nabla}\times\boldsymbol{w}) - \boldsymbol{w}\times(\boldsymbol{\nabla}\times\boldsymbol{v}) \\ &= 0 - 0 - \boldsymbol{v}\times(\boldsymbol{\nabla}\times\boldsymbol{w}) - 0 \\ &= -\boldsymbol{v}\times(\boldsymbol{\nabla}\times\boldsymbol{w}) = -\boldsymbol{v}\times(\boldsymbol{\nabla}\times(\boldsymbol{\nabla}\times\boldsymbol{v})) = -\boldsymbol{v}\times(\boldsymbol{\nabla}(\boldsymbol{\nabla}\cdot\boldsymbol{v}) - \nabla^2\boldsymbol{v}) \\ &= \boldsymbol{v}\times\nabla^2\boldsymbol{v}\end{aligned}$$

Thus we would have

$$\begin{aligned}\boldsymbol{\nabla}\times\boldsymbol{S} &= \boldsymbol{\nabla}\times(\boldsymbol{v}\times\nabla^2\boldsymbol{v}) \\ &= \boldsymbol{v}(\boldsymbol{\nabla}\cdot\nabla^2\boldsymbol{v}) - \nabla^2\boldsymbol{v}(\boldsymbol{\nabla}\cdot\boldsymbol{v}) + ((\nabla^2\boldsymbol{v})\cdot\boldsymbol{\nabla})\boldsymbol{v} - (\boldsymbol{v}\cdot\boldsymbol{\nabla})\nabla^2\boldsymbol{v} \\ &= 0 - 0 + (\nabla^2\boldsymbol{v}\cdot\boldsymbol{\nabla})\boldsymbol{v} - (\boldsymbol{v}\cdot\boldsymbol{\nabla})\nabla^2\boldsymbol{v} \\ &= (\nabla^2\boldsymbol{v}\cdot\boldsymbol{\nabla})\boldsymbol{v} - (\boldsymbol{v}\cdot\boldsymbol{\nabla})\nabla^2\boldsymbol{v}.\end{aligned}$$

So in the end we obtain

$$\begin{aligned}(\mathcal{B}(\boldsymbol{v},\boldsymbol{v}), A\boldsymbol{u}) &= \int_\Omega (\boldsymbol{\nabla}\times\boldsymbol{S})\cdot\boldsymbol{u}\, d\boldsymbol{x} \\ &= \int_\Omega ((\nabla^2\boldsymbol{v}\cdot\boldsymbol{\nabla})\boldsymbol{v})\cdot\boldsymbol{u}\, d\boldsymbol{x} - \int_\Omega ((\boldsymbol{v}\cdot\boldsymbol{\nabla})\nabla^2\boldsymbol{v})\cdot\boldsymbol{u}\, d\boldsymbol{x}.\end{aligned}$$

Taking into account that we can add or subtract terms of the form

$$\int_\Omega \boldsymbol{u}\cdot\boldsymbol{\nabla} p\, d\boldsymbol{x} = 0,$$

we can write

$$\begin{aligned}(\mathcal{B}(\boldsymbol{v},\boldsymbol{v}), A\boldsymbol{u}) &= \int_\Omega ((\nabla^2\boldsymbol{v}\cdot\boldsymbol{\nabla})\boldsymbol{v})\cdot\boldsymbol{u}\, d\boldsymbol{x} - \int_\Omega ((\boldsymbol{v}\cdot\boldsymbol{\nabla})\nabla^2\boldsymbol{v})\cdot\boldsymbol{u}\, d\boldsymbol{x} \\ &= -(\mathcal{B}(A\boldsymbol{v},\boldsymbol{v}),\boldsymbol{u}) + (\mathcal{B}(\boldsymbol{v},A\boldsymbol{v}),\boldsymbol{u}).\end{aligned}$$

Up to this point we have found a valuable representation of the term I in (A.10):

$$(\mathcal{B}(\boldsymbol{v},\boldsymbol{v}), A\boldsymbol{u}) = \underbrace{(\mathcal{B}(\boldsymbol{v},A\boldsymbol{v}),\boldsymbol{u})}_{J} - \underbrace{(\mathcal{B}(A\boldsymbol{v},\boldsymbol{v}),\boldsymbol{u})}_{K}. \tag{A.11}$$

Applying (A.2) and (A.8) identities to the terms J and K, respectively, we will obtain

$$(\mathcal{B}(\boldsymbol{v},\boldsymbol{v}), A\boldsymbol{u}) = -(\mathcal{B}(\boldsymbol{v},\boldsymbol{u}), A\boldsymbol{v}) - (\mathcal{B}(\boldsymbol{u},\boldsymbol{v}), A\boldsymbol{v}).$$

which is exactly (A.10).

1.E Estimates for the bilinear term involving the higher order of the Stokes operator

A term that has great impact on our analysis of the Navier–Stokes equation is

$$\big(\mathcal{B}(\boldsymbol{v},\boldsymbol{v}), A^2\boldsymbol{v}\big).$$

Having a good estimate for this term is vital in our work, but unfortunately no simpler representation is known for this term, only a useful upper bound. Using the equivalent form of the general 2D identity, (A.11), one obtains

$$\big(\mathcal{B}(\boldsymbol{v},\boldsymbol{v}),A^2\boldsymbol{v}\big) = (\mathcal{B}(\boldsymbol{v},\boldsymbol{v}),AA\boldsymbol{v}) \overset{\boldsymbol{u}\doteq A\boldsymbol{v}}{=} (\mathcal{B}(\boldsymbol{v},\boldsymbol{v}),A\boldsymbol{u}) \tag{A.12}$$

$$\overset{(A.11)}{=}(\mathcal{B}(\boldsymbol{v},A\boldsymbol{v}),\boldsymbol{u}) - (\mathcal{B}(A\boldsymbol{v},\boldsymbol{v}),\boldsymbol{u}) \tag{A.13}$$

$$= (\mathcal{B}(\boldsymbol{v},A\boldsymbol{v}),A\boldsymbol{v}) - (\mathcal{B}(A\boldsymbol{v},\boldsymbol{v}),A\boldsymbol{v}) \tag{A.14}$$

$$= -(\mathcal{B}(A\boldsymbol{v},\boldsymbol{v}),A\boldsymbol{v}) = (\mathcal{B}(A\boldsymbol{v},A\boldsymbol{v}),\boldsymbol{v}). \tag{A.15}$$

The above result is the best exact estimate that we could obtain using the general identity (A.10) (and consequently all other identities that we have proved so far). As this term appears in our functional estimates, it is necessary to come up with an upper bound. In order to obtain this estimate we will eventually require the Ladyzhenskaya inequality that we introduced before:

$$\big(\mathcal{B}(\boldsymbol{u},\boldsymbol{u}),A^2\boldsymbol{u}\big) = (\mathcal{B}(A\boldsymbol{u},A\boldsymbol{u}),\boldsymbol{u}) \overset{\boldsymbol{v}\doteq A\boldsymbol{u}}{=} (\mathcal{B}(\boldsymbol{v},\boldsymbol{v}),\boldsymbol{u}).$$

As we have shown earlier, the $\boldsymbol{\nabla} p$ term will vanish due to incompressibility, so

$$\begin{aligned}\big(\mathcal{B}(\boldsymbol{u},\boldsymbol{u}),A^2\boldsymbol{u}\big) &= (\mathcal{B}(\boldsymbol{v},\boldsymbol{v}),\boldsymbol{u})\\ &= \int_\Omega (\boldsymbol{v}\cdot\boldsymbol{\nabla}\boldsymbol{v})\cdot\boldsymbol{u}\,d\boldsymbol{x} = \int_\Omega \left(\frac{1}{2}\boldsymbol{\nabla} v^2 - \boldsymbol{v}\times(\boldsymbol{\nabla}\times\boldsymbol{v})\right)\cdot\boldsymbol{u}\,d\boldsymbol{x}\\ &= \int_\Omega \left(\frac{1}{2}\boldsymbol{\nabla} v^2\right)\cdot\boldsymbol{u}\,d\boldsymbol{x} - \int_\Omega (\boldsymbol{v}\times(\boldsymbol{\nabla}\times\boldsymbol{v}))\cdot\boldsymbol{u}\,d\boldsymbol{x}\\ &= 0 - \int_\Omega (\boldsymbol{v}\times\boldsymbol{\omega})\cdot\boldsymbol{u}\,d\boldsymbol{x} = \int_\Omega (\boldsymbol{\omega}\times\boldsymbol{v})\cdot\boldsymbol{u}\,d\boldsymbol{x}.\end{aligned}$$

Using the triple product identities we can write

$$\begin{aligned}
\big(\mathcal{B}(\boldsymbol{u},\boldsymbol{u}),A^2\boldsymbol{u}\big) &= \int_\Omega \boldsymbol{u}\cdot\boldsymbol{\omega}\times\boldsymbol{v}\,d\boldsymbol{x} = \int_\Omega \boldsymbol{\omega}\cdot\boldsymbol{v}\times\boldsymbol{u}\,d\boldsymbol{x} \\
&\overset{\text{Cauchy-Schwarz}}{\leq} \left(\int_\Omega |\boldsymbol{v}\times\boldsymbol{u}|^2\,d\boldsymbol{x}\right)^{1/2}\left(\int_\Omega |\boldsymbol{\omega}|^2\,d\boldsymbol{x}\right)^{1/2} \\
&\leq \left(\int_\Omega v^2u^2\,d\boldsymbol{x}\right)^{1/2}\left(\int_\Omega \omega^2 d\boldsymbol{x}\right)^{1/2} \\
&= \left(\int_\Omega A^2u^4\,d\boldsymbol{x}\right)^{1/2}\left(\int_\Omega \omega^2 d\boldsymbol{x}\right)^{1/2} \\
&= \left(\int_\Omega (A^{1/2}u)^4\,d\boldsymbol{x}\right)^{1/2}\left(\int_\Omega \omega^2 d\boldsymbol{x}\right)^{1/2}.
\end{aligned}$$

On the other hand we have

$$\begin{aligned}
\int_\Omega \omega^2 d\boldsymbol{x} &= \int_\Omega |\boldsymbol{\nabla}\times\boldsymbol{v}|^2 d\boldsymbol{x} = \int_\Omega A^2|\boldsymbol{\nabla}\times\boldsymbol{u}|^2 d\boldsymbol{x} \\
&= \int_\Omega A^2\boldsymbol{\nabla}\cdot(\boldsymbol{u}\times\boldsymbol{\omega})\,d\boldsymbol{x} + \int_\Omega A^2(\boldsymbol{u}\cdot(-\nabla^2\boldsymbol{u}))\,d\boldsymbol{x} \\
&= 0 + \int_\Omega A^2(\boldsymbol{u}\cdot A\boldsymbol{u})d\boldsymbol{x} = \int_\Omega A^2(A^{1/2}\boldsymbol{u}\cdot A^{1/2}\boldsymbol{u})d\boldsymbol{x} \\
&= \int_\Omega A^3u^2 d\boldsymbol{x} = \big|A^{3/2}\boldsymbol{u}\big|^2.
\end{aligned}$$

Thus we will obtain

$$\begin{aligned}
\big(\mathcal{B}(\boldsymbol{u},\boldsymbol{u}),A^2\boldsymbol{u}\big) &\leq \left(\int_\Omega (A^{1/2}u)^4\,d\boldsymbol{x}\right)^{1/2}\big|A^{3/2}\boldsymbol{u}\big| \\
&\overset{\text{Ladyzhenskaya}}{\leq} c_L||\boldsymbol{u}||\,|A\boldsymbol{u}|\,\big|A^{3/2}\boldsymbol{u}\big|.
\end{aligned}$$

Appendix B

Inequalities

Among many inequalities in the field of *functional analysis*, we now list those that are used in this work. The reader who is interested in studying their proofs and related inequalities, especially *Sobolev inequalities*, can refer to any standard functional analysis resource.

In this appendix we use the following notation:

- Ω: the domain of definition of functions;
- $\boldsymbol{u}$: $\boldsymbol{u}(\boldsymbol{x}), \quad \boldsymbol{x} \in \Omega \subset \mathbb{R}^3$, or $\Omega \subset \mathbb{R}^3$;
- $\boldsymbol{u_k}$: the discrete Fourier transform of $\boldsymbol{u}, \quad \boldsymbol{k} \in \mathbb{Z}^3 \backslash \{\boldsymbol{0}\}$, or $\boldsymbol{k} \in \mathbb{Z}^2 \backslash \{\boldsymbol{0}\}$;
- $A = -\nabla^2$: a self-adjoint linear operator.

For the sake of simplicity, we are going to ignore Ω in our notation; for example, we would write H^2 instead of $H^2(\Omega)$.

2.A Agmon inequalities

Let $\Omega \in \mathbb{R}^3$ and $\boldsymbol{u} \in H^2(\Omega) \cap H_0^1(\Omega)$. Then the 3D Agmon inequalities state that there exists constants C such that

$$|\boldsymbol{u}|_{L^\infty(\Omega)} \leq C|\boldsymbol{u}|^{1/2}_{H^1(\Omega)}|A\boldsymbol{u}|^{1/2}_{H^2(\Omega)},$$
$$|\boldsymbol{u}|_{L^\infty(\Omega)} \leq C|\boldsymbol{u}|^{1/4}_{L^2(\Omega)}|A\boldsymbol{u}|^{3/4}_{H^2(\Omega)}.$$

When $\Omega \subset \mathbb{R}^2$ and $\boldsymbol{u} \in H^2(\Omega) \cap H_0^1(\Omega)$, the 2D Agmon inequality states that there exists a constant C such that

$$|\boldsymbol{u}|_{L^\infty(\Omega)} \leq C|\boldsymbol{u}|^{1/2}|A\boldsymbol{u}|^{1/2}. \tag{B.1}$$

It must be noticed here that the constant C in each Agmon inequality is a universal constant that depends only on the space Ω, so in order to make use of this inequality for numerical simulations, having an explicit form of C is crucial. Thus, in the next section we are going to obtain an explicit form of this constant for the two-dimensional case.[1]

2.B Universal constant of the Agmon inequality in a 2D periodic domain

The main reason for finding an explicit value for the constant in the Agmon inequality is to obtain some useful bounds for our direct numerical simulation of 2D turbulence. As the numerical simulation is done on a lattice, we focus on the discrete form of the Agmon inequality and so all the integrals will turn to

[1] Proved by John C. Bowman [2016].

summations. On the other hand, because all of our simulations are naturally in Fourier space, we make use of the Fourier representation of our functions and the Agmon inequality.

We consider continuous functions on a bounded domain. The numerical simulations are done on a lattice on this domain, where suprema reduce to maxima. That is,

$$|\boldsymbol{u}|_{L^\infty(\Omega)} = \max_{\Omega} |\boldsymbol{u}|.$$

It is worth mentioning that *pseudospectral* numerical simulations of turbulence in a periodic domain use the N-point discrete Fourier transform

$$\hat{\boldsymbol{u}}_k = \frac{1}{\sqrt{N}} \sum_{j=0}^{N-1} \boldsymbol{u}_j e^{-\frac{2\pi i j k}{N}},$$

which has the inverse

$$\boldsymbol{u}_j = \frac{1}{\sqrt{N}} \sum_{k=0}^{N-1} \hat{\boldsymbol{u}}_k e^{\frac{2\pi i j k}{N}}.$$

The orthogonality relationship underlying this transform pair is elucidated on substituting $z = e^{2\pi i (j+\bar{j})/N}$:

$$\sum_{k=0}^{N-1} e^{2\pi i (j+\bar{j}) k/N} = \sum_{k=0}^{N-1} z^k = \begin{cases} N & \text{if} \quad j + \bar{j} = mN, \quad m \in \mathbb{Z}, \\ \frac{1-z^N}{1-z} = 0 & \text{otherwise.} \end{cases}$$

Taking into account the above definitions, one can easily obtain the convolution theorem for the product of two functions f and g:

$$\frac{1}{\sqrt{N}} \sum_{j=0}^{N-1} f_j g_j e^{-\frac{2\pi i k j}{N}} = \frac{1}{N\sqrt{N}} \sum_{j=0}^{N-1} e^{-\frac{2\pi i k j}{N}} \sum_{p=0}^{N-1} \hat{f}_p e^{-\frac{2\pi i p j}{N}} \sum_{q=0}^{N-1} \hat{g}_q e^{-\frac{2\pi i q j}{N}}.$$

Using the orthogonality condition

$$\sum_{j=0}^{N-1} e^{-\frac{2\pi i(p+q-k)j}{N}} = N\delta_{p+q-k,0},$$

yields

$$\frac{1}{\sqrt{N}} \sum_{j=0}^{N-1} f_j g_j e^{-\frac{2\pi ikj}{N}} = \frac{1}{\sqrt{N}} \sum_{j=0}^{N-1} \hat{f}_p \hat{g}_{k-p}.$$

So, taking $k = 0$ and $g = f$, we obtain the *Parseval identity*

$$\sum_{j=0}^{N-1} f_j^2 = \sum_{p=0}^{N-1} \hat{f}_p \hat{f}_{-p} = \sum_{p=0}^{N-1} \left|\hat{f}_p\right|^2. \tag{B.2}$$

Now using the fact that $(\max_\Omega |\boldsymbol{u}|)^2 \leq \sum_{\boldsymbol{x}} |\boldsymbol{u}|^2$ and $\sqrt{2} \leq \sqrt{1+k^2}$ for $\boldsymbol{k} \in \mathbb{Z}^2\backslash\{\boldsymbol{0}\}$, and applying the *Parseval identity* (B.2) and *Hölder inequality*, we find

$$\left(\max_{\Omega} |\boldsymbol{u}|\right)^2 \leq \sum_{\boldsymbol{x}} |\boldsymbol{u}|^2 = \sum_{\boldsymbol{k}} |\boldsymbol{u}_{\boldsymbol{k}}|^2 \leq \frac{1}{\sqrt{2}} \sum_{\boldsymbol{k}} |\boldsymbol{u}_{\boldsymbol{k}}|^2 \sqrt{1+k^2} \overset{\text{Hölder Ineq.}}{\leq} \frac{1}{\sqrt{2}} \left(\sum_{\boldsymbol{k}} |\boldsymbol{u}_{\boldsymbol{k}}|^2\right)^{1/2} \left(\sum_{\boldsymbol{k}} |\boldsymbol{u}_{\boldsymbol{k}}|^2 (1+k^2)\right)^{1/2}. \tag{B.3}$$

As a result, we will have:

$$\max_{\Omega} |\boldsymbol{u}| \leq \frac{1}{\sqrt[4]{2}} \left(\sum_{\boldsymbol{k}} |\boldsymbol{u}_{\boldsymbol{k}}|^2\right)^{1/4} \left(\sum_{\boldsymbol{k}} |\boldsymbol{u}_{\boldsymbol{k}}|^2 (1+k^2)\right)^{1/4}, \qquad \forall \boldsymbol{k} \in \mathbb{Z}^2\backslash\{\boldsymbol{0}\}. \tag{B.4}$$

Comparing to (B.1), we thus see that

$$C \leq \frac{1}{\sqrt[4]{2}}.$$

Bibliography

[Arnold 1964] V. I. Arnold, Soviet Mathematics, **5**:581, 1964.

[Basdevant 1983] C. Basdevant, Journal of Computational Physics, **50**:209, 1983.

[Batchelor 1948] G. Batchelor, Quarterly of Applied Mathematics, **6**:97, 1948.

[Batchelor 1969] G. K. Batchelor, Phys. Fluids, **12 II**:233, 1969.

[Boussinesq 1877] J. Boussinesq, *Essai sur la théorie des eaux courantes*, Imprimerie nationale, 1877.

[Bowman & Roberts 2011] J. C. Bowman & M. Roberts, SIAM J. Sci. Comput., **33**:386, 2011.

[Burgers 1948] J. M. Burgers, Advances in applied mechanics, **1**:171, 1948.

[Chapman & Tobak 1985] G. T. Chapman & M. Tobak, "Observations, theoretical ideas, and modeling of turbulent

flowsast, present, and future," in *Theoretical Approaches to Turbulence*, pp. 19–49, Springer, 1985.

[Comte-Bellot & Corrsin 1966] G. Comte-Bellot & S. Corrsin, Journal of Fluid Mechanics, **25**:657, 1966.

[Corrsin 1949] S. Corrsin, An experimental verification of local isotropy, 1949.

[Dascaliuc *et al.* 2005] R. Dascaliuc, M. Jolly, *et al.*, Journal of Dynamics and Differential Equations, **17**:643, 2005.

[Dascaliuc *et al.* 2010] R. Dascaliuc, C. Foias, & M. Jolly, Journal of differential Equations, **248**:792, 2010.

[Deardorff 1970] J. W. Deardorff, Journal of Fluid Mechanics, **41**:453, 1970.

[Domaradzki & Saiki 1997] J. A. Domaradzki & E. M. Saiki, Physics of Fluids (1994-present), **9**:2148, 1997.

[Echekki *et al.* 2001] T. Echekki, A. R. Kerstein, T. D. Dreeben, & J.-Y. Chen, Combustion and flame, **125**:1083, 2001.

[Emmons 1951] H. W. Emmons, Journal of the Aeronautical Sciences, **18**:490, 1951.

[Feigenbaum 1978] M. J. Feigenbaum, Journal of statistical physics, **19**:25, 1978.

[Foias *et al.* 2002] C. Foias, M. Jolly, O. Manley, & R. Rosa, Journal of Statistical Physics, **108**:591, 2002.

[Frisch 1995] U. Frisch, *Turbulence: The Legacy of A.N.Kolmogorov*, Cambdridge University Press, 1995.

[George 2013] W. K. George, *Lectures in Turbulence for 21st Century*, 2013.

[Germano *et al.* 1991] M. Germano, U. Piomelli, P. Moin, & W. H. Cabot, Physics of Fluids A: Fluid Dynamics (1989-1993), **3**:1760, 1991.

[Gibson 1968] C. H. Gibson, Physics of Fluids (1958-1988), **11**:2305, 1968.

[Gollub & Benson 1980] J. Gollub & S. Benson, Journal of Fluid Mechanics, **100**:449, 1980.

[Heisenberg 1948] W. Heisenberg, Proceedings of the Royal Society of London A, **195**:402, 1948.

[Kolmogorov 1941a] A. Kolmogorov, Dokl. Akad. Nauk SSSR, **30**:301, 1941, Reprinted in Proc. R. Soc. Lond. A434, 9–13,1991.

[Kolmogorov 1941b] A. Kolmogorov, Dokl. Akad. Nauk SSSR, **32**:16, 1941, Reprinted in Proc. R. Soc. Lond. A434, 15–17,1991.

[Kraichnan 1958] R. H. Kraichnan, Phys. Rev., **109**:1407, 1958.

[Kraichnan 1959] R. H. Kraichnan, J. Fluid Mech., **5**:497, 1959.

[Kraichnan 1961] R. H. Kraichnan, J. Math. Phys., **2**:124, 1961.

[Kraichnan 1967] R. H. Kraichnan, Phys. Fluids, **10**:1417, 1967.

[Kraichnan 1971] R. H. Kraichnan, J. Fluid Mech., **47**:525, 1971.

[Ladyzhenskaya 1963] O. Ladyzhenskaya, Viscous Incompressible Flow, **184**, 1963.

[Launder & Spalding 1974] B. E. Launder & D. Spalding, Computer methods in applied mechanics and engineering, **3**:269, 1974.

[Launder *et al.* 1975] B. Launder, G. J. Reece, & W. Rodi, Journal of fluid mechanics, **68**:537, 1975.

[Leith 1968] C. E. Leith, Phys. Fluids, **11**:671, 1968.

[Leray 1933] J. Leray, Thèses françaises de l'entre-deux-guerres, **142**:1, 1933.

[Leray 1934] J. Leray, Journal de Mathématiques pures et appliquées, **13**:331, 1934.

[Lorenz 1963] E. N. Lorenz, J. Atmos. Sci., **20**:130, 1963.

[Lumley & Newman 1977] J. L. Lumley & G. R. Newman, Journal of Fluid Mechanics, **82**:161, 1977.

[McDonough & Yang 2003] J. McDonough & T. Yang, "A new LES model applied to an internally-heated, swirling buoyant plume," in *Western States Section*, 2003.

[McDonough *et al.* 1998] J. McDonough, S. Mukerji, & S. Chung, Applied mathematics and computation, **95**:219, 1998.

[McDonough 2007] J. M. McDonough, Introductory lectures on turbulence, Unpublished lecture notes, 2007.

[McWilliams 1984] J. C. McWilliams, J. Fluid Mech., **146**:21, 1984.

[Mukerji *et al.* 1998] S. Mukerji, J. Mcdonougha, M. Mengüç, S. Manickavasagam, & S. Chung, International journal of heat and mass transfer, **41**:4095, 1998.

[Novikov 1964] E. A. Novikov, J. Exptl. Theoret. Phys. (U.S.S.R), **47**:1919, 1964.

[Obukhov 1949] A. Obukhov, "The local structure of atmospheric turbulence," in *Dokl. Akad. Nauk. SSSR*, volume 67, pp. 643–646, 1949.

[Patterson Jr. & Orszag 1971] G. S. Patterson Jr. & S. A. Orszag, Physics of Fluids, **14**:2538, 1971.

[Piomelli 1993] U. Piomelli, Physics of Fluids A: Fluid Dynamics (1989-1993), **5**:1484, 1993.

[Poincaré & Magini 1899] H. Poincaré & R. Magini, Il Nuovo Cimento (1895-1900), **10**:128, 1899.

[Pomeau & Manneville 1980] Y. Pomeau & P. Manneville, Communications in Mathematical Physics, **74**:189, 1980.

[Prandtl 1925] L. Prandtl, Z. Angew. Math. Mech, **5**:136, 1925.

[Reynolds 1894] O. Reynolds, Proceedings of the Royal Society of London, **56**:40, 1894.

[Ruelle & Takens 1971] D. Ruelle & F. Takens, Communications in mathematical physics, **20**:167, 1971.

[Schubauer & Skramstad 1947] G. B. Schubauer & H. K. Skramstad, Journal of Research of the National Bureau of Standards, **38**, 1947.

[Smagorinsky 1963] J. Smagorinsky, Mon. Weather Rev., **91**:99, 1963.

[Smale 1965] S. Smale, "Diffeomorphisms with many periodic," in *Differential and combinatorial topology: A symposium in honor of Marston Morse*, volume 27, p. 63, Princeton University Press, 1965.

[Taylor 1935] G. I. Taylor, "Statistical theory of turbulence," in *Proceedings of the Royal Society of London A: Mathematical, Physical and Engineering Sciences*, volume 151, pp. 421–444, The Royal Society, 1935.

[Townsend 1947] A. Townsend, "The measurement of double and triple correlation derivatives in isotropic turbulence," in *Mathematical Proceedings of the Cambridge Philosophical Society*, volume 43, pp. 560–570, Cambridge Univ Press, 1947.

[Tucker & Reynolds 1968] H. J. Tucker & A. Reynolds, Journal of fluid mechanics, **32**:657, 1968.

[von Karman 1948] T. von Karman, Proceedings of the National Academy of Sciences, **34**:530, 1948.

[Wygnanski & Fiedler 1970] I. Wygnanski & H. Fiedler, Journal of Fluid Mechanics, **41**:327, 1970.

[Yaglom 1948] A. Yaglom, Izv. Akad. Nauk. SSSR Ser. Geogr. i Geofiz, **12**:501, 1948.

[Yang *et al.* 2003] T. Yang, J. McDonough, & J. Jacob, AIAA journal, **41**:1690, 2003.

Index